

The Post-Transcriptional Regulation of Antioxidant Enzymes

BY

EMILY N. REINKE

B.Sc., University of St. Andrews, 2006
M.S., Washington State University, 2008

THESIS

Submitted as partial fulfillment of the requirements
for the degree of Doctor of Philosophy in Pathology
in the Graduate College of the
University of Illinois at Chicago, 2013

Chicago, IL

Defense Committee:

Alan Diamond, Chair and Advisor
Larisa Nonn
Bao-Shiang Lee, Research Resources Center
Rajendra Mehta, Illinois Institute of Technology
Chiayeng Wang, Oral Sciences

ACKNOWLEDGEMENTS

The assistance of several people was necessary for the completion of this dissertation, without which I might never have made it. Firstly, I would like to thank my advisor Dr. Alan Diamond, whose patience, guidance and support throughout my dissertation project provided me with the means to go beyond what I thought I was capable of academically. He has taken the time to provide instruction in a broad range of academic and research aspects, which have greatly aided in my professional development and my readiness to pursue the next stage of my career. I would also like to thank my committee, Drs. Larisa Nonn, Wancai Yang, Chiayeng Wang, Bao-Shiang Lee and Rajendra Mehta, whose guidance and suggestions have helped to complete this project. Great appreciation goes out to the current and former members of the Diamond lab, for insightful conversation, technical suggestions and most importantly the support to make it through, especially Marci Gutt, Dr. Anita Jerome-Morais, Dr. Frank Weinberg and Dr. Soumen Bera. Thank you to the other Diamond lab grad students Dede Ekoue and Emmanuel Ansong, for providing extra hands when two just weren't enough. I'd also like to acknowledge my parents Donn and Kathi Terry and my siblings Kristin, Armando and the Larios family, who have supported me in all of my pursuits and instilled a never ceasing love of learning and curiosity. Finally, I would like to thank my husband, Adam Reinke, for his love, extreme patience, and support throughout this entire pursuit and into the future.

TABLE OF CONTENTS

<u>CHAPTER</u>	<u>PAGE</u>
I. INTRODUCTION	1
A. Generation of reactive oxygen species	1
1. Superoxide is generated primarily by cellular metabolism.....	1
2. Superoxide dismutase enzymes protect against superoxide-induced cell damage	2
3. Hydrogen peroxide is produced in multiple cellular compartments	4
4. Hydrogen peroxide is a vital component in pathogen defense and in signal transduction.....	5
5. Excess reactive oxygen species levels can be detrimental to cell function and DNA fidelity.....	6
B. Multiple antioxidant proteins regulate hydrogen peroxide levels.....	7
1. Catalase reduces hydrogen peroxide under oxidative stress.....	8
2. Thioredoxin and thioredoxin reductase maintain antioxidant reductive capacity	9
3. Thioredoxin reductase is an antioxidant selenoprotein.....	9
4. Thioredoxin reductase 1 has more than antioxidant properties	11
C. The glutathione peroxidase family: antioxidant selenoproteins	12
1. Glutathione peroxidase activity is dependent on the antioxidant substrate glutathione.....	12
2. Glutathione peroxidase enzymes detoxify hydrogen peroxide and lipid peroxides	13
3. Glutathione peroxidase selenoprotein expression is dependent on selenium status	13
4. The glutathione peroxidase selenoprotein family members	14
5. The antioxidant glutathione peroxidase 4 regulates fertility, cell viability, and inflammation	15
6. Cytosolic glutathione peroxidase 1 is a ubiquitous antioxidant protein ...	16
7. Properties of glutathione peroxidase that affect cell growth and proliferation.....	17
8. Glutathione peroxidase is associated with risk or progression of multiple diseases	19
a. Glutathione peroxidase is deleted in multiple cancer types.....	19
b. Allelic variations in glutathione peroxidase enzyme activity	19
c. Cancer risk is increased by glutathione peroxidase 1 polymorphisms.....	21
d. Obesity and increased reactive oxygen species increase diabetes risk via glutathione peroxidase 1	22
e. Glutathione peroxidase 1 and selenium intake affect onset of cardiomyopathies	23

TABLE OF CONTENTS (continued)

<u>CHAPTER</u>	<u>PAGE</u>
9. Regulation of glutathione peroxidase 1	23
10. Glutathione peroxidase 1 transcription is dependent on reactive oxygen species levels.....	24
11. Glutathione peroxidase 1 translation is increased in a selenium-dependent manner.....	25
12. Post-translational modifications of glutathione peroxidase 1 affect enzyme activity.....	27
D. Understanding the regulation of glutathione peroxidase 1	28
II. CHANGES IN THE ACTIVITY OF THE GLUTATHIONE PEROXIDASE 1 ANTIOXIDANT SELENOENZYME IN MONONUCLEAR CELLS FOLLOWING IMATINIB TREATMENT	28
A. Introduction.....	28
B. Materials and methods	28
C. Results.....	30
1. Assay reliability	30
2. Changes in glutathione peroxidase activity following imatinib therapy ..	32
D. Discussion	34
III. THE <i>IN VITRO</i> EFFECTS OF IMATINIB AND RAPAMYCIN ON ANTIOXIDANT PROTEIN LEVELS AND ACTIVITY	36
A. Introduction.....	36
B. Materials and methods	36
1. Tissue culture	36
2. Cell lysis, protein and RNA isolation, and cDNA synthesis	38
3. Protein analysis and enzyme activity	39
4. Analysis of transcript levels.....	41
5. Retroviral SECIS reporter construct synthesis and analysis of reporter signal	41
6. Statistical analysis	43
C. Results.....	43
1. Treatment of chronic myelogenous leukemia cell lines with imatinib increases antioxidant enzymes	43
a. Subcloning KU812 and determining a cytostatic imatinib dose... 43	
b. Imatinib treatment increases glutathione peroxidase 1 protein and enzyme levels.....	44
c. The increase in glutathione peroxidase 1 protein levels is not from altered transcript levels or protein decay	45
d. Imatinib also increases glutathione peroxidase 1 in the chronic myelogenous leukemia cell line MEG-01.....	45

TABLE OF CONTENTS (continued)

<u>CHAPTER</u>	<u>PAGE</u>
<ul style="list-style-type: none"> <ul style="list-style-type: none"> <ul style="list-style-type: none"> e. Imatinib treatment does not increase glutathione peroxidase 1 in non-Bcr-Abl-expressing cell lines 46 f. Ectopic Bcr-Abl expression in LNCaP decreases glutathione peroxidase 1 levels 46 g. Imatinib treatment increases antioxidant proteins in addition to glutathione peroxidase 1 47 2. Rapamycin and mTOR inhibition regulates selenoprotein levels 57 <ul style="list-style-type: none"> a. Selenoprotein levels are increased by inhibition of mTOR 57 b. UGA readthrough by the SECIS is not enhanced by rapamycin treatment 58 3. Inhibition of PI3K decreases glutathione peroxidase activity 64 D. Discussion 66 <ul style="list-style-type: none"> 1. Inhibition of Bcr-Abl by imatinib increases protein and activity levels of multiple antioxidant proteins 66 <ul style="list-style-type: none"> a. Steady-state mRNA levels of glutathione peroxidase 1 and manganese superoxide dismutase are not altered by Bcr-Abl inhibition 67 b. Inhibition of Bcr-Abl by imatinib increases antioxidant protein levels post-transcriptionally 68 c. Increased glutathione peroxidase 1 levels are not a result of decreased rates of protein decay 71 d. Evidence that post-translational modifications also affect glutathione peroxidase 1 and manganese superoxide dismutase activity 71 e. Increased antioxidant protein levels following imatinib treatment are Bcr-Abl dependent 72 2. Inhibition of mTOR by rapamycin increases the protein levels of specific selenoproteins 74 <ul style="list-style-type: none"> a. Increased selenoprotein levels following mTOR inhibition are independent of Bcr-Abl 74 b. Increased glutathione peroxidase 1 levels by inhibition of mTOR may be independent of PI3K regulation. 75 c. Increased glutathione peroxidase 1 levels following inhibition of mTOR are not dependent on the selenocysteine insertion sequence element for UGA recoding 77 d. Mammalian target of rapamycin may alter levels of glutathione peroxidase 1 and other selenoproteins by altering translation initiation or elongation 78 	
IV. CONCLUSIONS AND FUTURE DIRECTIONS.....	80
APPENDICES	85
APPENDIX A.....	85

TABLE OF CONTENTS (continued)

<u>CHAPTER</u>	<u>PAGE</u>
APPENDIX B	95
APPENDIX C	97
APPENDIX D	104
CITED LITERATURE	108
VITA.....	141

LIST OF TABLES

<u>TABLE</u>	<u>PAGE</u>
TABLE I. PATIENT INFORMATION AND DEGREE OF CHANGE IN GPX ACTIVITY FOLLOWING IMATINIB TREATMENT	33
TABLE II. BAND INTENSITY AS DETERMINED BY DENSITOMETRY INDICATING THE EFFECT OF IMATINIB TREATMENT OF KU812A ON SELECTED ANTIOXIDANT PROTEINS	85
TABLE III. BAND INTENSITY AS DETERMINED BY DENSITOMETRY INDICATING THE EFFECT OF CYCLOHEXIMIDE \pm IMATINIB TREATMENT OF KU812A PROTEIN DECAY RATE OF GPX1	86
TABLE IV. BAND INTENSITY AS DETERMINED BY DENSITOMETRY INDICATING THE EFFECT OF IMATINIB TREATMENT OF MEG-01 ON SELECTED ANTIOXIDANT PROTEINS	87
TABLE V. BAND INTENSITY AS DETERMINED BY DENSITOMETRY INDICATING THE EFFECT OF IMATINIB TREATMENT OF GM10832 ON SELECTED ANTIOXIDANT PROTEINS	88
TABLE VI. BAND INTENSITY AS DETERMINED BY DENSITOMETRY INDICATING THE EFFECT OF IMATINIB TREATMENT OF LNCAP ON SELECTED ANTIOXIDANT PROTEINS	89
TABLE VII. BAND INTENSITY AS DETERMINED BY DENSITOMETRY INDICATING THE TRANSFECTION OF BCR-ABL INTO LNCAP ON GPX1	90
TABLE VIII. BAND INTENSITY AS DETERMINED BY DENSITOMETRY INDICATING THE EFFECT OF RAPAMYCIN TREATMENT OF KU812A ON SELECTED ANTIOXIDANT PROTEINS	91
TABLE IX. BAND INTENSITY AS DETERMINED BY DENSITOMETRY INDICATING THE EFFECT OF RAPAMYCIN TREATMENT OF MEG-01 ON SELECTED ANTIOXIDANT PROTEINS	92
TABLE X. BAND INTENSITY AS DETERMINED BY DENSITOMETRY INDICATING THE EFFECT OF RAPAMYCIN TREATMENT OF GM10832 ON SELECTED ANTIOXIDANT PROTEINS	93
TABLE XI. BAND INTENSITY AS DETERMINED BY DENSITOMETRY INDICATING THE EFFECT OF RAPAMYCIN TREATMENT OF LNCAP ON SELECTED ANTIOXIDANT PROTEINS	94

LIST OF FIGURES

<u>FIGURE</u>	<u>PAGE</u>
Figure 1. Reproducibility of the GPx enzyme assay.....	31
Figure 2. GPx activity in MNC extracts derived from patients before and after imatinib therapy.	33
Figure 3. No difference in growth between parental and clonal KU812 cell lines following imatinib treatment.	48
Figure 4. GPx1 protein and activity levels are enhanced by 7-day treatment of KU812a CML cells with 150 nM imatinib.	49
Figure 5. GPx1 protein and activity levels are enhanced in a dose- and time-dependent manner following imatinib treatment of KU812a cells.	50
Figure 6. Increases in GPx1 protein are not a result of increased steady-state transcript levels or increased protein decay rates.	51
Figure 7. GPx1 protein and activity levels are increased in MEG-01 following 300 nM imatinib treatment.	52
Figure 8. GPx1 protein and activity levels are unaffected by imatinib treatment of LNCaP and GM10832 cells.....	53
Figure 9. GPx1 protein and activity levels are decreased by exogenous Bcr-Abl in LNCaP...	54
Figure 10. Imatinib increases MnSOD protein and activity levels and TrxR1 protein levels following treatment with imatinib in CML cell lines.	55
Figure 11. Imatinib does not affect catalase or GPx4 protein levels in KU812a or MEG-01 cell lines.....	56
Figure 12. Imatinib does not affect catalase, GPx4 or TrxR1 protein levels in GM10832 or LNCaP cell lines.	56
Figure 13. Overexpression of Bcr-Abl in LNCaP does not result in decreased expression of MnSOD and TrxR1 protein levels.	57
Figure 14. Rapamycin enhances GPx protein and enzyme activity levels in KU812a and MEG-01.	59
Figure 15. Rapamycin treatment did not affect mRNA transcript levels for GPx1 and MnSOD following rapamycin treatment in KU812a.	60

LIST OF FIGURES (continued)

<u>FIGURE</u>	<u>PAGE</u>
Figure 16. Rapamycin treatment in non-CML cell lines significantly increases GPx1 protein and activity levels.	61
Figure 17. Rapamycin increases levels of GPx4 and TrxR1 protein levels in cell lines.	62
Figure 18. MnSOD protein and activity levels are not increased following rapamycin treatment.	63
Figure 19. The translational efficiency of UGA readthrough by the GPx1 SECIS is not enhanced by rapamycin treatment.	64
Figure 20. Treatment of KU812a by 20 μ M LY294002 for 4 days inhibits PI3K phosphorylation activity and decreases GPx activity levels.	65
Figure 21. Proposed signaling cascade for the regulation of GPx1 transcription and translation.	82

LIST OF ABBREVIATIONS

4EBP1	Eukaryotic translation initiation factor 4E-binding protein 1
ADP	Adenosine diphosphate
AP-1	Activator protein-1
ATP	Adenosine triphosphate
Bax	Bcl-2-associated X protein
Bcl-2	B-cell lymphoma-2 protein
Bcr	Breakpoint cluster region
CD95	Cluster of differentiation 95
Cdk	Cyclin-dependent kinase
CHO	Chinese hamster ovary
CML	Chronic myelogenous leukemia
Ct	Cycle threshold
Cys	Cysteine
DM	Diabetes mellitus
dNTP	Deoxyribonucleotide triphosphates
ECL	Enhanced chemiluminescence
eIF	Eukaryotic initiation factor
EJC	Exon-junction complex
Erk	Extracellular signal-regulated kinase
FAD	Flavin adenine dinucleotide
FBS	Fetal bovine serum

LIST OF ABBREVIATIONS (continued)

GFP	Green fluorescence protein
GPx	Glutathione peroxidase
GSH	Glutathione
GS	Glutathione anion
GSSG	Glutathione disulfide
hOGG1	Human 8-oxoguanine DNA N-glycosylase 1
JAK-STAT	Janus kinase signal transducer and activator of transcription
kDa	Kilodalton
LD ₅₀	Lethal dose 50%
Leu	Leucine
MAPK	Mitogen-activated protein kinase
Mn	Manganese
MNC	Mononuclear cell
MnSOD	Manganese superoxide dismutase
mTOR	Mammalian target of rapamycin
mTORC	mTOR complex
NADPH/NAD ⁺	Nicotinamide adenine dinucleotide phosphate
NF-κB	Nuclear factor κB
NQO2	NADPH-quinone oxidoreductase
ORE	Oxygen response element
p70S6K	p70S6 kinase
PBS	Phosphate-buffered saline

LIST OF ABBREVIATIONS (continued)

PCR	Polymerase chain reaction
PDGFR	Platelet-derived growth factor receptor
PI3K	Phosphatidylinositol 3 kinase
PMSF	Phenylmethanesulfonylfluoride
pS6	Phospho S6 ribosomal protein
Pro	Proline
PVDF	Polyvinylidene fluoride
RHEB	Ras homolog enriched in brain protein
ROS	Reactive oxygen species
RT-qPCR	Reverse transcription quantitative PCR
SBP2	SECIS-binding protein 2
S.D.	Standard deviation
Se	Selenium
Sec	Selenocysteine
SECIS	Selenocysteine insertion sequence
Ser	Serine
SFCA	Surfactant-free cellulose acetate
SOD	Superoxide dismutase
TAE	Tris-acetic acid-EDTA
TBP	TATA-binding protein
TE	Tris-EDTA
TGR	Thioredoxin glutaredoxin reductase

LIST OF ABBREVIATIONS (continued)

TOR	Target of rapamycin
tRNA	Transfer RNA
Trx	Thioredoxin
TrxR	Thioredoxin reductase
UTR	Untranslated region

SUMMARY

A study was conducted exploring the post-transcriptional regulation of four antioxidant enzymes: glutathione peroxidase 1 (GPx1), manganese superoxide dismutase (MnSOD), glutathione peroxidase 4 (GPx4), and thioredoxin reductase 1 (TrxR1). Glutathione peroxidase activity was analyzed in clinical samples from imatinib-treated patients with chronic myelogenous leukemia (CML), which is characterized by the presence of Bcr-Abl. Studies were also conducted in the following human cell lines: KU812 and MEG-01 (CML), LNCaP (prostate cancer), and GM10832 (immortal B lymphocyte). Breakpoint Cluster Region-Abelson (Bcr-Abl) and Mammalian Target of Rapamycin (mTOR) were pharmacologically inhibited because their expression was expected to inhibit the protein levels of the selected antioxidants. Levels of antioxidant protein and activity were measured in cell lines treated with imatinib or rapamycin, the latter of which inhibits mTOR.

Glutathione peroxidase activity was found to increase in 4 of 7 CML patient sample sets, which was recapitulated in the two CML cell lines utilized for this study, in which MnSOD and TrxR1 were also increased in response to imatinib treatment. The increase of these three antioxidant proteins occurred only in CML cell lines. The ectopic expression of Bcr-Abl in the prostate cancer cell line LNCaP significantly decreased GPx1 protein; however, MnSOD and TrxR1 were unaltered. This indicates that GPx1 is potentially inhibited by Bcr-Abl, while MnSOD and TrxR1 could be increased in response to the intracellular effects of imatinib. In imatinib-treated CML cells, GPx1 and MnSOD activity levels increased only marginally in comparison to protein levels. This indicates that GPx1 and MnSOD may be post-translationally modified and that their activity is regulated independently of the post-transcriptional regulation that increased protein levels.

SUMMARY (continued)

Treatment of both CML and non-CML cell lines with rapamycin, which inhibits mTOR, significantly increased protein levels for GPx1, GPx4, and TrxR1, suggesting that the post-transcriptional regulation of these proteins is dependent on the control of translation by mTOR and its downstream targets. These are all members of the selenoprotein family, the translation of which is dependent on the recoding of the selenocysteine codon by a selenocysteine insertion sequence (SECIS) found in the 3'-UTR of selenoprotein mRNA. The increase in these antioxidant proteins by mTOR inhibition illustrates a potential route by which selenoprotein translation may be regulated independent of selenium availability. Analysis of the effect of mTOR inhibition on a reporter construct dependent on the GPx1 SECIS element for expression did not reveal a difference in activity in the presence of rapamycin. This suggests that the mTOR-dependent translation of GPx1, GPx4, and TrxR1 may be via translation initiation and/or polypeptide chain elongation.

I. INTRODUCTION

A. Generation of reactive oxygen species

Historically, reactive oxygen species (ROS) such as superoxide and hydrogen peroxide (H_2O_2) were considered to be harmful to the cell and were culprits in DNA mutagenesis, cancer onset, aging, and cellular senescence [1]. Recent research has shown that while these molecules and their products can be harmful to the cell, they can also play a vital role in cellular homeostasis and signal transduction [2]. The presence of these radicals is also physiologically vital for immune function via inflammation and in signal transduction and cell cycle regulation [3,4]. Multiple antioxidant enzymes have evolved to aid in the maintenance of the balance of free radicals, and it is only when this balance is disrupted that ROS become harmful.

1. Superoxide is generated primarily by cellular metabolism

There are multiple intracellular sources of ROS that partition into different subcellular organelles. For example, the mitochondria produce the majority of the cellular superoxide as a by-product of the electron transport chain-driven production of adenosine triphosphate (ATP) [5-7]. The process of ATP production utilizes oxygen and electron transfer to drive the oxidative phosphorylation of adenosine diphosphate (ADP) to form ATP, a primary energy source of the cell [6,8]. Of the four protein complexes involved in this process, complexes I and III leak electrons to molecular oxygen, producing superoxide. The presence of an unpaired electron on this molecule makes it highly reactive, and in the absence of the mitochondrial superoxide dismutase (SOD) enzyme, damage can occur to mitochondrial DNA or membranes [2]. Superoxide produced in the mitochondrial intermembrane space can also be actively transported across the outer membrane to the cytosol via voltage-dependent ion channels

[9]. The presence of SODs can quickly dismutate exported superoxide and maintain the superoxide at its site of production.

2. Superoxide dismutase enzymes protect against superoxide-induced cell damage

The SOD antioxidant enzyme family consists of three distinct proteins, each containing a transition metal at their active site, and their primary function is to dismutate superoxide to H_2O_2 , which is more stable and less reactive than superoxide [2,10]. The mitochondrial SOD is encoded by the *SOD2* gene, and the constitutive homotetrameric protein contains manganese (Mn) at its active site, which must be inserted for maturation of the protein [11-14]. Manganese is inserted at the active site of manganese superoxide dismutase (MnSOD) following translocation of the immature protein into the mitochondrial matrix. Superoxide produced by the electron transport chain is dismutated by the now-mature protein via an alternating reduction and re-oxidation of the Mn at the active site [12,14-17].

Manganese SOD is an essential protein, as has been demonstrated in transgenic mice with a targeted deletion of *SOD2* [18,19]. Transgenic deletion of *SOD2* in mice is not embryonic lethal, but newborn pups are affected by cardiomyopathies, metabolic acidosis, and neurodegeneration, which are lethal within 10-21 days of parturition. The overexpression of the cytosolic isoform of SOD had been hypothesized to overcome the deletion of MnSOD; however, there is no difference in phenotype between MnSOD-null mice and MnSOD-null mice that overexpress the cytosolic SOD [20]. Decreased MnSOD levels have been associated with the onset of renal disorders, and the targeted deletion of MnSOD in mice induces mild renal damage with kidney-specific increases in superoxide [21]. Additionally, autophagy and mitochondrial biogenesis appear to be inhibited in the absence of MnSOD expression, which results in severe

alterations in mitochondrial morphology and dysfunction [22,23]. Cell growth and proliferation are also regulated by MnSOD expression and activity. Overexpression of MnSOD in NIH3T3 mouse embryo fibroblasts and in multiple cancer lines inhibits cell growth and alters cell cycle progression [24-26]. The inhibition of cellular proliferation by MnSOD *in vitro* is further supported by ablation of MnSOD via RNA interference in vascular smooth muscle cells, which increases migratory and proliferative capacity as assessed through wound-healing and proliferation assays [27]. The activity of MnSOD in cell cycle progression decreases as the cell moves from G1 to S to G2, indicating that active MnSOD may inhibit cell proliferation [28]. This decrease in activity was correlated with alterations in post-translational modifications of MnSOD, such as the addition of a methyl-group. Additional post-translational modifications such as acetylation and phosphorylation have also been proposed, where phosphorylation may be dependent on cyclin-dependent kinase 1 (Cdk1)/cyclin B1 activity and activates MnSOD, whereas acetylation is inhibitory and activity is dependent on deacetylation by Sirtuin protein 3 (Sirt3) [29-31].

The inhibition of proliferation by MnSOD indicates that this antioxidant protein may be inhibitory in developing cancer. For example, the expression of MnSOD is decreased in tumor tissues as compared to adjacent cancer-free tissue in at least breast and lung cancers [10,32,33]. However, it also appears that MnSOD levels are increased during cancer progression, as multiple studies have indicated high levels of MnSOD are associated with poorer outcome [10]. Expression of MnSOD in a skin cancer model of mice was inhibited early in carcinogenesis, but expression increased as the tumor progressed [34]. For example, maintained expression of MnSOD in tumors was associated with poor survival in lung cancer; in lung cancer cells, overexpression of MnSOD promoted tumor invasion and anchorage-independent growth *in vivo*

[35]. Thus, the overall impact of MnSOD in cancer initiation and progression is not entirely clear, as multiple studies have shown decreases in MnSOD in cancer tissue, but others have demonstrated an increase in expression concurrent with poorer outcome.

The export of superoxide from the mitochondria, as well as the production of superoxide by cytosolic proteins such as nicotinamide adenine dinucleotide phosphate (NADPH) oxidase and xanthine oxidoreductase, necessitates the presence of additional SODs outside of the mitochondria. There are two non-mitochondrial SODs: cytosolic SOD (Cu/ZnSOD) and extracellular SOD (ecSOD), both of which contain copper and zinc at their active sites [36-41]. Extracellular SOD is synthesized and secreted by cells in organs where there is a high potential for ROS production, such as the lungs, pancreas, heart, kidneys, liver and skeletal muscle [42-45]. Mice with deletions of either of these SODs are found to have normal phenotypes, except when challenged with a hyperoxic environment [46-51].

3. Hydrogen peroxide is produced in multiple cellular compartments

The production of superoxide within the mitochondria is a by-product of cellular respiration, and is potentially detrimental to the cell. However, the production of superoxide in the cytosol is necessary in order to produce H_2O_2 , an essential component of multiple cellular functions, such as signal transduction, gene transcription and host defense against invading pathogens [2]. The presence of multiple SODs catalyzes the rapid dismutation of superoxide to H_2O_2 . Xanthine oxidoreductase and NADPH oxidase are two of the cytosolic components responsible for the production of H_2O_2 via superoxide synthesis [52,53]. H_2O_2 is also readily produced at the peroxisomes, which are the main site of β -oxidation of fatty acids, the dismutation of cytosolic superoxide, and enzymatic reactions of flavin oxidase [54].

Regardless of its site of production, H_2O_2 must move throughout the cell as a component of signal transduction or outside of the cell for immune defense. Hydrogen peroxide appears to be freely diffusible across both mitochondrial membranes, but in other less permissive lipid bilayers (such as the peroxisomes or the cell membrane), the movement of H_2O_2 across the membrane is dependent upon aquaporins [55-58]. Once within the cytosol or the appropriate subcellular organelle, H_2O_2 is able to interact with its signaling partners or is reduced to water by either catalase or one of the glutathione peroxidases (GPx) [59].

4. Hydrogen peroxide is a vital component in pathogen defense and in signal transduction

Hydrogen peroxide is a component in multiple cellular processes. One is the defense against invading pathogens by an oxidative burst [52]. One primary cytosolic source of H_2O_2 and superoxide for the oxidative burst is NADPH oxidase, and H_2O_2 and superoxide are produced by neutrophils and monocytes at sites of inflammation and infection. This high level of total ROS production for host protection can be both beneficial and harmful, as long-term exposure to ROS can lead to chronic inflammation, potentially resulting in irreversible tissue damage [60-62]. While the oxidative burst serves as host protection, ROS also participate in more finely controlled signal transduction and gene transcription, generally resulting in increased proliferation and survival.

Transcription factors, kinases and phosphatases are the primary targets of ROS-induced signal transduction. Hydrogen peroxide has been found to interact with many of these proteins through the oxidation of amino acid residues, such as cysteine, and by the formation of disulfide bonds [63,64]. Activity of H_2O_2 -modified proteins is modulated by thiol-oxidation of redox-sensitive cysteine residues known as s-glutathionylation, which changes protein structure, DNA

binding capabilities, and the ability to bind protein partners [63-66]. Protein tyrosine phosphatases are inactivated in the presence of H_2O_2 in a completely reversible manner by modification of a cysteine, while ataxia telangiectasia mutated (ATM) is activated by the H_2O_2 -induced formation of disulfide bonds [63,64]. These modifications appear to result in a pro-proliferative and anti-apoptotic signal, which can lead to altered cell profiles and affect disease onset, such as in cancer. The proliferative effects of H_2O_2 are only observed at low levels, typically less than 10 μM exogenously [67-72]. Doses above this are considered supraphysiologic and result in the induction of oxidative stress and an apoptotic response within cells. This suggests that H_2O_2 has a biphasic effect within the cell, where low levels are proliferative, but higher levels are apoptotic, inducing the extracellular signal-regulated kinase (Erk) and p38 apoptotic pathways [70]. The addition of the antioxidant catalase *in vitro*, either by ectopic expression of the gene or through exogenous exposure in tissue culture media, resulted in inhibition of proliferation and cell survival in response to H_2O_2 signaling, demonstrating the cellular interplay between oxidants and antioxidants [73,74].

5. Excess reactive oxygen species levels can be detrimental to cell function and DNA fidelity

While H_2O_2 production has many benefits in cellular growth and signal transduction, excess levels can be harmful to the health of the cell, and the excess levels of H_2O_2 often result in the induction of apoptosis or necrosis. An increase in total ROS production can lead to an overabundance of H_2O_2 and other ROS molecules, such as superoxide and the hydroxyl radical. ROS overproduction can result from overstimulation of NADPH oxidase or xanthine oxidase; however, the electron transport chain is responsible for the majority of excess ROS production [8,75-77]. High levels of superoxide are produced by the electron transport

chain when there is an alteration in the proton gradient, which under normal conditions flows from the intermembrane space into the matrix, and is altered if the availability of ADP for conversion to ATP is low. A build-up of protons in the intermembrane space causes the components to be in a continuous reduced state, resulting in greater superoxide leakage from the transport pathway and damage to the mitochondria, which ultimately can damage the cell [8].

Cellular damage also can occur from exposure to exogenous ROS. Environmental sources of ROS, such as ionizing radiation, cigarette smoke and toxin exposure, also contribute to unmanageable ROS levels within the cell, and can have negative consequences on cell survival [78-80]. ROS within the cell can attack lipid membranes, protein and DNA. Oxidation of lipid membranes can lead to membrane breakdown and leakage of harmful materials through the affected membrane. Additionally, the damage can be propagated along the membrane, as the oxidized lipid reacts with neighboring lipid particles. Proteins are also negatively regulated by H_2O_2 , resulting in a cleavage of the peptide chain or oxidation of amino acids, which affects protein function or stability. DNA can be modified by ROS indirectly (as a result of peroxidation of nearby proteins or lipids) or directly (by inducing base modifications).

B. Multiple antioxidant proteins regulate hydrogen peroxide levels

Excess superoxide must be managed by MnSOD or its cytosolic counterpart; in the absence of adequate SOD levels, superoxide can damage the mitochondria or other components within the cell [2]. Where SOD levels are able to maintain the dismutation of superoxide, excess H_2O_2 levels can lead to induction of apoptosis, altered signal transduction, and gene transcription or prolonged inflammation [67-72]. The maintenance of H_2O_2 levels is dependent on multiple antioxidant enzymes, including catalase, the thioredoxin system, and the GPx family.

1. Catalase reduces hydrogen peroxide under oxidative stress

Hydrogen peroxide is reduced to water and molecular oxygen in order to control the levels of H_2O_2 within the cell. Because H_2O_2 is found in multiple cellular compartments, several enzymes have evolved to manage its levels, such as the cytosolic and peroxisomal antioxidant enzyme catalase [81-83]. As with the SODs, a metal ion is found at the active site of the enzyme; in this instance, catalase contains heme [84]. The catalytic heme ion of the active site is located deep within a small hydrophobic channel, effectively limiting access to only hydroperoxides. The reductive capability of heme is maintained by the cycling of the heme ion from a reduced to oxidized and back to a reduced state. While catalase is maintained at a basal level, it is primarily induced in response to hyperoxic conditions and by the presence of pro-oxidants, including exogenous sources of ROS [85,86]. Deletion of catalase in transgenic C57BL/6 mice delayed the rate of H_2O_2 decomposition, but no overt changes in phenotype were demonstrated in comparison to wild-type mice [87]. There was no increase in susceptibility to lung injury as assessed for the whole organ in these same catalase-deficient mice following 72-hour exposure to hyperoxic conditions. However, the damage incurred in these mice may not have been detectable at the whole organ level, as wild-type BALB/c mice exposed to hyperoxia for 24 hours showed histological evidence of lung damage [86].

The induction of catalase in response to a pro-oxidant environment is not immediate, and is dependent upon prolonged exposure to hyperoxia, further demonstrating the necessity of catalase in oxidative stress conditions. BALB/c mice exposed to hyperoxic conditions for 12-48 hours did not demonstrate a marked increase in catalase enzyme levels until after 48-hours of exposure [86]. Exposure of tracheobronchial epithelial cells to exogenous, nontoxic levels of H_2O_2 resulted in a 3-fold increase in mRNA levels following an 18-hour exposure period [85].

Catalase deficiency, while not lethal, does lead to systemic disorders, particularly diabetes. Prolonged exposure to pharmacologically induced oxidative stress in catalase-deficient male mice resulted in the onset of a diabetic phenotype [88]. This association was also seen in humans with a rare congenital disorder, acatalasia, which results in a near-complete lack of catalase [89]. Analysis of familial groups afflicted with acatalasia has shown an increased frequency of diabetes in the affected population as compared to the general population [90].

2. Thioredoxin and thioredoxin reductase maintain antioxidant reductive capacity

Much of the maintenance of H_2O_2 levels within the cell is dependent on Thioredoxin (Trx), which is a substrate for the reduction of hydroperoxides [91]. The dithiol/disulfide active site of Trx cycles between oxidized and reduced states. The maintenance of multiple antioxidant enzyme functions, such as peroxiredoxin, is dependent on the availability of reduced Trx to act as an electron donor [92]. In order to maintain Trx in a reduced state, the thioredoxin reductase family of proteins reduces the cysteine dithiol at the active site of Trx [93,94]. The active site of TrxRs is unique, in that while the antioxidant SODs and catalase utilize a transition metal at their active sites, TrxRs are dependent upon the selenium-containing selenocysteine for their activity.

3. Thioredoxin reductase is an antioxidant selenoprotein

The TrxRs belong to a group of proteins known as selenoproteins, which are defined by the presence of a co-translationally inserted selenocysteine (Sec), a selenium-containing homolog of cysteine, at their active site [95,96]. The selenium at the active site is utilized as an antioxidant in a similar manner to the sulfur in cysteines, where the selenium is

converted between the reduced selenenylsulfide and the oxidized selenothiol forms for activity [93,97].

The structure and function of each of the isoforms of the thioredoxin reductase (TrxR) protein family are similar. All TrxR family members are homodimers arranged in a head-to-tail conformation, where both members of the dimer depend on the presence of the reactive Sec [93,98,99]. The reduced form of TrxR is made by a series of reductions, beginning with NADPH reducing a flavin adenine dinucleotide (FAD) bound to one of the TrxR subunits, which ultimately results in the formation of a selenothiol between the two subunits [93]. With the formation of the selenothiol, the protein is able to reduce other TrxRs, or react with Trx to reduce the disulfide at the active site. Because the Trx system is dependent upon TrxR to maintain its redox state, it is dependent on the selenium (Se) status of the cell [100,101]. Decreases in Se availability affect the expression and activity of TrxR, which can cascade to affect peroxiredoxin and other Trx-dependent antioxidant turnover, as well as the turnover of other small molecule antioxidants like Vitamin C [102]. It is also possible that the TrxR family is involved in the maintenance of the availability of Se, as it has been shown that at least TrxR1 and possibly TrxR2 are able to convert selenite to selenide, the form of Se necessary for Sec synthesis [103,104].

The main antioxidant function for all TrxR proteins is the same: to maintain Trx in a reduced state. Where the three isoforms differ is in their localization and their overall importance to survival. TrxR1 and TrxR2 are differentially located within the cell, with TrxR1 localized primarily in the cytosol and TrxR2 primarily in the mitochondria, although some spliceoforms have been detected in the cytosol [105,106]. Deletion of either TrxR1 or TrxR2 is embryonic lethal at the midpoint of pregnancy in mice, indicating that these proteins are essential

for viability [107,108]. The third TrxR, known as thioredoxin glutathione reductase (TGR), is unique, in that it has the properties of a glutathione reductase and a thioredoxin reductase. The amino-terminal of the protein contains a glutaredoxin domain, while the carboxyl-terminal has the canonical TrxR motif [109,110]. In mammals, TGR is found in elongating spermatids at the mitochondrial sheath, but is not detected in mature sperm, indicating that it may have a role in maturation and development of sperm [111]. Additionally, the primary intracellular effects of TGR enzyme activity are in the formation of disulfide bonds via the glutaredoxin domain.

4. Thioredoxin reductase 1 has more than antioxidant properties

In addition to its antioxidant properties, TrxR1 is necessary for growth and survival, where it is involved in multiple cellular functions, including the prevention of apoptosis, cellular proliferation, and DNA repair and synthesis [112]. Its direct involvement in multiple cellular pathways demonstrates its importance in cell growth and survival, and indicates that alterations in its expression and activity can be detrimental to health. Indeed, TrxR1 is increased in oral cancer tissue as compared to normal tissue, and its expression is associated with poor prognosis in breast and tongue cancers [113-115]. Inhibition of TrxR1 inhibits growth of different tumor cell lines and increases cellular sensitivity to anticancer treatments; in xenografted mice, decreased TrxR1 limited invasive potential of the cells and tumor growth [116-119]. Increased levels of TrxR1 could create a permissive environment for progression of disease states, by inducing antioxidative stress and providing antioxidant protection against therapeutics that are effective by increased oxidative stress.

C. The glutathione peroxidase family: antioxidant selenoproteins

1. Glutathione peroxidase activity is dependent on the antioxidant substrate glutathione

Another important family of antioxidant enzymes is the GPx family. Made up of both selenoprotein and non-selenoprotein members, these antioxidants have important roles in cell signaling, growth and survival, as well as being the primary reducers of hydroperoxides and lipid peroxides. The GPx family is dependent on the presence of the small antioxidant molecule glutathione (GSH) as its substrate for catalysis of peroxide reduction [120]. GSH is a small tripeptide antioxidant molecule which is readily synthesized by the cell when necessary. In addition to its role as a substrate for antioxidant proteins, GSH protects cells by detoxifying against drugs and other toxins, is a component in signal transduction (such as nuclear factor [NF]- κ B activation and mitogen-activated protein kinase [MAPK] phosphorylation), and can act as a pro-oxidant [121]. It is a ubiquitous molecule, found in high intracellular concentrations ranging from 1 to 10 mM [36]. The antioxidant properties of GSH against ROS occur via enzymatic interactions with several different cofactors, such as the GPx family, or by a non-enzymatic oxidation at the active site of the thiol group on cysteine [122,123]. GPx enzymes utilize GSH to convert H_2O_2 to water and molecular oxygen, which oxidizes GSH to glutathione disulfide (GSSG) [121]. The non-enzymatic oxidation of GSH via ROS can lead to the production of a thiyl radical and create a volatile compound of GSH; however, interaction between two glutathione anion (GS) radicals also forms GSSG. The levels of GSH are maintained by the subsequent reduction of GSSG back to two GSH molecules by glutathione reductase [121]. In instances of extreme oxidative stress, where GSSG levels overwhelm glutathione reductase, or where glutathione reductase is otherwise impaired, multiple membrane-

associated proteins export GSSG out of the cell [124]. Maintenance of GSH levels is critical to sustaining adequate GPx activity levels, especially in circumstances where ROS levels are high.

2. Glutathione peroxidase enzymes detoxify hydrogen peroxide and lipid peroxides

The antioxidant GPx family consists of five Sec-containing members and three non-Sec-containing members [125,126]. These antioxidant enzymes detoxify H₂O₂ and lipid peroxides via the oxidation of GSH and are found within multiple cellular compartments as well as in plasma. As with the active site of TrxR1, the active site of the selenoprotein portion of the GPx family contains Sec, which is conserved across the five different GPx selenoprotein isoforms [127]. The mechanism of peroxide reduction appears to be the same for all of the isoforms, a multistep Ping-Pong type mechanism, oxidizing GSH as a substrate to catalyze the reaction [5,7]. The selenol group of the Sec is oxidized to selenenic acid following interaction with peroxides, which is subsequently reduced by GSH to a glutathiolated selenol intermediate. To return the active site back to its reduced state, an additional GSH molecule is oxidized, converting the glutathiolated selenol to a selenol.

3. Glutathione peroxidase selenoprotein expression is dependent on selenium status

All members of the GPx family are responsive to Se status. However, there is a hierarchy within which different selenoproteins are preferentially translated, where GPx1 and GPx3 levels and translation are most sensitive to Se deficiency [128,129]. The translation of GPx4 and GPx2 is less affected by Se deficiency; in some cases, GPx2 expression is increased during deficiency [130,131]. The mechanism by which this differential regulation occurs is unclear, but at least for GPx1, it has been shown that its mRNA is less stable during deficiency,

when the transcript is susceptible to nonsense-mediated decay [132,133]. Additionally, the translation of selenoproteins is dependent on the binding of the multiple accessory proteins to the selenocysteine insertion sequence (SECIS), a stem-loop structure in the 3'-UTR of selenoprotein mRNA, which is necessary for recoding the selenocysteine UGA codon [134]. One of these proteins, SECIS-binding protein 2 (SBP2), binds the base of the SECIS stem-loop structure, and its binding site there can be blocked by eukaryotic initiation factor (eIF)4a3, which appears to only bind those selenoproteins most susceptible to inhibition during Se deficiency [135-138]. In Se-adequate conditions, eIF4a3 does not bind the SECIS, allowing for access of SBP2 at the base of the stem-loop structure in the SECIS element. This mechanism reveals a way by which a cell maintains the expression of its most vital selenoproteins while allowing less important proteins to decrease in expression. This demonstrates the redundancy that the antioxidant system has in protecting from ROS, as the loss of multiple antioxidant selenoproteins is not catastrophic to the cell.

4. The glutathione peroxidase selenoprotein family members

The GPx family members have similar structure and function, with the exception of GPx4. They are all homotetrameric proteins, with subunit molecular weights of approximately 23 kilodaltons (kDa); however, GPx4, the phospholipid hydroperoxide GPx, is monomeric, but with a similar molecular weight [139-143]. GPx1 and GPx4 are both ubiquitous selenoproteins, whereas GPx6 and GPx2 are only found within certain organs. GPx6 has only been found within the olfactory epithelium, and very little is known or has been characterized about this selenoprotein [125]. GPx3 is found in the plasma as a secreted antioxidant protein following synthesis within the proximal tubule of the kidney [144]. In cancer, GPx3 is found to have decreased expression compared to normal tissue, potentially as a result of hypermethylation

of the gene [145-148]. GPx2 is a cytosolic GPx found primarily in the epithelial cells of the gastrointestinal tract, including in the esophagus, but has also been detected in the liver [149]. Inflammation and pathogens are common in the gastrointestinal tract, and it is possible that GPx2 has a primary role in protecting against damage as a result of inflammation and pathogenic attack [150-152]. GPx2 is a potential factor in the onset of pre-cancerous lesions such as Barrett's esophagus or in colorectal adenoma, where GPx2 expression is associated with increased cellular proliferation [153-155]. Increased expression has also been detected in lungs exposed to cigarette smoke [156,157]. Initiation of a malignant phenotype of these pre-cancerous lesions decreases GPx2 expression [158].

5. The antioxidant glutathione peroxidase 4 regulates fertility, cell viability, and inflammation

The reduction of phospholipid hydroperoxides is targeted by GPx4, which is the only member of the GPx family that targets this substrate [159,160]. Thus, it is primarily found at lipid membranes, with three isoforms localizing to the mitochondria, nucleus, or cytosol [161]. The three isoforms are transcribed from the same gene, but with alternative promoter regions and start sites. GPx4 is found in most tissues and is an essential protein, as it is the only member of the GPx family where transgenic deletion of GPx4 is embryonic lethal in mice, and pups die mid-gestation [162,163].

In addition to its antioxidant properties, GPx4 also affects male fertility, protects against apoptosis and mediates inflammation. GPx4 is a necessary component in spermatogenesis and in the viability of mature spermatozoa [164]. It is not enzymatically active, but is instead a structural protein within the mitochondrial sheath [164-166]. Mice that are carrying targeted deletions of total GPx4 in spermatocytes are infertile, with a severe decrease in sperm count, and

the targeted deletion of the mitochondrial isoform in spermatocytes confers infertility [165,167]. Overexpression of GPx4 *in vitro* demonstrates that both the nuclear and mitochondrial isoforms of the protein protect against apoptosis by limiting the release of cytochrome c from the mitochondria [168,169]. GPx4 is also involved in the inflammatory process, by inhibiting lipoxygenase activity through the availability of lipid hydroperoxides and thus limiting the production of the inflammatory mediator leukotrienes [170,171]. Therefore, GPx4 has multiple important roles within the cell: as antioxidant, in inflammation and cell death, and as a structural protein in spermatogenesis.

Overall, the antioxidant properties of GPx4 affect inflammation and apoptosis by limiting the availability of phospholipid hydroperoxides or by limiting the ability of cytochrome c to exit the mitochondria; it achieves both of these by protecting against the generation of pro-apoptotic ROS [168]. Both inflammation and apoptosis can have consequences in the onset of disease. Decreased GPx4 expression in a mouse xenograft model resulted in a more highly vascularized tumor than grafts with normal GPx4 expression levels, and the decreased GPx4 levels corresponded with increased lipoxygenase activity, indicating that GPx4 levels affect tumor phenotype and aggressiveness [172]. Indeed, GPx4 levels are found to be negatively correlated with breast cancer tumor grade, where higher-grade tumors have lower GPx4 levels [173]. These data indicate that GPx4 is protective against tumor development, and that the inhibition of GPx4 expression could have negative consequences related to tumor initiation and progression.

6. Cytosolic glutathione peroxidase 1 is a ubiquitous antioxidant protein

The most abundant member of the GPx selenoenzyme family is GPx1. This antioxidant is ubiquitously expressed, and was first described as a selenoprotein in 1973 [174]. While it is predominately a cytosolic protein, GPx1 has also been found localized to the

mitochondria, despite the lack of a mitochondrial-targeting sequence in its amino terminus [175]. The mechanism by which GPx1 enters into the mitochondria is not yet elucidated, but its presence indicates that it may play a role in protecting the mitochondria against high levels of oxidative stress or in the regulation of mitochondrial-dependent cell signaling via H_2O_2 levels [176-178]. Deletion of GPx1 in transgenic mice results in no abnormal phenotype, unless they are challenged with excessive levels of oxidative stress [179]. Treatment of GPx1-null mice with the oxidative stress-inducers paraquat or diquat at levels far below the LD_{50} in wild-type mice is lethal, which indicates that GPx1 is vital in the presence of excessive oxidative stress [180]. In another mouse model with targeted GPx1 deletion, cigarette smoke exposure increased markers of inflammation, which were reversed following exposure to the GPx1 mimic ebselen [181]. Both of these models indicate that, while GPx1 is not essential to normal growth and development, it is essential to survival in the presence of excess levels of ROS [176-178,180,181].

7. Properties of glutathione peroxidase that affect cell growth and proliferation

Glutathione peroxidase 1 has been shown to be involved as a regulator of apoptosis, and has potential as a modulator of protection against DNA damage and decreased proliferative capacity. The first demonstration of GPx1 inhibiting apoptosis was shown *in vitro* utilizing GPx1 overexpression in B-cells deprived of interleukin-3 [182]. It had been hypothesized that the apoptotic inhibitor B-cell lymphoma-2 protein (Bcl-2) prevents apoptosis via an antioxidant pathway, which was demonstrated by the overexpression of GPx1. GPx1 overexpression in a breast cancer cell line was shown to inhibit the cluster of differentiation 95 (CD95)-induced apoptotic response through the inhibition of effector caspase activation and DNA fragmentation [183,184]. Inhibition of GPx1 by GSH depletion resulted in the induction of

apoptosis. The inhibition of apoptosis by GPx1 was upstream of the mitochondrial release of apoptotic factors, as overexpression inhibited the release of cytochrome c and cleavage of caspase-3. In human endothelial cells, the overexpression of GPx1 resulted in a decrease in the pro-apoptotic signaling protein Bcl-2-associated X (Bax) mRNA and protein levels [185]. Analysis of hepatocytes from GPx1-null mice showed an increased susceptibility to ROS-induced apoptosis as compared to hepatocytes from wild-type mice [186].

Glutathione peroxidase 1 has also been implicated as a potential factor in the prevention of DNA damage. The MCF7 breast cancer cell line does not express endogenous GPx1, making it an ideal model system with which to investigate the effects of the presence or absence of GPx1 [187]. Ectopic expression of GPx1 in MCF7 cells treated with UV-radiation decreased the number of micronuclei formed as a result of DNA damage compared to cells which did not express GPx1 [188]. This protection was independent of Se supplementation, which has also been implicated in prevention of DNA damage. Protection against DNA damage is decreased in mice with a targeted deletion of GPx1 and a deficiency in MnSOD [189]. These mice have increased levels of both DNA and protein oxidation, indicating that both GPx1 and MnSOD may be protective against DNA damage.

While GPx1 is shown to potentially inhibit apoptosis and protect against DNA damage, there is evidence that GPx1 may also regulate proliferation. This is demonstrated *in vitro*: T-helper cells with deletion of GPx1 had increased ROS levels and faster proliferation rates than T-helper cells that expressed GPx1 [190]. The overexpression of GPx1 in Chang liver cells attenuates cellular proliferation as determined by [³H]-thymidine incorporation, supporting that GPx1 may inhibit proliferation by decreasing the activation of EGFR [177]. *In vivo*, ventricular mass and rates of cardiac hypertrophy were increased by transgenic deletion of GPx1 and

treatment with angiotensin II, a vasoconstrictor that can induce hypertension [191]. The role of GPx1 in regulating cellular proliferation and protecting against DNA damage may potentially indicate why GPx1 has been found deleted or decreased in multiple cancer types when compared to normal tissue [187,192-195].

8. Glutathione peroxidase is associated with risk or progression of multiple diseases

GPx1 is associated with susceptibility or development of several types of diseases, such as cancer, diabetes and cardiovascular disease. The involvement of GPx1 in these diseases can be attributed to alterations in the management of oxidative stress, such as from environmental factors that increase ROS levels or from functional alterations as a result of single nucleotide polymorphisms (SNPs) [196-198].

a. Glutathione peroxidase is deleted in multiple cancer types

Decreased GPx1 levels have been found in multiple cancer types, with the loss in GPx1 resulting from deletion of its chromosomal region (3p21) and was been detected in cancers of the head and neck, breast, lung and colon [187,192-195]. These deletion studies indicate that GPx1 may be deleted early in cancer; however, the sample sets were generally small (< 100 cancer sets), and the loss of GPx1 may have been a bystander effect to the loss of the DNA repair enzyme human 8-oxoguanine DNA N-glycosylase 1 (hOGG1), which is in the same chromosomal region as GPx1 [188,193-195]. The loss of both GPx1 and hOGG1 may result in an overall increase in DNA damage and could increase cellular proliferation rates.

b. Allelic variations in glutathione peroxidase enzyme activity

Genetic variations in GPx1 may alter its function, such that it could affect disease onset and severity. GPx1 is polymorphic, with approximately 38 polymorphisms, most

of which are not found within the open reading frame but in the 5' and 3' flanking regions [196]. The most well characterized is a C>T alteration in codon 198, which results in a proline to leucine (Pro198Leu) alteration in the polypeptide chain. There is also a trinucleotide repeat near the amino terminus, which modifies the number of alanines present within the polypeptide chain, resulting in the presence of five to seven alanines. The functional consequences of Pro198Leu are not completely understood, but it has been implicated as a risk factor in cancer. *In vitro*, the leucine (Leu) allele is shown to have a decreased responsiveness to selenium supplementation; the induction of GPx1 is lower for an equivalent selenium treatment in recombinant MCF7 cells expressing the Leu allele than for those expressing the Pro allele [187]. When the Pro198Leu polymorphism was combined with the trinucleotide repeat variation in MCF7 cells, GPx1 activity was generally lowest in cells with five alanines and the Leu allele, but it also had the highest level of induction following Se supplementation [199].

The Pro198Leu polymorphism affects GPx activity *in vivo*. In humans, carriers of the Leu allele of GPx1 had lower GPx activity in comparison to Pro carriers; the effect was greater in males than females and depended on Se levels [200-202]. As with the above-mentioned MCF7 supplementation study, humans with similar plasma Se levels but different GPx1 genotypes had significantly different GPx activity and responded differently to Se supplementation [199,202]. In a study to assess the effect of Se supplementation on GPx activity in relation to Pro198Leu, significant differences in GPx activity were detected only when basal plasma Se levels were below 1.15 μM [203]. In the general population, no difference in plasma GPx enzyme activity was detected between Pro carriers and Leu carriers. When those study participants were stratified by baseline Se status, a significant interaction was detected between genotype and supplementation; Pro carriers had a twofold higher induction in activity over Leu

carriers, indicating that the polymorphic effect was most pronounced when Se levels were low enough to have not yet maximized GPx activity.

c. **Cancer risk is increased by glutathione peroxidase 1 polymorphisms**

The allelic differences in GPx1 not only change enzyme activity, but also have been associated with increased risk of disease. There was an association between the Leu variant and the risk of developing bladder and breast cancer, especially when polymorphisms of MnSOD were also included in risk analysis [204,205]. The Pro198Leu polymorphism was associated with increased risk of lung, prostate, colorectal, bladder and liver cancers and was weakly associated with lymphoma [206-211]. Many of these studies were small or were confounded by multiple environmental factors that also confer risk, such as alcohol and smoking. Multiple other studies have shown no association between Pro198Leu and risk of cancer. In a meta-analysis of 35 journal articles pertaining to GPx1 polymorphisms and cancer, there was no association between Pro198Leu and cancer risk from publications that the meta-analysis authors assessed to be of higher quality; factors affecting study quality were related to control selection (generally, lower quality publications had no matched controls or hospital-based controls) [212]. A similar meta-analysis of studies on prostate cancer risk had a similar result, although study quality was not assessed [213]. Multiple additional factors affect susceptibility of cancer in association with the polymorphisms, including race, cigarette exposure, age and presence of additional polymorphisms. Risk of colorectal cancer is only increased for Leu carriers when alcohol consumption and smoking are factored in [214]. Conversely, genotype and smoking were not associated with risk of prostate cancer in a large cohort assessing the effects of β -carotene and retinol supplementation on the risk of lung cancer [215]. These studies indicate a

potential role that genetics may play in cancer susceptibility; however, the associations between Pro198Leu and cancer have not yet been completely elucidated.

d. Obesity and increased reactive oxygen species increase diabetes risk via glutathione peroxidase 1

Altered regulation of GPx1 has been implicated as a potential factor in the development of metabolic diseases such as diabetes mellitus (DM). Diabetes mellitus is characterized by the presence of high blood glucose and poor tissue glucose uptake due to insulin resistance or hyperinsulinemia [216]. One of the greatest risk factors for DM is obesity stemming from a high-fat diet [217]. Excess fat cells secrete factors that contribute to the desensitization of the insulin receptor and its response to insulin, thus negatively affecting glucose uptake [198]. Increased bodyfat levels also lead to an overall increase in ROS levels and oxidative stress levels, which can increase GPx1 levels and impact insulin production in humans, mice and rats [197,218,219]. Mice overexpressing GPx1 exhibited hyperglycemia, hyperinsulinemia, and increased leptin levels and had a higher body-fat percentage [220]. Increased GPx activity in pregnancy is correlated with an increase in insulin resistance over the course of gestation in humans [221]. Pregnant mice fed a high-selenium diet (which increases GPx activity) developed gestational diabetes or diabetes shortly following parturition, and offspring developed diabetes as adults, indicating that increased GPx activity alters susceptibility to diabetes in both the mother and in offspring [222]. GPx1-null mice have decreased plasma insulin levels and increased islet β -cell mass in the pancreas as compared to wild-type controls, further demonstrating how GPx1 modifies insulin levels and affects the onset of DM [223]. Mice fed a high-fat, Western style diet can develop insulin resistance, but, in the absence of GPx1, insulin resistance does not occur [224]. This effect is reversible by concomitant treatment

with n-acetyl-cysteine, a potent antioxidant which can substitute the effects of GPx1. Interestingly, when GPx1 is overexpressed exclusively in the pancreas, it is found to decrease hyperglycemia in mice with streptozotocin-induced diabetes [225]. Unlike in cancer, where GPx1 levels are sometimes decreased, increased GPx1 levels appear to increase risk of DM in conjunction with obesity, which is associated with an increase in ROS levels.

e. **Glutathione peroxidase 1 and selenium intake affect onset of cardiomyopathies**

Low GPx activity can alter susceptibility to developing severe cardiomyopathies, such as Keshan disease. Keshan disease is a severe cardiomyopathy endemic to regions of China where soil Se is low, creating a severe Se deficiency in the population [226]. In these regions, extremely low Se intake results in severely decreased GPx1 levels, and where Se supplementation programs exist, disease incidence has decreased significantly [227]. The susceptibility of developing Keshan disease is associated with concurrent infection with the Cocksackie virus [228]. Selenium-deficient mice infected with Cocksackie virus have increased incidence of myocarditis [229]. The onset of a cardiomyopathy is dependent on GPx1 expression, as transgenic GPx1 knockout mice infected with Cocksackie virus develop myocarditis, whereas uninfected knockout mice and wild-type Cocksackie-infected mice do not [230]. Further evidence of a protective effect against cardiomyopathies by GPx1 is shown in mice that overexpress GPx1 and are treated with the cardiotoxin doxorubicin; these mice have a lower incidence of cardiomyopathies than wild-type control mice [231].

9. **Regulation of glutathione peroxidase 1**

Regulation of GPx1 occurs at multiple levels, from transcription initiation to post-translational modifications. The association of GPx1 with onset of multiple diseases indicates

how important it is to understand regulation of GPx1 expression and how this can impact management of oxidative stress and disease. Transcriptionally, the *GPX1* gene contains multiple common promoter elements which both up- and down-regulate its rate of transcription. Transcript stability and translation are highly dependent on the availability of Se, as well as on accessory proteins which aid in recoding the UGA Sec codon from a stop codon. Finally, there is evidence of modification of GPx1 through either phosphorylation or acetylation [232,233].

10. Glutathione peroxidase 1 transcription is dependent on reactive oxygen species levels

The *GPX1* promoter region contains multiple promoter sites that are responsive to ROS levels. These promoter sites include the oxygen response element (ORE), the p53 consensus-binding site and NF-κB and activator protein-1 (AP-1) binding sites [234-237]. Binding to these promoter sites is regulated by changes in oxygen tension and ROS levels as detected in the cytosol. The two ORE sites within the *GPX1* promoter region regulate GPx1 transcription under normoxic conditions, while under hypoxic conditions the associated ORE-binding proteins dissociate from the DNA, silencing GPx1 transcription [234]. Conversely, the NFκB and AP-1 sites are activated under oxidative stress and hyperoxia, which result in enhanced rates of GPx1 transcription and increased antioxidant capacity in the cell [236]. The NFκB and AP-1 transcription factors are both activated in the cytosol and translocate to the nucleus in response to cell stressors (e.g., increased ROS, cytokines, and pathogens), and activate the transcription of a variety of antioxidant response genes, including MnSOD and catalase [238,239]. Binding of p53 to the promoter regions increases transcription of GPx1 (possibly in response to increased oxidative stress) and may contribute to the regulation of the apoptotic response by p53 [235,237]. The transcriptional regulation of GPx1 is primarily in response to

alterations of the cellular environment, especially in response to ROS and increased oxygen levels, demonstrating the importance of GPx1 and other antioxidant enzymes in the maintenance of steady-state ROS levels.

11. Glutathione peroxidase 1 translation is increased in a selenium-dependent manner

While many ROS-sensitive elements regulate GPx1 transcription, the post-transcriptional regulation of GPx1 is in response to availability of Se and is regulated via the unique features of selenoproteins. GPx1 is a Se-sensitive enzyme, where expression is decreased in Se-deficient conditions, as described in Keshan disease [227]. In Se deficiency, GPx1 mRNA is sensitive to nonsense-mediated decay, where mRNA is degraded following detection of a premature stop codon (such as UGA) by the ribosomal translation machinery [132]. The UGA codon also encodes for the selenocysteine amino acid, which is found in the first exon at codon 46 of GPx1 [240]. Recoding the UGA codon from a stop codon to a selenocysteine codon requires the SECIS element within the 3'-untranslated region (UTR); in Se deficiency, the SECIS is unable to recode the UGA, leading to the detection of a premature stop codon and decay of the transcript [134]. Detection of a nonsense codon is dependent on its location relative to an exon-exon boundary, where an exon-junction complex (EJC) of multiple proteins is bound [133]. If the nonsense codon is detected upstream of the EJC during translation, the transcript is signaled for degradation within the cytoplasm [241].

The SECIS is a critical element in the recoding of the UGA codon, and it is bound by multiple accessory proteins that regulate Sec incorporation into the growing polypeptide chain [138,242-245]. Most of these proteins bind the SECIS or the Sec transfer RNA (tRNA), regardless of Se status. The protein SBP2 binds the SECIS stem-loop structure and recruits the

selenoprotein-specific elongation factor and tRNA^{[Ser]Sec} to the ribosomal complex [135,136]. Without this protein, SECIS-recoding does not occur in the majority of selenoproteins, with the exception of Selenoprotein P, GPx2 and GPx4, which are translated regardless of Se status [128,130,131]. Deficiencies in SBP2 have been detected in humans; while it is not fatal, it does result in a multi-system selenoprotein deficiency with a complex disease phenotype affecting multiple organ systems [246]. Levels of the majority of the 25 selenoproteins are decreased, with consequences on thyroid hormone levels, muscle development, fertility and fat mass, highlighting the importance of selenoproteins in prevention of multiple disorders. The binding of SBP2 to the SECIS is interrupted by eIF4a3, which senses Se availability in the cell and binds the mRNA of those selenoproteins which are most sensitive to Se availability [138]. Both eIF4a3 and SBP2 compete for the same binding site on the SECIS, and when eIF4a3 is bound, it blocks the ability of SBP2 to bind, preventing UGA recoding. Glutathione peroxidase 1 is one of the most Se-sensitive proteins, and thus is susceptible to inhibition by eIF4a3 [129].

Selenium levels also affect the distribution of the tRNA isoacceptors necessary for Sec insertion into the polypeptide chain. The addition of a methyl-group onto the methylcarboxymethyl-5'-uridine at the wobble position (position 34) of the anticodon is dependent on selenium availability; in Se sufficient conditions 2'-*O*-methylation occurs, and the presence of 2'-*O*-methylation is considered the mature form of tRNA^{[Ser]Sec} [247]. Transgenic mice with mutations of the isopentenyladenosine at position 37 of the tRNA have altered distributions between methylated and unmethylated tRNA^{[Ser]Sec}, with a shift towards the less active unmethylated form [248]. Analysis of selenoprotein expression in these animals reveals that expression of multiple selenoproteins is decreased by the shift away from the mature tRNA^{[Ser]Sec}, including GPx1, which was found to be significantly decreased in all tissues

investigated [247]. The methylation state of the tRNA is changed by Se availability, which is detected in an unknown manner by SECp43 and soluble liver antigen [248,249]. The availability of Se alters accessibility of the SBP2-binding site in the 3'-UTR and the methylation state of the tRNA^{[Ser]Sec}, both of which can potentially affect GPx1 levels and thus are potential pathways to investigate additional routes of post-transcriptional regulation of GPx1.

12. Post-translational modifications of glutathione peroxidase 1 affect enzyme activity

Glutathione peroxidase 1 is regulated post-translationally, either through irreversible modification of the Sec by ROS or modification of the peptide chain by the addition of functional groups such as phosphate or acetate. When high levels of ROS are present, the Sec at the active site of GPx1 can be converted to a dehydroalanine, permanently inactivating the enzyme activity of GPx1 [250,251]. Lifestyle factors such as smoking or obesity can increase ROS levels and negatively impact GPx1 function by inactivating the protein [156,157,198]. Obesity or smoke exposure can increase GPx1 levels in response to high ROS levels, but ROS increases can inactivate GPx1, resulting in an imbalance of antioxidant and oxidant levels.

Glutathione peroxidase 1 may also be regulated by reversible modifications, such as acetylation and phosphorylation. A proteomic screen for acetylated proteins indicated that GPx1 is predicted to be acetylated at lysine 88, which may inhibit its activity, and that it may be deacetylated by Sirt3, a mitochondrial deacetylase [233,252]. Acetylation of multiple proteins is increased by chronic alcohol intake, and GPx1 is acetylated in rats fed a high-alcohol diet [252,253]. Inhibition of GPx1 by acetylation could be a factor in alcohol-induced liver damage, as chronic alcohol consumption increases ROS levels in the liver, with negative effects on

proteins, DNA, and lipids [254]. Finally, the non-receptor tyrosine kinases c-Abl and Arg have been shown to phosphorylate GPx1 at tyrosine-96, increasing enzymatic activity [232].

Inhibition of c-Abl via the Abl-specific inhibitor imatinib mesylate (STI-571, Gleevec) decreased GPx1 enzyme activity in HEK 293 and SH-SY5Y cells [232]. FLAG-tagged GPx1 was found to co-immunoprecipitate with a Myc-tagged c-Abl, with a phosphorylation site determined to be the tyrosine at codon 96. However, a study by our laboratory was unable to confirm a phosphorylation site in GPx1 by direct analysis of the protein by mass spectrometry, phosphoprotein detection assays, or through the mutation of the phosphorylation site [199]. The addition of a tag to either the amino- or carboxyl-terminus of GPx1 can potentially affect the structure of the protein and the interaction between subunits [196,199]. The presence of even a small tag could modify the tertiary structure of the protein and affect binding affinities between proteins or the expression levels of the proteins of interest, potentially inducing an interaction which does not occur *in vivo* [255,256]. The terminus utilized for FLAG-tagging can alter expression, with differential effects in tagging the amino- versus the carboxyl-terminus [255]. It is evident that there is a potential for regulation of GPx1 by post-translational modifications; though a direct mechanism of regulation by c-Abl has not been confirmed, treatment of neuroblastoma cells with imatinib decreased GPx activity, and overexpression of c-Abl in HEK293 cells increased endogenous levels of GPx1 [199,232]. These data indicate that there is regulation of GPx1 by c-Abl, which could have impacts on the expression and regulation of GPx1 and the maintenance of ROS levels in the cell.

D. Understanding the regulation of glutathione peroxidase 1

Changes in GPx1 levels may impact the maintenance of cell viability and human disease by H₂O₂, affecting proliferation and apoptosis, and potentially damaging the cell [2,120]. The

post-transcriptional regulation of GPx1, independent of Se levels, is not well understood, nor is the effect of post-translational modifications in regulation of enzyme activity. The evidence of regulation by the non-receptor tyrosine kinase c-Abl indicates a previously unexplored mechanism by which GPx1 levels may be modified [232]. It was not investigated if c-Abl affected GPx1 transcript or protein levels, but provides compelling enough evidence of an alternative route of regulation to warrant further investigation. In order to determine whether the observed *in vitro* effects of imatinib on GPx1 levels were biologically significant and occurred in treated individuals, clinical samples were obtained by our lab for analysis.

II. CHANGES IN THE ACTIVITY OF THE GLUTATHIONE PEROXIDASE 1 ANTIOXIDANT SELENOENZYME IN MONONUCLEAR CELLS FOLLOWING IMATINIB TREATMENT¹

A. Introduction

The non-receptor tyrosine kinase c-Abl and its derivative oncogene breakpoint cluster region Abelson (Bcr-Abl) are directly inhibited by the targeted kinase inhibitor imatinib, which also targets c-Kit and platelet-derived growth factor receptor (PDGFR) [257,258]. Imatinib is the preferred first-round treatment for chronic myelogenous leukemia (CML), which is characterized by the presence of Bcr-Abl, a fusion protein that is the result of reciprocal translocation between the c-Abl region of chromosome 9 and the Bcr of chromosome 22 [259,260]. Bcr-Abl is a constitutively active cytosolic tyrosine kinase that effects the malignant transformation of myeloid cells and in addition to other pathways, signals for increased cellular proliferation and survival via the PI3K/Akt/mTOR pathway [261]. The fusion of Bcr to c-Abl maintains all but the first exon of c-Abl, preserving the majority of its regulatory domains [262,263]. Because GPx activity levels have been shown to be directly affected by c-Abl and imatinib treatment in culture, it was investigated whether this observed phenomenon occurs in CML patients treated with imatinib for disease.

B. Materials and methods

GPx activity was determined from archived mononuclear cells obtained from patients before and after undergoing imatinib therapy. Because the amount of protein available was insufficient to perform the assay multiple times, the reproducibility of the assay was established.

¹ Adapted from Terry, EN et al. *Changes in the activity of the GPx-1 anti-oxidant selenoenzyme in mononuclear cells following imatinib treatment*. Leuk Res, 2011. **35**(6): p. 831-3.

Protein extracts were prepared from the KU812 and MEG-01 human CML cell lines (American Type Culture Collection, ATCC, Manassas, VA) by sonication in 0.1 M NaPO₄ buffer and spun at 14,000 rpm to pellet cell debris. Extracts were freeze-thawed and assayed for GPx activity by a coupled spectrophotometric assay, which measures the oxidation of NADPH at 339 nm [264]. Oxidation of NADPH (0.25 mM, Sigma-Aldrich Corporation, St. Louis, MO) occurs by the reduction of GSH (5 mM, Sigma-Aldrich) by GSH reductase (1 U/mL, Sigma-Aldrich), and this is coupled to the reduction of H₂O₂ (65 μM, Sigma-Aldrich) by GPx. The rate of oxidation of NADPH is coupled to the rate of H₂O₂ reduction by GPx. The linear rate of decay for NADPH was measured and averaged for 3.5 minutes, and the nmoles NADPH oxidized per minute per milligram of protein were calculated as below:

$$\text{GPx activity} = (\text{sample rate of decay} - \text{background rate of decay}) / (0.00622 \mu\text{M}^{-1}\text{cm}^{-1} * [\text{protein } \mu\text{g}/\mu\text{L}])$$

The extinction coefficient for NADPH is 0.00622 μM⁻¹cm⁻¹.

To assess the variation in GPx activity expected to occur in samples from the same individuals over a period of time similar to that of patients treated with imatinib, mononuclear cells (MNC) were obtained from participants in a lycopene supplementation study (UIC IRB# 2005-0828, Peter Gann) and assayed for GPx activity. Samples were also obtained from patients before and after 3–6 months imatinib therapy as part of a study to predict clinical responsiveness (Oregon Health & Science University IRB# MOL-01018-L, B. Drucker; UIC IRB# 2009-1005, Alan M. Diamond). MNCs were isolated by Ficoll gradient centrifugation, frozen either as dry pellets

(maintaining viability) or made into protein lysates. Extracts were prepared and assayed for GPx activity.

C. Results

1. Assay reliability

In order to determine the reproducibility of the GPx assay, extracts prepared from KU812 and MEG-01 cells were subjected to multiple freeze–thaw cycles and assayed on different days spanning a 4-month period. Four KU812 and 2 MEG-01 extracts were assayed (Fig. 1A); it was apparent that the variation from the mean did not exceed 20% for any of the tested extracts.

To determine the anticipated variation in GPx activity expected in MNCs from the same individuals over an approximately 6-month period, extracts were prepared from deidentified MNC cells from participants in a nutritional supplementation study not including drugs or substances that were likely to alter GPx activity (unpublished observations). Five pairs of samples were studied (Fig. 1B). The variation in measured activity for each of these sample sets was less than 20%, similar to the assay variation observed in the multiple retesting studies shown in Fig. 1A.

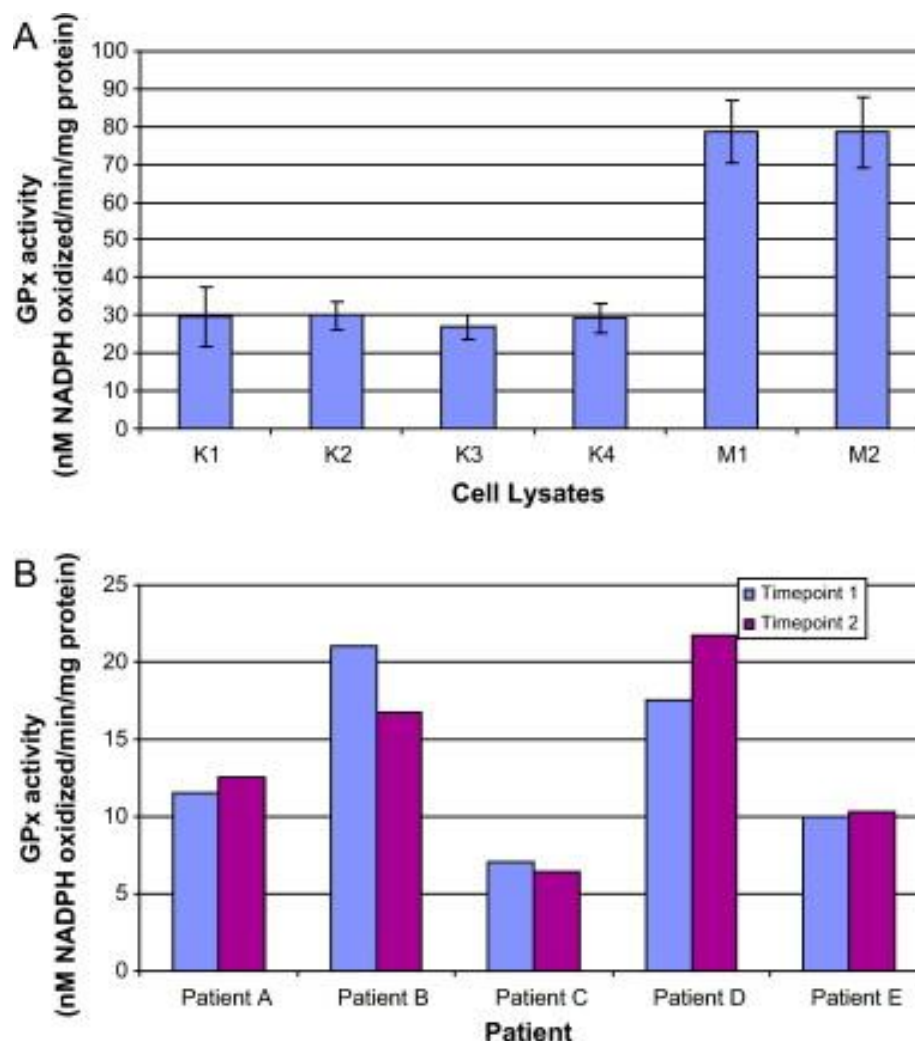


Figure 1. Reproducibility of the GPx enzyme assay.

(A) Extracts were prepared from separate KU812 and MEG-01 cultures, and GPx activity was assayed following 4 freeze–thaw cycles. Extracts were prepared from 4 individual cultures of KU812 cells (K1–4) and 2 individual cultures of MEG-01 cells (M1 and M2). (B) Extracts were prepared from MNCs derived from the same subjects 6–9 months apart and assayed for GPx activity. Individual patients are indicated by letters. GPx activity is presented as nmoles of NADPH oxidized/mg protein, and the error bars indicate the S.D.

2. Changes in glutathione peroxidase activity following imatinib therapy

GPx activity was assessed in paired samples obtained from the individuals before and after treatment with 400 mg/day imatinib as shown graphically in Fig. 2. Patient information including gender, age, and duration of treatment are included in Table I. Of the 7 sample sets presented, 5 showed changes in enzyme activity that exceeded 20%, and 2 did not. Of the 5 that did, 1 showed a decrease in activity of 42%, and 4 demonstrated increases ranging from 33% to 208%. The sample set showing decreased GPx activity had the highest baseline level prior to treatment, and the 2 demonstrating the greatest increases following treatment (166% and 208%) exhibited the lowest pre-treatment levels and were derived from the only 2 females in the patient sample group examined.

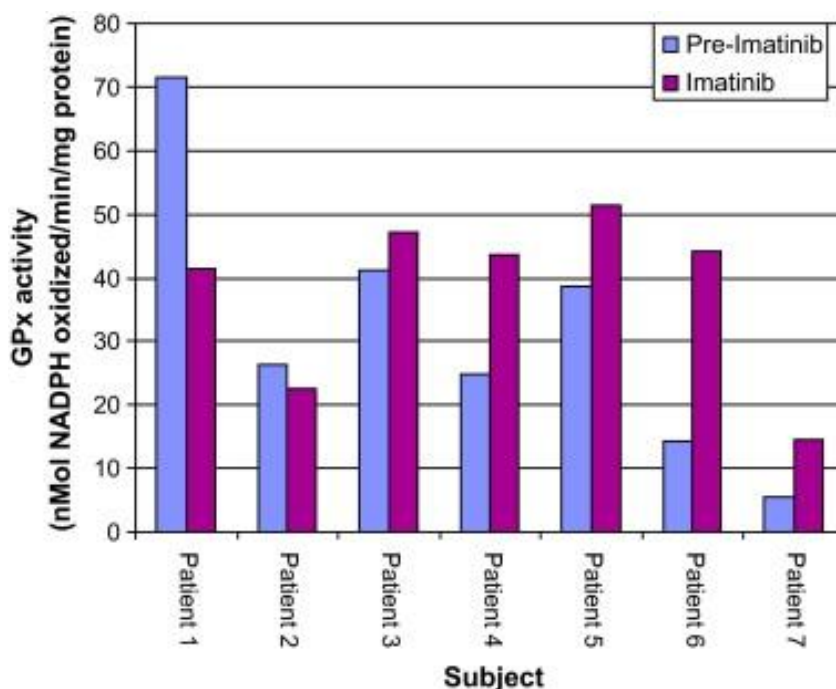


Figure 2. GPx activity in MNC extracts derived from patients before and after imatinib therapy.

Extracts were prepared from frozen and viable MNCs derived from patients prior to beginning imatinib treatment and after several months of receiving the drug (see Table I for details). GPx activity is presented as nmoles of NADPH oxidized/min/mg protein.

TABLE I. PATIENT INFORMATION AND DEGREE OF CHANGE IN GPX ACTIVITY FOLLOWING IMATINIB TREATMENT

Patient	Gender	Age (years)	Duration of treatment (months)	% change
1	M	45	4	-42
2	M	54	3	-
3	M	71	6	-
4	M	28	2	+75
5	M	64	6	+33
6	F	62	6.5	+208
7	F	53	12	+166

Patients 1, 2, 5, 6, and 7 achieved complete or near-complete cytogenetic and/or molecular responses to imatinib therapy; patient 3's response was considered sub-optimal; and patient 4's disease was considered resistant to imatinib therapy.

D. Discussion

In contrast to published data, a tyrosine phosphorylation of GPx1 was not detected nor was there an effect by mutating out tyrosine 97, the likely Abl substrate [199,232]. Thus, there may be cell culture- or cell type-specific determinants of Abl phosphorylation of GPx1. There are a number of limitations to this study of the effect of imatinib treatment on GPx activity in CML patients. The amount of protein available for analysis permitted only a single assay per sample, although our assessments on assay variability indicated the data obtained is likely to be correct. Due to the large variation in the changes seen in the imatinib-treated patients, coupled with the ability to perform only one assay per sample, we were unable to detect any statistical difference ($P = 0.18$) between treatment and control sets via a two-sample *t*-test with equal variance. However, the biological differences were evident with 5 of the 7 individuals showing changes in excess of what was observed in untreated individuals. The sample size was also too small to make conclusions regarding any associations between changes in GPx activity and responsiveness to imatinib treatment, as only 1 of the patients (Patient 4) had disease that did not improve with the drug. Nonetheless, most of the sample pairs examined showed a change in GPx1 in MNCs following treatment.

GPx may have a significant impact in influencing disease management and long-term health of treated patients. Because GPx is a major antioxidant enzyme, altered levels of it may influence the risk of DNA oxidation products leading to disease. In support of this, numerous reports have shown that a variant GPx1 allele expected to exhibit reduced enzyme activity was associated with increased risk of a variety of diseases, including cancer [199]. Alternatively, enhanced GPx1 activity may result in increased risk of diseases such as diabetes or negatively affect therapeutic effectiveness by inhibiting apoptosis, as was first shown in T cells and

subsequently in a variety of cell types [182,220]. These studies indicate the need for additional work to evaluate changes in GPx activity in patients undergoing treatment with Abl kinase inhibitors and to determine whether these changes impact the therapeutic outcome.

III. THE *IN VITRO* EFFECTS OF IMATINIB AND RAPAMYCIN ON ANTIOXIDANT PROTEIN LEVELS AND ACTIVITY

A. Introduction

Motivated by the initial observation of the post-translational modification of GPx1 [232], the effect of imatinib treatment on GPx enzyme activity was investigated in CML patients, yielding the surprising result that GPx activity was frequently stimulated by imatinib [265]. To investigate this phenomenon further, *in vitro* tissue culture methods were used in order to study how GPx1 levels are altered by imatinib under conditions of limited variables. To achieve this, established Bcr-Abl-positive cell lines were used.

B. Materials and methods

1. Tissue culture

Four cell lines were obtained from ATCC: KU812 and MEG-01 human CML cell lines, LNCaP human prostate cancer cells, and Chinese hamster ovary (CHO)-AA8 cells. The GM10832 human immortal B lymphocyte cell line was obtained from the National Institute of General Medical Sciences Human Genetic Cell Repository of the Coriell Institute (Camden, NJ). CHO cells were maintained in Modified Essential Medium, alpha (Cellgro, Manassas, VA); all other cells were maintained in RPMI-1640 (ATCC). All media was supplemented with 10% fetal bovine serum (FBS, Gemini Biosciences, West Sacramento, CA), 100 units/mL penicillin, and 100 µg/mL streptomycin (Gibco, Grand Island, NY). KU812 cells were subcloned by methylcellulose colony formation in MethoCult™ (Stemcell Technologies, Vancouver, BC) by the following protocol. KU812 cells (3×10^3) in 0.3 mL IMDM media (Stemcell Technologies) with 10% FBS were mixed with 3.0 mL methylcellulose previously prepared with 10% IMDM and 10% FBS. The mixture was vortexed, and bubbles dissipated (5 minutes); 1.1 mL of

mixture was layered onto a 35-mm dish. Visible colonies were picked after 14 days by extraction using a 200- μ L pipette tip bent to prevent suction of the cell mass beyond the first 1/3 of the tip. Recovered cells were mixed with fresh media and grown. For all pharmacological treatments, non-adherent cells (KU812, MEG-01 and GM10832) were plated at 2×10^5 cells/mL and treated with 150-300 nM imatinib mesylate (Novartis, Basel, Switzerland) for 3-7 days or 1 ng/mL rapamycin (Cayman Chemical, Ann Arbor, MI) for 3 days. For protein half-life studies, KU812 also received 25 μ g/mL cycloheximide (one group with imatinib; one group without) for 3 days or 20 μ M LY294002 (Cayman) for 4 days. Media was removed, and fresh media with specified treatments was applied to cells every 3 days. To measure KU812 and KU812 clonal growth rates, 2×10^5 cells/mL were treated with selected doses of imatinib (0-250 nM) and counted every 1 to 3 days for 20 days using a hemacytometer. Old media was removed, and fresh media and drug treatments were applied every 3 days. LNCaP cells were plated 1 day prior to treatment; 12.5% of a confluent plate of cells was plated for imatinib treatment, and 25% of a confluent plate of cells was plated for rapamycin treatment. Fresh media was applied, and cells were treated with 500 nM imatinib for 7 days or 1 ng/mL rapamycin for 3 days. Cells were maintained at 37° C and 5% CO₂ in a humidified incubator.

The retroviral Bcr-Abl expression construct, which also expresses green fluorescence protein (GFP), was generously provided by Dr. WenYong Chen [2]. LNCaP cells were transfected with empty vector, Bcr-Abl, and kinase-deficient Bcr-Abl with X-tremeGENE HP DNA transfection reagent (Roche Applied Science, Indianapolis, IN). Cells were co-transfected with pSV2-hph (ATCC) at a 1:40 molar ratio for hygromycin B (Cellgro) selection. Following selection in 400 μ g/mL hygromycin B, GFP-positive colonies were detected by fluorescence microscopy and isolated by trypsin and cloning rings, and recovered cells were expanded.

GP293 retroviral packaging cells (Clontech, Mountain View, CA) were maintained in high-glucose Dulbecco's Modified Eagle Medium with 10% FBS, 100 units/mL penicillin and 100 µg/mL streptomycin. GP293 were co-transfected for 4 hours with the pVSV-G pantropic packaging vector (Clontech) and pLNCX-UGA or pLNCX-UGA-GPx1 SECIS reporter constructs using Lipofectamine-2000 (Invitrogen); fresh RPMI-1640 was applied to cells following removal of transfection media. Forty-eight hours after transfection, the virus-containing supernatant was filtered with a 40-µm low-binding surfactant-free cellulose acetate (SFCA) filter (Corning, Tewksbury, MA) to remove cells and debris. Polybrene (4 µg/mL, Santa Cruz Biotechnologies, Santa Cruz, CA) was added to the supernatant. LNCaP cells were plated such that they were approximately 25% confluent 1 day prior to retroviral infection on 35-mm tissue culture plates. LNCaP cells were infected for 6 hours with 1 mL of viral supernatant ($>1 \times 10^6$ multiplicity of infection). After 6 hours, an additional 1 mL of RPMI-1640 containing 4 µg/mL polybrene was added, and infection proceeded for another 18 hours. Following the 24-hour infection, media was removed; fresh RPMI-1640 applied; and cells were treated with 1 ng/mL rapamycin and/or 100 nM sodium selenite (Sigma-Aldrich-Aldrich, St. Louis, MO) for 3 days. All cell treatments and subsequent analyses were performed in triplicate at least two times.

2. Cell lysis, protein and RNA isolation, and cDNA synthesis

Following the specified treatment times, cells were lysed for protein or RNA. Cells were washed 1x in ice-cold phosphate-buffered saline (PBS, Gibco), and adherent cells were dislodged by scraping. For protein harvest, cells were resuspended in Cell Lysis Buffer (Cell Signaling Technologies, Boston, MA) with 200 µM phenylmethanesulfonylfluoride (PMSF) protease inhibitor (Sigma-Aldrich) and passively lysed on ice for 30 minutes, with 15 seconds of vortexing every 10 minutes. Lysates were centrifuged at 14,000 rpm in a refrigerated

microfuge at 4° C for 10 minutes, and the cleared lysate was transferred to a new tube. Protein concentration was determined by the Bio-Rad colorimetric assay (Hercules, CA) [266]. Bovine Serum Albumin (New England Biolabs, Ipswich, MA) was used to create a standard curve between 0.05 µg/µL to 1.0 µg/µL. Protein lysates were utilized immediately for enzyme activity and Western blot analysis, and excess lysate was stored at -20° C. RNA was isolation from treated cells using the RNeasy RNA isolation kit (Qiagen, Valencia, CA), and total RNA was quantified by NanoDrop (Thermo Scientific, Wilmington, DE). Two µg of total RNA in a 40-µL reaction was reverse-transcribed with the High Capacity cDNA Reverse Transcription kit (Applied Biosystems, Grand Island, NY). In brief, total RNA was combined in a polymerase chain reaction (PCR) tube with reaction buffer, random primers, deoxyribonucleotide triphosphate (dNTP) mix, reverse transcriptase, and nuclease-free water, and samples were incubated for 10 minutes at 25° C, 120 minutes at 37° C, and 5 minutes at 85° C. RNA and cDNA were stored at -80° C until quantitative PCR analysis.

3. Protein analysis and enzyme activity

Proteins of interest were analyzed by Western blot analysis. Fifteen µg total protein per sample was prepared in NuPAGE® LDS sample buffer (Invitrogen, Grand Island, NY) with NuPAGE® sample-reducing agent and boiled at 100° C for 10 minutes, to make a 3x master mix for each sample. Five µg was loaded onto a 4-12% Bis-Tris denaturing polyacrylamide gel (Invitrogen) and electrophoresed for 40 minutes at 200 volts in the XCell electrophoresis chamber (Invitrogen). A protein ladder (Thermo) was also electrophoresed for band size estimation after blotting. Protein was transferred onto a methanol-activated polyvinylidene fluoride (PVDF) membrane for 70 minutes at 30 volts using the XCell Blot Module (Invitrogen). Following transfer, membranes were blocked against non-specific

antibody binding with 5% milk in TBS-Tween-20 (TBST, Bio-Rad and Fisher) for 1 hour at room temperature. PVDF membranes were incubated overnight on a rocker at 4° C with primary antibodies against the proteins of interest. Antibodies against the following proteins were used: GPx1 (mouse, MBL, International, Woburn, MA), MnSOD (mouse, BD Biosciences, San Jose, CA), Catalase (rabbit, Abcam, Cambridge, MA), GPx4 (rabbit, Abcam), TrxR1 (rabbit, Proteintech, Inc., Chicago, IL), phospho-S6 (rabbit, pS6, Cell Signaling) for verification of rapamycin activity, and β -actin (rabbit, Abcam) was used as a standard. All antibodies were diluted 1:1000 in 5% milk-TBST except pS6 (1:1000 in 5% BSA-TBST) and β -actin (rabbit, 1:10,000 in 5% milk-TBST). Following overnight incubation, membranes were washed 2 times for 5 minutes each in 1x TBST. Membranes were incubated 1 hour at room temperature in species-appropriate secondary antibody (Anti-rabbit or anti-mouse, 1:2000 dilution in 5% milk-TBST, Cell Signaling). Following secondary antibody incubation, the membrane was washed 3 times for 20 minutes each in 1x TBST. The blot was imaged by enhanced chemiluminescence (ECL) with ECL plus (GE Lifesciences, Pittsburgh, PA). Density of protein bands was analyzed using ImageJ software (NIH, Washington, DC) and normalized to β -actin band density.

Total GPx enzyme activity was analyzed by a coupled spectrophotometric GPx assay, as previously described [264]. Activity of MnSOD was measured by a colorimetric spectrophotometric assay (Cayman). This assay measures the dismutation of superoxide produced by xanthine oxidase and hypoxanthine, which is coupled to the conversion of tetrazolium salt to formazan dye. The addition of 2 mM sodium cyanide to the final reaction inhibits Cu/ZnSOD and ecSOD activity, allowing for MnSOD specificity. Samples were measured at 440 nm in a 96-well plate on a plate reader (BioTek, Winooski, VT), and MnSOD

activity was calculated from a standard curve. Samples were normalized to protein concentration to give a final result of SOD units/mg protein.

4. Analysis of transcript levels

RNA was isolated and cDNA reverse-transcribed as described in section 2. MnSOD and GPx1 cDNA levels were quantified via real-time reverse-transcription polymerase chain reaction (RT-qPCR). Primer-probe pairs were obtained from Applied Biosystems for GPx1, MnSOD, TATA-binding protein (TBP), and 18s. Gene Expression Master Mix (Applied Biosystems) was combined with primer-probe pairs and 50 ng cDNA in a 10 μ L reaction. Expression was analyzed in a 96-well plate format with a Step-One Plus Instrument (Applied Biosystems) with the following protocol: 50° C for 2 minutes, 95° C for 10 minutes, followed by 40 cycles of 15 seconds at 95° C and 1 minute at 60° C. Cycle threshold (Ct) value was determined, and changes in expression relative to untreated controls were calculated using the $2^{-\Delta\Delta C_t}$ method [267]. The Ct values for Gpx1 and MnSOD were normalized to the Ct value of selected housekeeping genes. Three independent cultures were analyzed in triplicate for each treatment condition. Mean Ct of each triplicate was utilized for gene expression analysis.

5. Retroviral SECIS reporter construct synthesis and analysis of reporter signal

The pLNCX retroviral vector [268] was used as a backbone for the construction of a UGA or UGA-GPx1 readthrough luciferase reporter construct, which contains a UGA codon downstream of β -galactosidase, but upstream of the luciferase gene. The UGA-GPx1 sequence contains the GPx1 SECIS element downstream of the luciferase gene, which recodes the in-frame UGA for Sec insertion and luciferase expression. For construction of the pLNCX-UGA vector, the β -galactosidase and luciferase reporter sequences were excised from a pBPLUGA reporter construct at HindIII and XmaI (New England Biolabs) [269]. The fragment was

isolated by excising the 3-kb band from a 1% agarose gel and electroeluting the DNA band into Tris-acetic acid-EDTA (TAE) buffer in dialysis tubing. DNA was precipitated using a standard alcohol precipitation adding 1/10 volume 3 M sodium acetate and 2 volumes of 100% ethanol. Following a brief vortex, the solution was placed at -80° C for 10 minutes. The solution was spun at 14,000 rpm in a microfuge for 6 minutes to pellet DNA, supernatant was removed, and the pellet was allowed to dry for 5 minutes. The pellet was then resuspended in Tris-EDTA (TE) and DNA quantified on a NanoDrop for cloning into pLNCX. Two nucleotide strands were synthesized containing XmaI and ClaI restriction sites (IDT, Coralville, IA, 5'-CCGGGTTAGCTGAGGTCAGAT-3'; 5'-CGATCTGACCTCAGCTAAC-3') and annealed at room temperature for 20 minutes. These were used as polylinkers to convert the XmaI site in the reporter fragment to a ClaI site for directional insertion into pLNCX, which contains a HindIII and ClaI site in its multiple cloning sequence. One hundred fifty ng of reporter fragment, 150 ng of pLNCX, and 0.5 ng of annealed polylinker were combined with T4 DNA ligase (Promega, Madison, WI) for ligation, which proceeded for 1 hour at room temperature. Following ligation, 5 µL of ligation reaction was transformed into subcloning efficiency DH5a *E. coli* (Invitrogen). One hundred µL of the transformation was plated on LB agar (Fisher) made with 100 µg/mL ampicillin (Sigma-Aldrich), and colonies were grown overnight at 37° C. Ten colonies were selected for expansion in LB broth containing 100 µg/mL ampicillin and were shaken overnight at 37° C. pLNCX-UGA DNA was isolated from the bacteria with the QIAprep spin miniprep kit (Qiagen) and digested with HindIII and ClaI to verify insertion of the reporter fragment. Clones positive for fragment insertion were transfected into CHO-AA8 cells to confirm β-galactosidase activity and minimal luciferase activity by the β-galactosidase and luciferase assay systems following the manufacturer's protocol (Promega). One clone was selected for further use. The

pLNCX-UGA-GPx1 reporter construct was constructed in the same way as the pLNCX-UGA construct, except that the fragment from pBPLUGA-GPx1 was excised with HindIII and KpnI (New England Biolabs). A polylinker was synthesized that converted KpnI to ClaI (5'-CGTTAGCTGAGGTCAGA-3'; 5'-CGATCTGACCTCAGCTAACGGTAC-3'). Following successful insertion of the fragment and selection of clones, transfection into CHO-AA8 verified both β -galactosidase and luciferase activity. Inducibility of luciferase activity was verified by treating transfected CHO-AA8 cells with 100 nM sodium selenite (Sigma-Aldrich) for 72 hours. Production of viral particles by GP-293 and multiplicity of infection was also verified by infection of CHO-AA8 cells.

6. Statistical analysis

The statistical significance of the observed differences of target proteins and mRNA transcripts in response to drug treatment was determined by a two-tailed Student's *t* test. Significance was set at $P < 0.05$.

C. Results

1. Treatment of chronic myelogenous leukemia cell lines with imatinib increases antioxidant enzymes

a. Subcloning KU812 and determining a cytostatic imatinib dose

The observation that GPx activity was enhanced in CML patients treated with imatinib led us to investigate whether this observation also occurs in CML cell lines *in vitro*. The established Bcr-Abl-positive CML cell line KU812 was selected for *in vitro* imatinib studies [270]. This cell line has the properties of immature basophils and was established from a male Japanese CML patient in blast crisis. Established cell lines maintained in culture eventually become heterogeneous, affecting the reproducibility of experimental replicates. To

isolate a homogeneous population of KU812, the cell line was sub-cloned in methylcellulose. Growth rates of the clonal and parental KU812 cell lines were found to be similar. A dose-response curve was generated for multiple clones, and it was found that 250 nM imatinib was the maximum cytostatic dose for the KU812 clones (Fig. 3). All subsequent experiments utilized the KU812a clonal cell line.

b. Imatinib treatment increases glutathione peroxidase 1 protein and enzyme levels

Glutathione peroxidase enzyme levels obtained from patient samples indicated that the enzyme activity levels were increased in 4 out of 7 patients by 6 months' treatment with imatinib [265]. In order to determine if GPx activity is also altered by imatinib *in vitro*, KU812a cells were exposed to imatinib for a period of 7 days at 150 nM. Following 7-day treatment, GPx activity levels were increased 2.5-fold from baseline activity levels (Fig. 4A). The increase in GPx activity was not as great as the increase in protein levels, which increased 7-fold from baseline, as determined by densitometry (Fig. 4B, Table II, Appendix A). KU812a cells were treated with 100 or 150 nM imatinib for a period of 3 to 7 days to show both a dose and time response. The increase in GPx1 protein and activity was both dose- and time-dependent; 100 nM treatment marginally increased GPx activity (1.5-fold, Fig. 5A), while an approximately 4-fold increase in protein was observed (Fig. 5C, Table II, Appendix A). The time-dependent response in protein levels to imatinib treatment was more apparent at 3 days, with a 4-fold increase in protein, with only a marginal increase above that for the 7-day treatment, as compared to the dose response (Fig. 5C, Table II, Appendix A). The increase in enzyme activity was again approximately 1.5-fold (Fig. 5B).

c. **The increase in glutathione peroxidase 1 protein levels is not from altered transcript levels or protein decay**

In order to determine if the GPx1 protein level increase observed upon treatment with imatinib was a result of increased steady-state transcript levels or altered protein decay, mRNA expression and protein decay rates were determined. Glutathione peroxidase 1 cDNA was measured by RT-qPCR following reverse-transcription from imatinib-treated and untreated KU812a. Levels of GPx1 cDNA were not increased following 150 nM imatinib treatment (Fig. 6A). KU812a cells were treated with the protein translation inhibitor cycloheximide (25 µg/mL) and/or 150 nM imatinib for a period of 72-96 hours in order to determine if GPx1 protein decay rates were altered. The half-life of GPx1 was determined to be approximately 72 hours in KU812a cells. The rates of GPx1 decay following protein translation inhibition were not significantly different between cycloheximide controls and cells co-treated with cycloheximide and imatinib (Fig. 6B, C Table III, Appendix A).

d. **Imatinib also increases glutathione peroxidase 1 in the chronic myelogenous leukemia cell line MEG-01**

The observation that imatinib treatment of KU812a increases GPx1 protein levels recapitulates the observation that GPx1 is increased in CML patients following imatinib treatment [265]. In order to determine whether the increase in GPx1 was generalized to another CML cell line, the MEG-01 CML cell line was selected for study. This established cell line was isolated from megakaryoblasts of a Japanese male in blast crisis of CML [271]. It was determined that growth in 300 nM of imatinib was cytostatic for this cell line, and this amount was used for subsequent studies. Cells were treated with 300 nM imatinib for 7 days, and GPx1

protein and enzyme activity were again increased (4-fold, Table IV, Appendix A and 1.6-fold respectively, Fig. 7).

e. **Imatinib treatment does not increase glutathione peroxidase 1 in non-Bcr-Abl-expressing cell lines**

In order to see if the imatinib effect was restricted to CML cells, because imatinib increased GPx1 in two different CML cell lines, the effect of imatinib on GPx1 in the immortalized B-lymphocyte line GM10832 and the prostate cancer line LNCaP [272] was determined, neither of which carry the Bcr-Abl translocation. It was determined that growth of GM10832 cells is inhibited at a dose of 300 nM imatinib and that growth of LNCaP cells is inhibited at an imatinib dose of 500 nM. Seven-day treatment of both of these cell lines did not increase GPx1 protein and activity levels (Fig. 8, Table V and VI, Appendix A). The lack of response in these Bcr-Abl-negative cells indicates that the presence of Bcr-Abl may be necessary for the imatinib-induced increase in GPx1.

f. **Ectopic Bcr-Abl expression in LNCaP decreases glutathione peroxidase 1 levels**

The observation that GPx1 enzyme and protein levels were increased following imatinib treatment only in cells that expressed Bcr-Abl indicates that this effect may be dependent on Bcr-Abl. LNCaP cells do not express a Bcr-Abl translocation; thus, these cells were selected to determine if the addition of Bcr-Abl to these cells decreased GPx1 levels. LNCaP cells were transfected with empty vector, Bcr-Abl, and kinase-deficient Bcr-Abl constructs [2], and GPx1 protein levels and enzyme activity were determined. The ectopic expression of Bcr-Abl in LNCaP cells resulted in a significant decrease (0.6-fold) of GPx activity levels, which was dependent on the presence of an active kinase domain in Bcr-Abl (Fig.

9B). GPx1 protein was also significantly decreased in the presence of Bcr-Abl (0.5-fold, Fig. 9C, Table VII, Appendix A). Surprisingly, GPx1 protein was also significantly decreased by the kinase-deficient Bcr-Abl (0.75-fold, Fig. 9C, Table VII, Appendix A).

g. Imatinib treatment increases antioxidant proteins in addition to glutathione peroxidase 1

Glutathione peroxidase 1 is an antioxidant enzyme that was increased by imatinib treatment; therefore, it was examined whether additional antioxidant proteins may also be induced following imatinib treatment. Manganese SOD, GPx4, TrxR1 and catalase were selected as representative antioxidant proteins. MnSOD and TrxR1 protein levels were both significantly increased by imatinib treatment in both KU812a and MEG-01 cells (4-fold for both proteins, Fig. 10A, Table II and IV, Appendix A). MnSOD activity was measured in KU812a and MEG-01 and was increased 2.5-fold in both cell lines (Fig. 10C). The imatinib-induced increase in MnSOD was not a result of increased mRNA steady-state levels (Fig. 10B). Levels of GPx4 and catalase were unaffected by imatinib treatment of either CML cell line (Fig. 11, Table II and IV, Appendix A). Imatinib treatment did not increase MnSOD, GPx4 and TrxR1 in LNCaP or GM10832 (Figure 12, Table V and VI, Appendix A). However, catalase was decreased (0.6-fold) in GM10832 after 300 nM imatinib treatment (Fig. 12, Table V, Appendix A). Overexpression of Bcr-Abl in LNCaP also did not inhibit MnSOD or TrxR1 protein, as observed in Bcr-Abl-expressing cells (Fig. 13, Table VII, Appendix A).

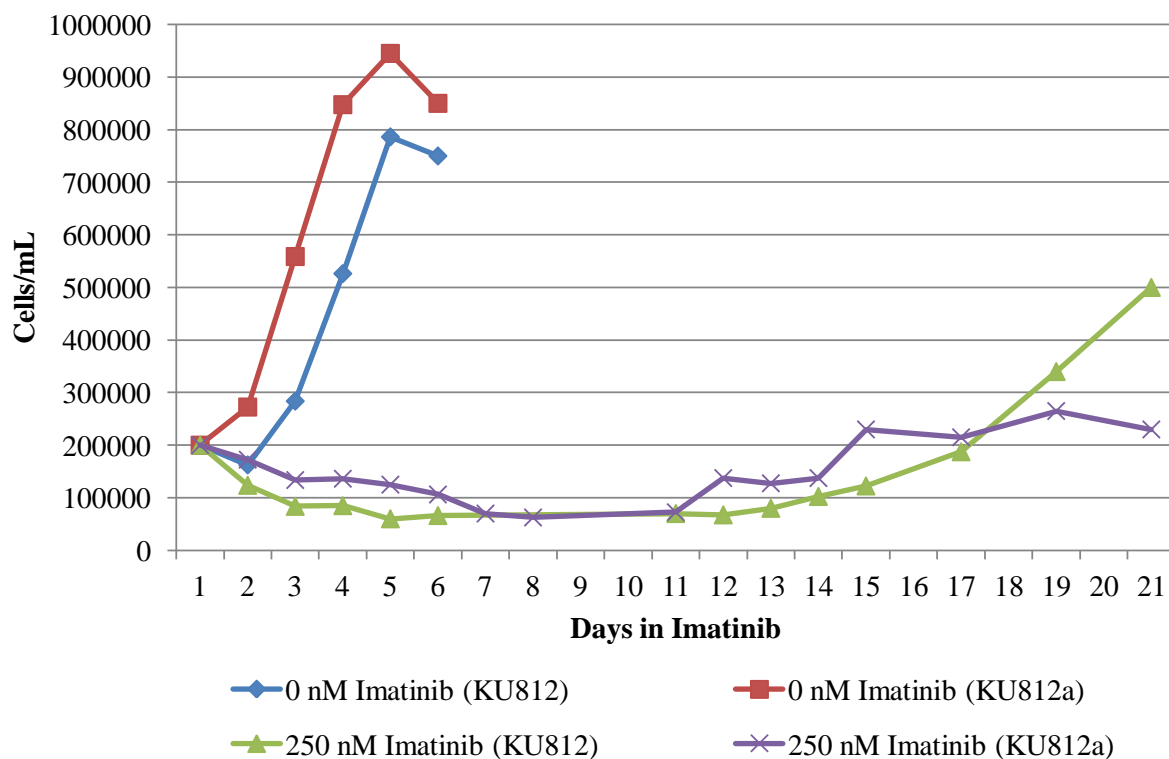


Figure 3. No difference in growth between parental and clonal KU812 cell lines following imatinib treatment.

(A) The effect of imatinib on growth of parental KU812 cells (A) and the sub-clonal cell line KU812a (B) as determined by counting on a hemacytometer. Cells were no longer counted once they reached a density of 1×10^6 cells/mL. Error bars indicate the S.D.

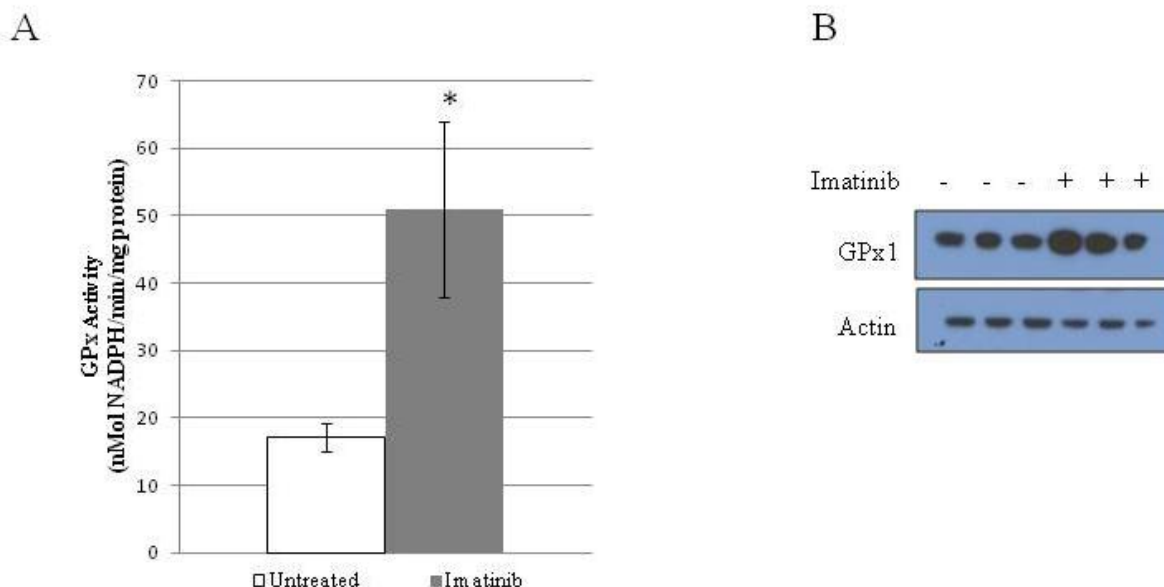


Figure 4. GPx1 protein and activity levels are enhanced by 7-day treatment of KU812a CML cells with 150 nM imatinib.

The effect of 150 nM imatinib on GPx enzyme activity (A) and GPx1 protein (B) as determined by the coupled spectrophotometric GPx assay and immunoblotting for GPx1 and actin. GPx activity was increased 2.5-fold, and protein increased 7-fold ($P = 0.02$) by imatinib treatment. Data shown is representative of one experiment. Three independent experiments were performed. * = $P < 0.001$. Error bars indicate the S.D.

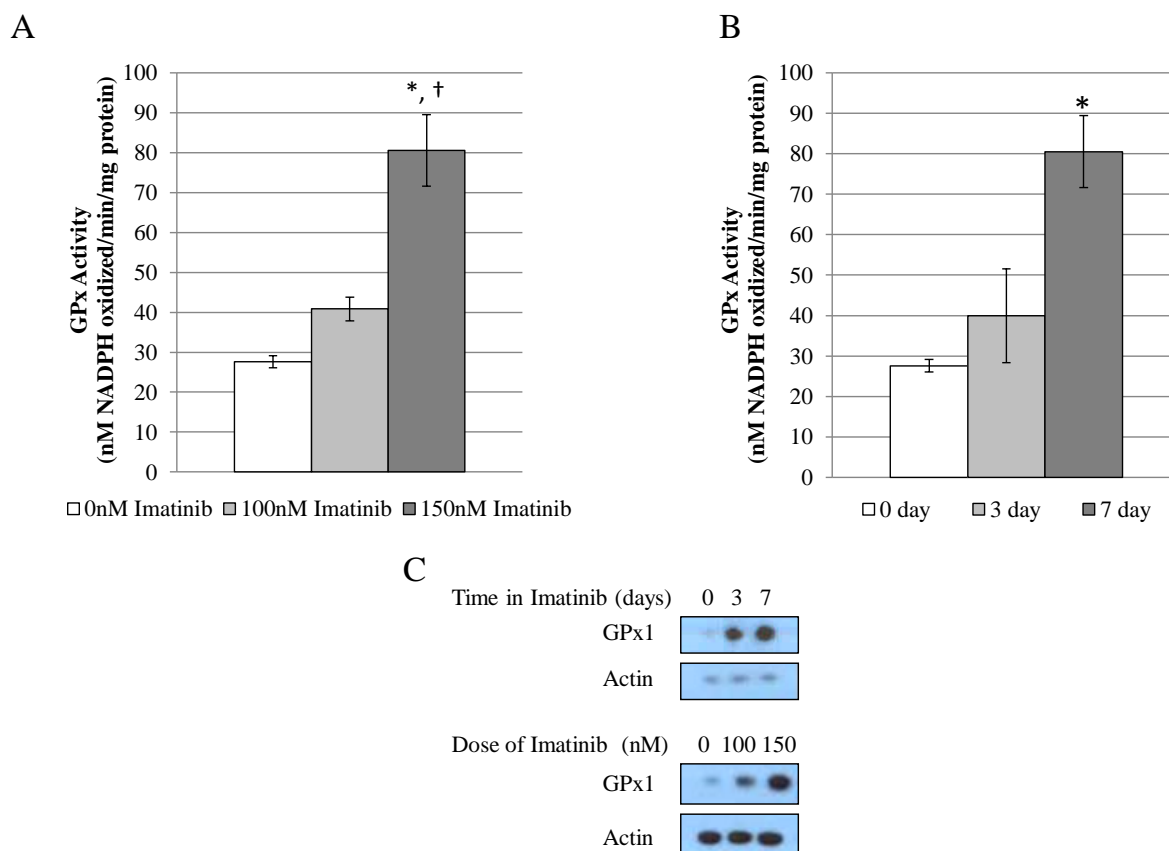


Figure 5. GPx1 protein and activity levels are enhanced in a dose- and time-dependent manner following imatinib treatment of KU812a cells.

The dose- and time-dependent increases in GPx activity following 100 nM and 150 nM imatinib treatment for 7 days (A) or 150 nM imatinib treatment for 3 or 7 days (B) was detected by the coupled spectrophotometric GPx assay. GPx activity was increased 1.3-fold by 100 nM imatinib and 2.5-fold by 150 nM imatinib. No significant increase in GPx activity was detected following 150 nM imatinib treatment for 3 days, but GPx activity increased 2.5-fold following 150 nM imatinib treatment for 7 days. The effect of imatinib treatment time and dose on GPx1 protein (C) as detected following immunoblotting for GPx1 and actin. GPx1 protein levels increased 7-fold following 7 days of imatinib treatment with 150 nM imatinib ($P = 0.02$). Data shown is representative of one experiment. Three independent experiments were performed.

* = $P < 0.001$, † = $P < 0.05$, compared to 100 nM or 3-day imatinib treatment. Error bars indicate S.D.

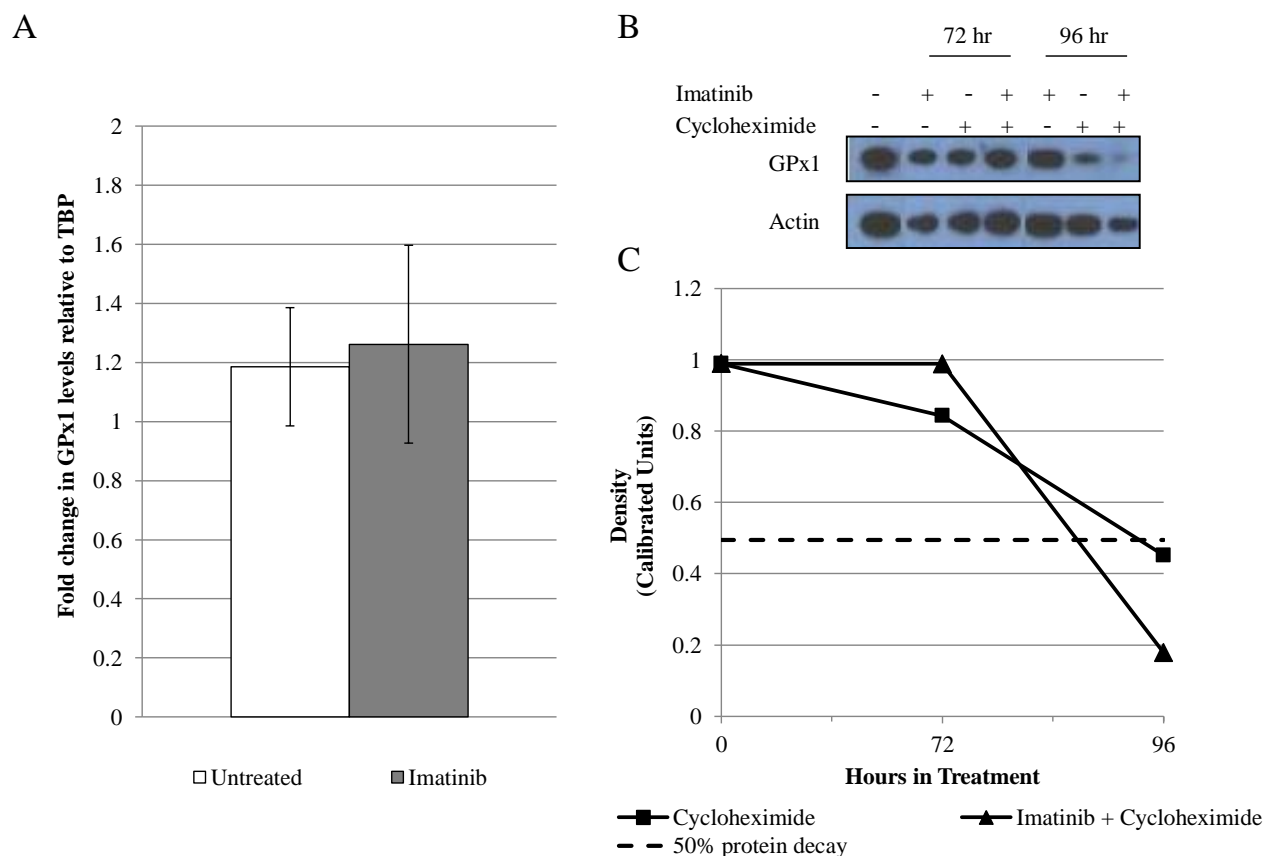


Figure 6. Increases in GPx1 protein are not a result of increased steady-state transcript levels or increased protein decay rates.

GPx1 transcript levels were measured following 150 nM imatinib treatment for 7 days (A) by RT-qPCR. GPx1 Ct values were normalized to the Ct values for the housekeeping gene TBP. GPx1 mRNA transcript levels are not affected by 150 nM imatinib treatment for 7 days. The effect of imatinib on GPx1 protein decay rate following treatment with 25 μ g/mL cycloheximide \pm 150 nM imatinib for 72 or 96 hours (B) was detected by immunoblotting for GPx1 and actin. Rates of decay in the presence of 150 nM imatinib, as determined by densitometry, were not different in the presence of 150 nM imatinib (C). Error bars indicate the S.D.

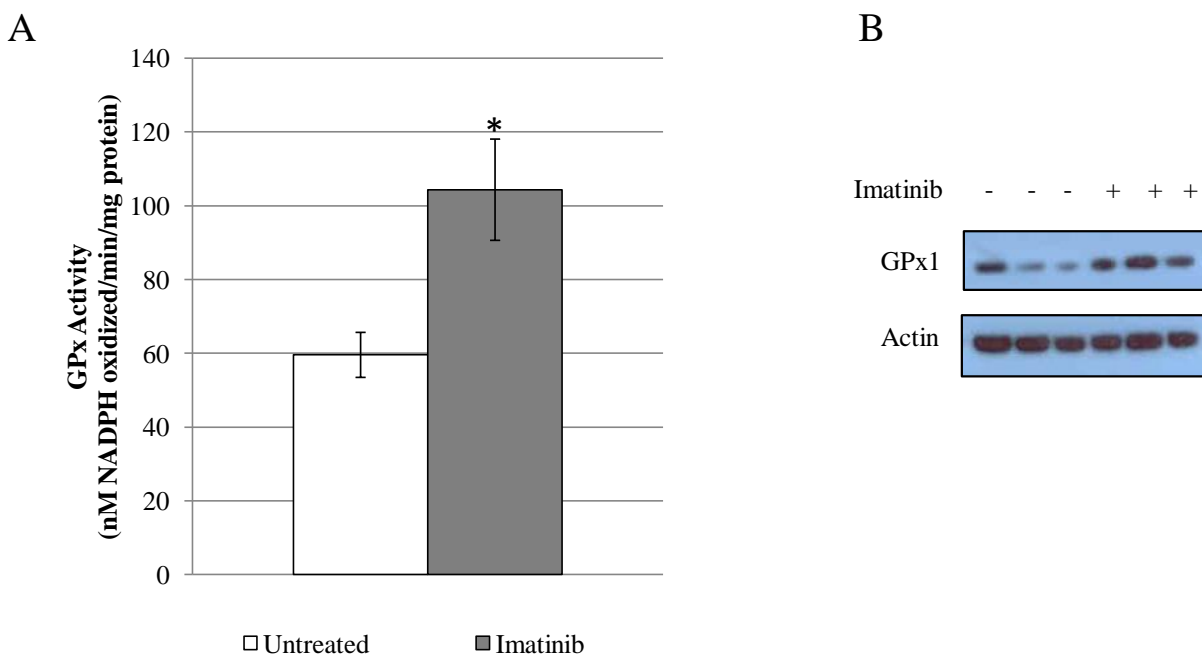


Figure 7. GPx1 protein and activity levels are increased in MEG-01 following 300 nM imatinib treatment.

The effect of 300 nM imatinib on GPx enzyme activity (A) and GPx1 protein (B) in MEG-01 as determined by the coupled spectrophotometric GPx assay and immunoblotting for GPx1 and actin. GPx activity was increased 2-fold, and protein increased 4-fold ($P < 0.01$) by imatinib treatment. Data shown is representative of one experiment. Three independent experiments were performed. * = $P < 0.001$. Error bars indicate S.D.

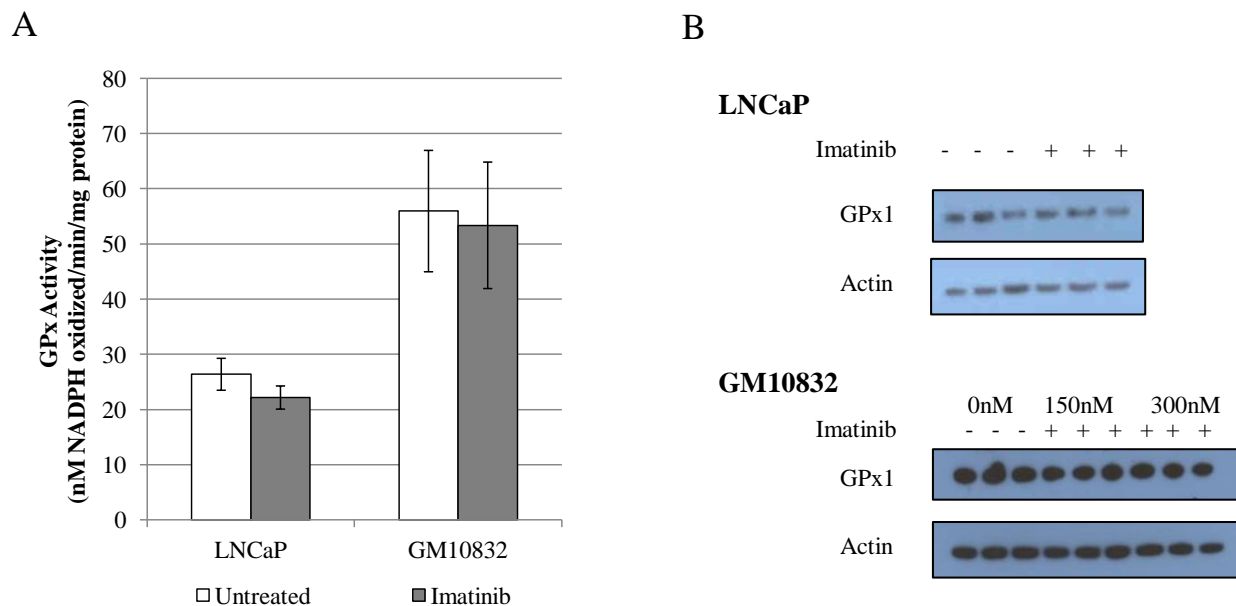


Figure 8. GPx1 protein and activity levels are unaffected by imatinib treatment of LNCaP and GM10832 cells.

The effect of imatinib on GPx enzyme activity (A) and GPx1 protein (B) in LNCaP and GM10832 as determined by the coupled spectrophotometric GPx assay and immunoblotting for GPx1 and actin. There was no effect of imatinib on GPx1 in either cell line. Data shown is representative of one experiment. Three independent experiments were performed. Error bars indicate S.D.

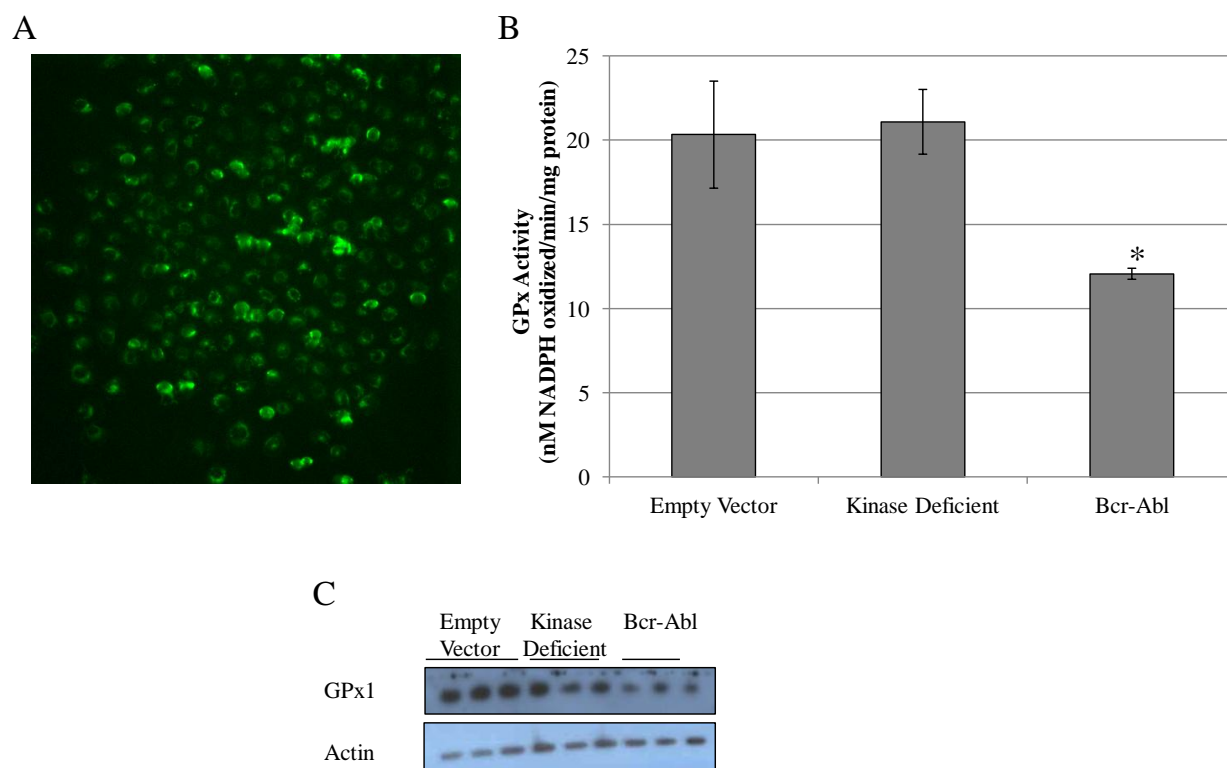


Figure 9. GPx1 protein and activity levels are decreased by exogenous Bcr-Abl in LNCaP.

GFP expression in Bcr-Abl-positive LNCaP cells transfected with a GFP-tagged Bcr-Abl vector (A) as assessed by fluorescence microscopy. The effect of the presence of Bcr-Abl on GPx enzyme activity (B) and GPx1 protein (C) in LNCaP as determined by the coupled spectrophotometric GPx assay and immunoblotting for GPx1 and actin. GPx activity was decreased 0.6-fold by Bcr-Abl, and protein decreased 0.75-fold by Bcr-Abl ($P = 0.02$) and 0.5-fold by kinase-deficient Bcr-Abl ($P = 0.006$). Data shown is representative of one experiment. Two independent experiments were performed. * = $P < 0.001$. Error bars indicate S.D.

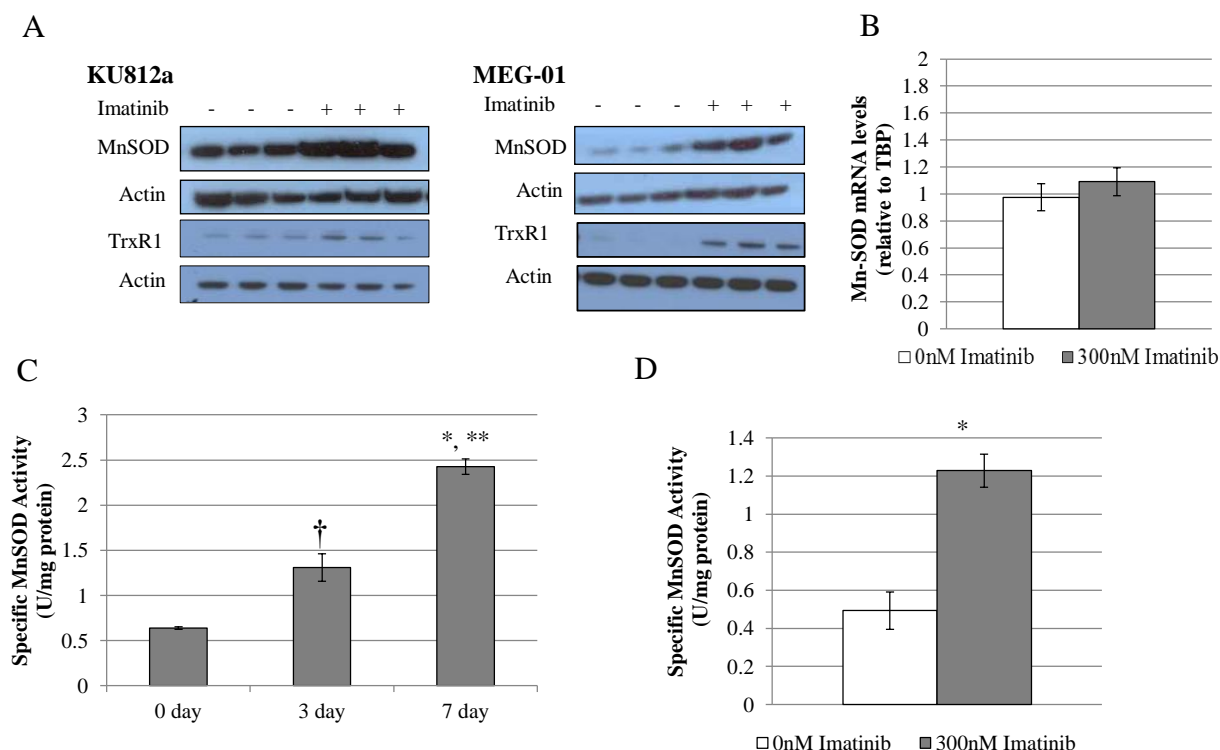


Figure 10. Imatinib increases MnSOD protein and activity levels and TrxR1 protein levels following treatment with imatinib in CML cell lines.

Effect of imatinib on MnSOD and TrxR1 protein in KU812a and MEG-01 (A) as determined by immunoblotting for MnSOD, TrxR1, and actin. There was no effect of imatinib on MnSOD and TrxR1 in either cell line. Effect of imatinib on MnSOD steady-state transcript levels (B) and MnSOD activity (C) in KU812a following 150 nM imatinib treatment for up to 7 days as assessed by RT-qPCR and the colorimetric MnSOD activity assay. MnSOD Ct values were normalized to Ct values for the housekeeping gene TBP. MnSOD transcript levels were unaffected by 150 nM imatinib; however, MnSOD activity was increased up to 5-fold after 150 nM imatinib for up to 7 days. Effect of 300 nM imatinib on MnSOD activity in MEG-01 (C) as assessed by the colorimetric MnSOD assay. MnSOD activity was increased 2.4-fold by 300 nM imatinib treatment for 7 days. Western blots are representative of one experiment. Three independent experiments were performed for each Western blot. * = $P < 0.001$, ** = $P < 0.01$, † = $P < 0.05$. Error bars indicate the S.D.

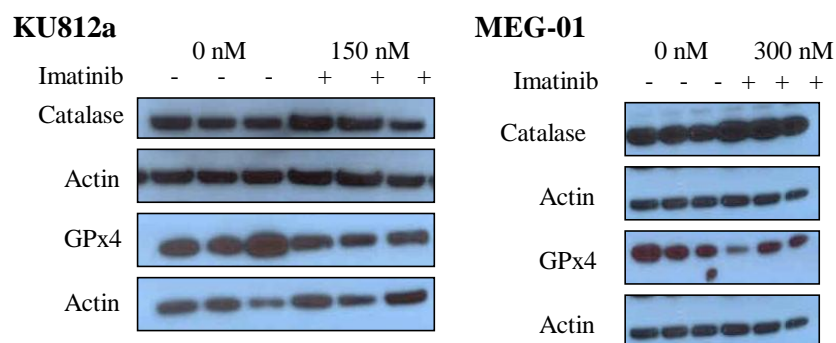


Figure 11. Imatinib does not affect catalase or GPx4 protein levels in KU812a or MEG-01 cell lines.

The effect of imatinib on catalase and GPx4 protein in KU812a and MEG-01 as assessed by immunoblotting for catalase, GPx4, and actin. There was no effect of imatinib on either antioxidant protein in either cell line. Data shown is representative of one experiment. Three independent experiments were performed. $P > 0.1$ for all samples.

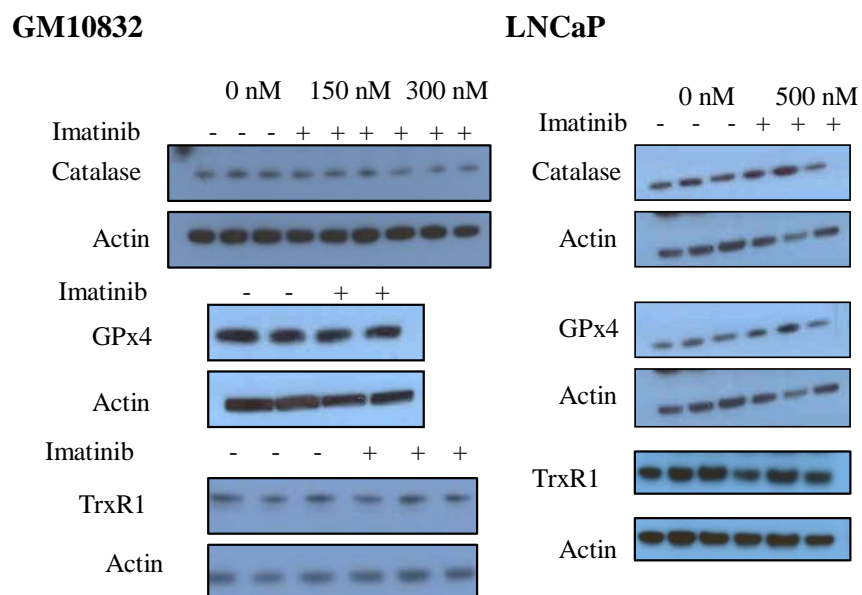


Figure 12. Imatinib does not affect catalase, GPx4 or TrxR1 protein levels in GM10832 or LNCaP cell lines.

The effect of imatinib on catalase, GPx4 and TrxR1 protein in GM10832 and LNCaP as assessed by immunoblotting for catalase, GPx4, TrxR1 and actin. There was no effect of imatinib on catalase and GPx4 in either cell line ($P > 0.09$). Catalase was decreased slightly in GM10832 ($P = 0.05$). Data shown is representative of one experiment. Three independent experiments were performed.

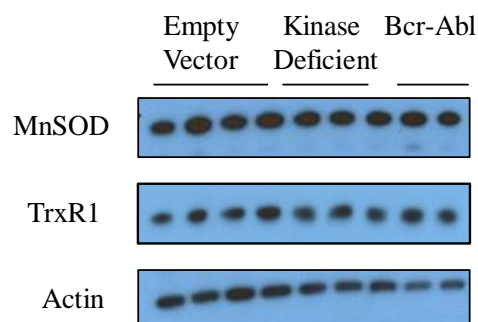


Figure 13. Overexpression of Bcr-Abl in LNCaP does not result in decreased expression of MnSOD and TrxR1 protein levels.

The effect of Bcr-Abl on MnSOD and TrxR1 protein in LNCaP as determined by immunoblotting for MnSOD, TrxR1 and actin. Protein levels were not affected by the presence of Bcr-Abl ($P > 0.1$). Data shown is representative of one experiment. Two independent experiments were performed.

2. Rapamycin and mTOR inhibition regulates selenoprotein levels

a. Selenoprotein levels are increased by inhibition of mTOR

The mammalian target of rapamycin (mTOR) translation pathway is regulated by the phosphatidylinositol 3 kinase (PI3K) pathway, which is one of the pathways induced by Bcr-Abl signal transduction [261,273]. The antibiotic/immunosuppressant rapamycin directly inhibits the mTOR complex I (mTORC1), which regulates protein translation initiation [274,275]. The increased levels of GPx1, MnSOD and TrxR1 after imatinib treatment could be controlled by mTOR-regulated translation, as the increases appear to be post-transcriptional. In order to determine if inhibition of mTOR also increased GPx1, MnSOD and TrxR1, KU812a cells were treated with 1 ng/mL rapamycin for 3 days. Rapamycin treatment of KU812a resulted in a moderate increase in GPx1 protein (3-fold) and activity (2-fold, Fig. 14A,

C, Table VIII, Appendix A). As with imatinib treatment, the increase in GPx1 was not as a result of increased steady-state mRNA levels (Fig. 15). A similar increase in GPx1 protein and activity was seen in MEG-01 cells (Fig. 14B, C, Table IX, Appendix A). Surprisingly, GPx1 was also found to increase in both LNCaP and GM10832 cells (Fig. 16). In LNCaP, GPx activity increased 3-fold and protein increased 1.7-fold (Table XI, Appendix A). In GM10832, GPx activity increased 1.7-fold and GPx1 protein increased 1.8-fold (Table X, Appendix A). Levels of GPx4 significantly increased in both LNCaP and GM10832 (8.6-fold and 4.7-fold, respectively, Tables IX and X, Appendix A), but not in KU812a or MEG-01 (Fig. 17, Table VII and VIII, Appendix A). TrxR1 was found to significantly increase only in GM10832 (2-fold, Fig 17, Table X, Appendix A). Unlike with the effects observed with imatinib treatment, MnSOD protein levels were unaffected by rapamycin in any cell line; however, activity did increase 1.4- to 1.6-fold in KU812a and LNCaP (Fig. 18, Tables VIII-XI, Appendix A).

b. UGA readthrough by the SECIS is not enhanced by rapamycin treatment

The increase in antioxidant protein levels following rapamycin treatment was only observed for selenoproteins, and the overall effect was greater in non-CML cell lines. Translation initiation is regulated by mTOR, and it was hypothesized that the inhibition of mTOR would result in an increase in selenoprotein translation. All selenoproteins rely on the presence of a SECIS element in the 3'-UTR to recode the in-frame UGA for Sec insertion [134]. A retroviral UGA-readthrough luciferase reporter construct was cloned in order to investigate the effects of rapamycin treatment on UGA readthrough (Fig 19C). LNCaP cells were infected with a reporter construct containing a GPx1 SECIS to allow for UGA readthrough 5' of the luciferase gene. As a control, LNCaP cells were transfected with a reporter construct that did not contain a

SECIS. Following infection, cells were treated with rapamycin for 72 hours, and luciferase enzyme levels were determined. There was no significant increase in UGA readthrough following rapamycin treatment (Fig. 19A).

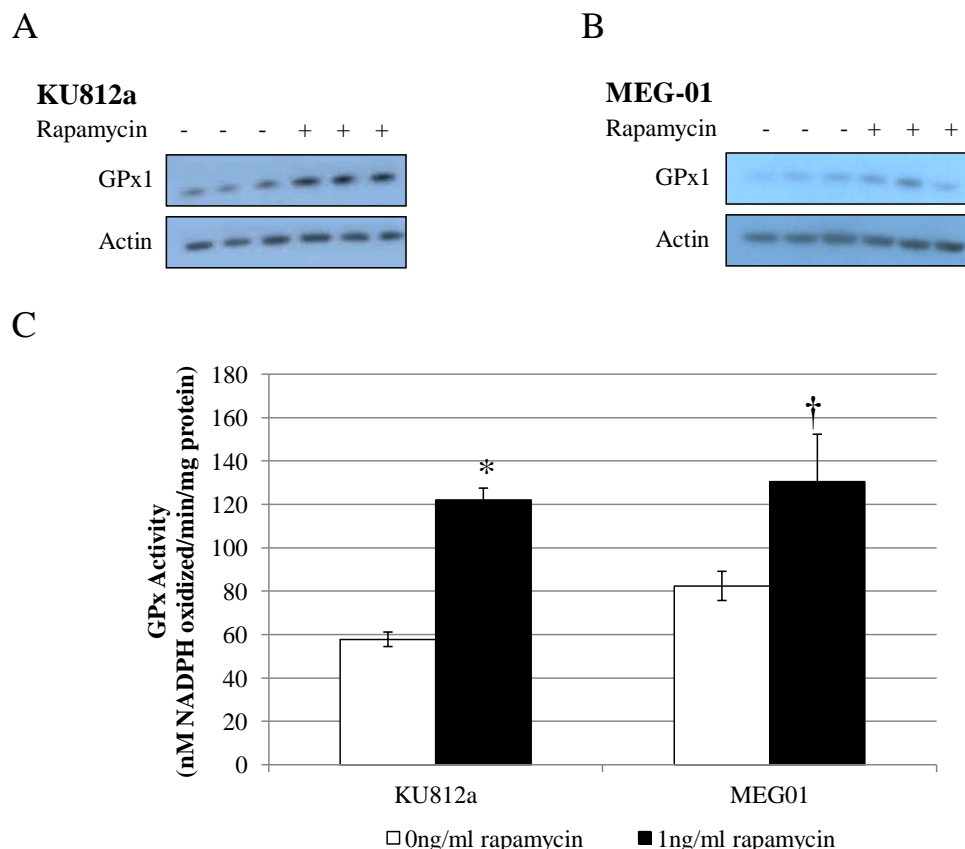


Figure 14. Rapamycin enhances GPx protein and enzyme activity levels in KU812a and MEG-01.

The effect of rapamycin on GPx1 protein (A, B) and enzyme activity (C) in KU812a or MEG-01 as determined by immunoblotting for GPx1 and actin or by the coupled spectrophotometric GPx assay. Rapamycin significantly increased protein respectively 3-fold and 1.3-fold in KU812a and MEG-01 ($P = 0.05$). GPx activity was increased 2-fold and 1.5-fold in KU812a and MEG-01, respectively. Data shown is representative of one experiment. Three independent experiments were performed. * = $P < 0.001$, † = $P < 0.05$. Error bars indicate S.D.

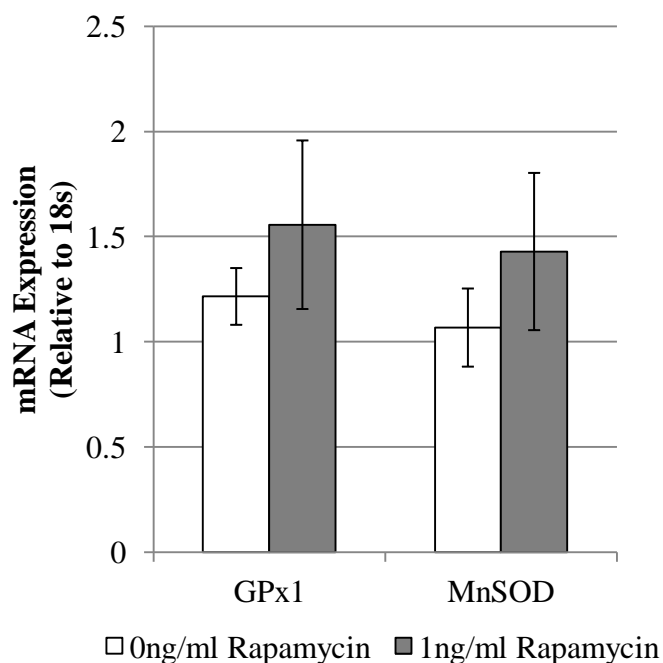


Figure 15. Rapamycin treatment did not affect mRNA transcript levels for GPx1 and MnSOD following rapamycin treatment in KU812a.

Effect of rapamycin on GPx1 and MnSOD steady-state transcript levels following 1 ng/mL rapamycin in KU812a as assessed by RT-qPCR. GPx1 Ct values were normalized to the Ct values for the housekeeping gene 18s. mRNA transcript levels were unaffected by rapamycin treatment for either GPx1 or MnSOD. Error bars indicate the S.D.

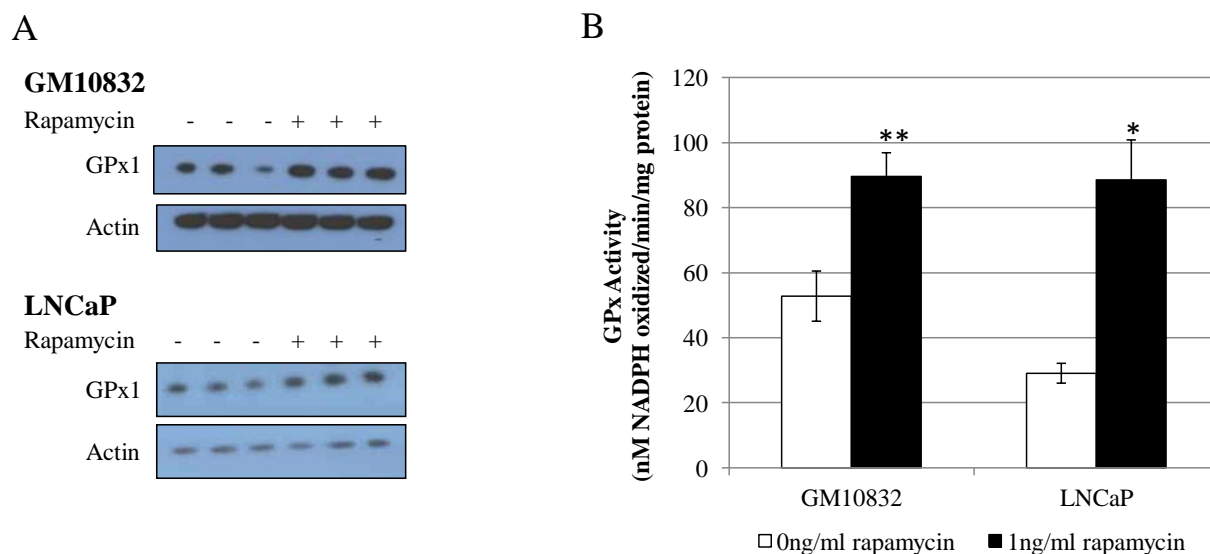


Figure 16. Rapamycin treatment in non-CML cell lines significantly increases GPx1 protein and activity levels.

Effect of treatment with 1 ng/mL rapamycin for 3 days in GM10832 and LNCaP cells on GPx1 protein (A) and GPx activity (B) as assessed by immunoblotting for GPx1 and actin and by the coupled spectrophotometric GPx assay. GPx1 protein was increased respectively 1.8-fold and 1.7-fold for GM10832 and LNCaP ($P < 0.04$). GPx activity was increased respectively 1.8-fold and 3.5-fold in GM10832 and LNCaP. Data shown is representative of one experiment. Three independent experiments were performed. * = $P < 0.001$, ** = $P < 0.01$. Error bars indicate the S.D.

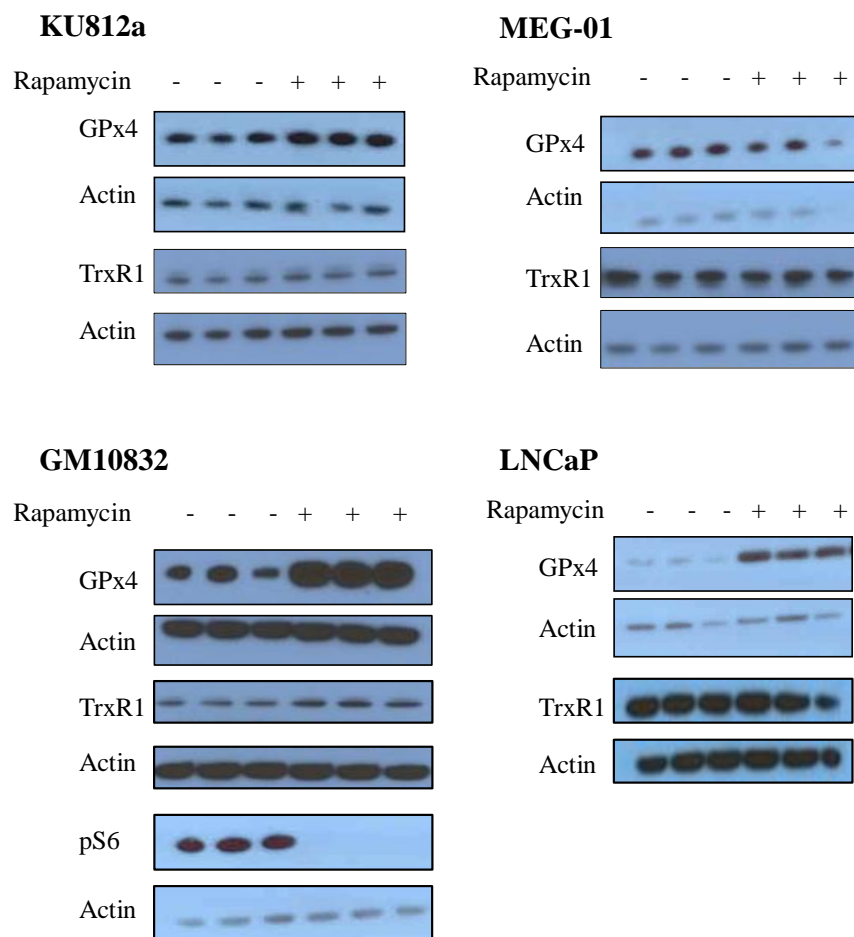


Figure 17. Rapamycin increases levels of GPx4 and TrxR1 protein levels in cell lines.

Effect of 1 ng/mL rapamycin on GPx4 and TrxR1 protein levels in KU812a, MEG-01, GM10832 and LNCaP and effect on pS6 in GM10832 as assessed by immunoblotting for GPx4, TrxR1 and actin. GPx4 and TrxR1 were unchanged by 3-day 1 ng/mL rapamycin treatment in KU812a and MEG-01 ($P > 0.2$), but both were increased in GM10832 (3-fold for GPx4 [$P = 0.05$] and 2-fold for TrxR1 [$P = 0.002$]). GPx4 was increased by rapamycin treatment in LNCaP cells (6-fold, $P = 0.02$). pS6 in GM10832 is representative for all cell lines and indicates inhibition of mTOR target pS6, following rapamycin treatment. Data shown is representative of one experiment. Three independent experiments were performed.

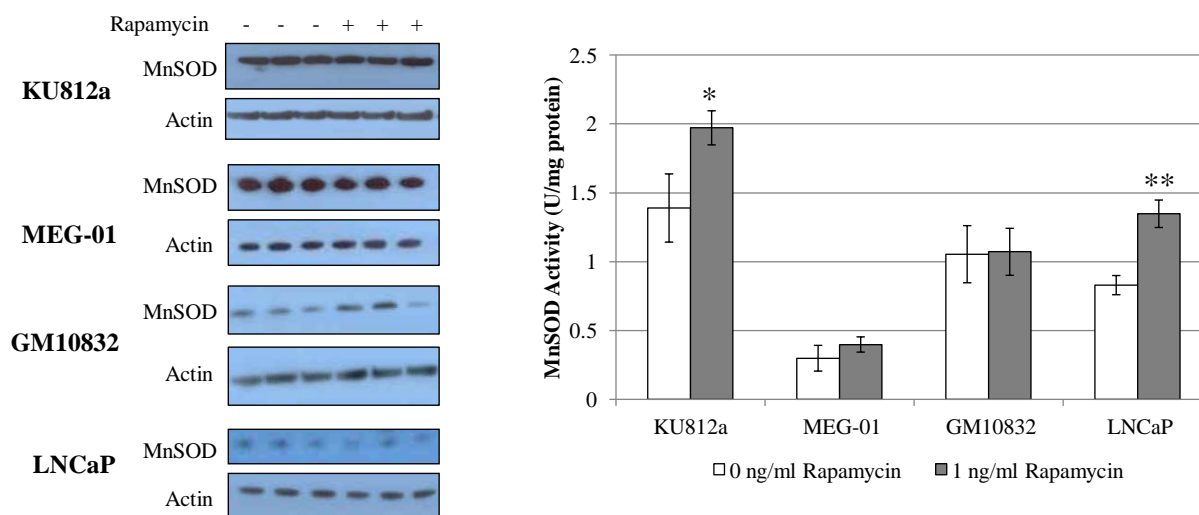


Figure 18. MnSOD protein and activity levels are not increased following rapamycin treatment.

Effect of rapamycin treatment on MnSOD protein and enzyme activity in KU812a, MEG-01, GM10832 and LNCaP as assessed by immunoblotting for MnSOD and actin and by the colorimetric MnSOD activity assay. None of the investigated cell lines showed an increase in MnSOD protein ($P > 0.2$); however, enzyme levels increased in KU812a and LNCaP following 1 ng/mL rapamycin treatment for 3 days. Western blots shown are representative of one experiment, three independent experiments were performed. * = $P < 0.02$, ** = $P < 0.01$. Error bars indicate the S.D.

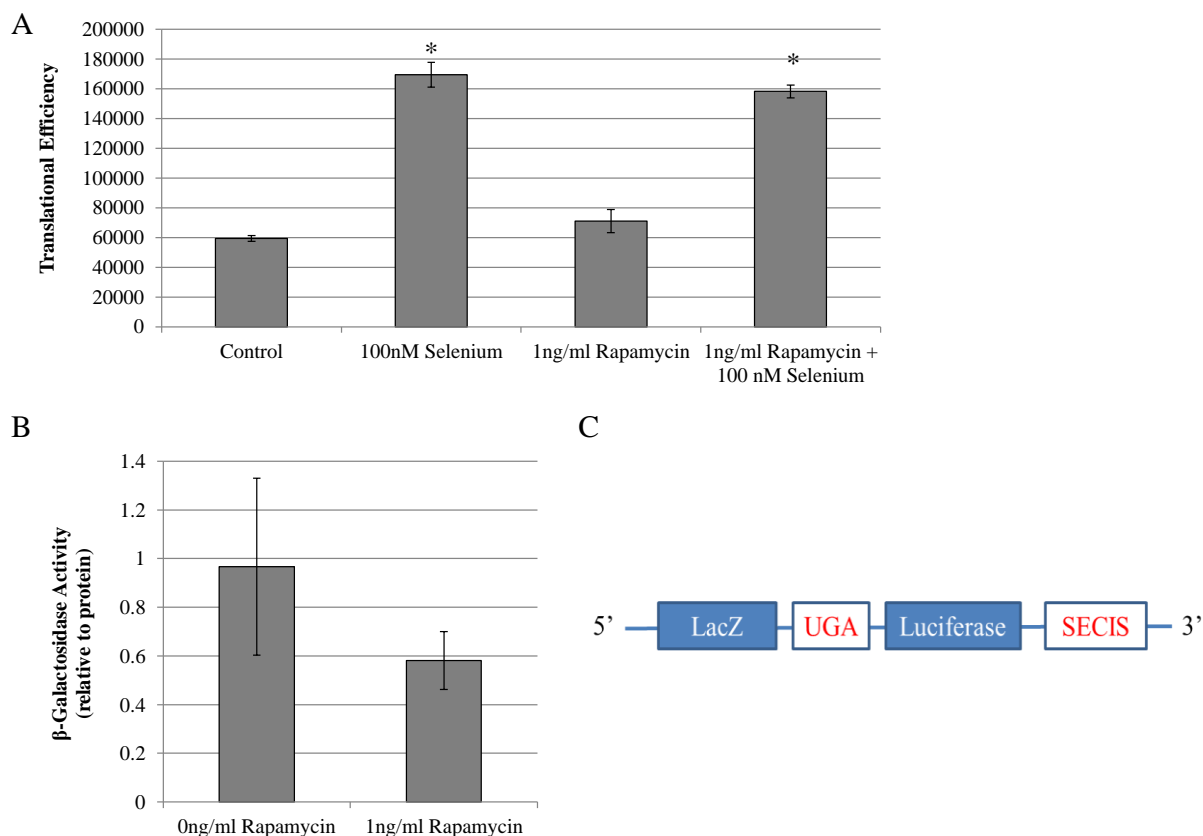


Figure 19. The translational efficiency of UGA readthrough by the GPx1 SECIS is not enhanced by rapamycin treatment.

Effect of rapamycin (1 ng/mL), selenium (100 nM), or both on the translational efficiency of UGA readthrough in LNCaP cells infected with the pLNCX-UGA-GPx1 SECIS reporter construct (A) as assessed by a luciferase assay; relative luciferase levels were normalized to β -galactosidase levels to calculate translational efficiency. SECIS-dependent translational efficiency was not increased following 1 ng/mL rapamycin treatment, but was increased 2.6-fold by Se. Assessment of rapamycin on β -galactosidase levels in LNCaP infected with the pLNCX-UGA control vector (B). β -galactosidase levels were normalized to cell lysate protein levels. (C) Diagrammatic representation of pLNCX-UGA-GPx1 containing the GPx1 SECIS element. Data shown is representative of one experiment. Two independent experiments were performed. * = $P < 0.001$. Error bars indicate the S.D.

3. Inhibition of PI3K decreases glutathione peroxidase activity

Bcr-Abl inhibition increased GPx activity only in CML cells, and mTOR inhibition increased GPx activity in all cell lines investigated. Bcr-Abl regulates mTOR

signaling via the PI3K pathway [261,273]. In order to determine if the increase of GPx1 following inhibition of Bcr-Abl by imatinib or inhibition of mTOR by rapamycin was propagated via the inhibition of PI3K, LY294002 (a morpholine derivative of quercetin) was utilized to inhibit PI3K. It was expected that inhibition of PI3K would increase GPx activity in a manner similar to rapamycin or imatinib treatment. 20 μ M treatment of KU812a for 4 days with LY294002 resulted in significant decrease of GPx activity (0.75-fold, Fig. 20). Combinatorial treatment with imatinib with LY294002 decreased GPx activity 0.2-fold, whereas rapamycin treatment overcame the inhibition of GPx activity by LY294002.

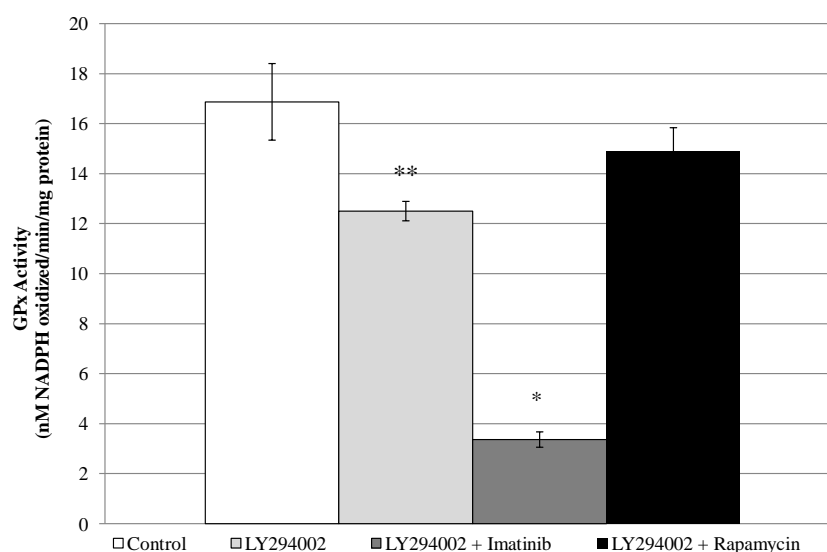


Figure 20. Treatment of KU812a by 20 μ M LY294002 for 4 days inhibits PI3K phosphorylation activity and decreases GPx activity levels.

Effect of LY294002 treatment of KU812a on GPx activity levels alone or in combination with 150 nM imatinib or 1 ng/mL rapamycin as assessed by the coupled spectrophotometric GPx enzyme assay. LY294002 decreased GPx activity 0.75-fold, while LY294002 in combination with imatinib decreased GPx activity 0.2-fold. Treatment of KU812a with both LY294002 and rapamycin recovered GPx activity to control levels. Data shown is representative of one experiment. Three independent experiments were performed for LY294002 treatment.

* = $P < 0.001$, ** = $P < 0.01$.

D. Discussion

The initial goal of this study was to determine if the inhibition of Bcr-Abl by the targeted kinase inhibitor imatinib induced GPx1 protein and activity *in vitro*. The imatinib-induced increase of GPx activity in 4 of 7 CML patient samples following imatinib treatment led to the hypothesis that inhibition of Bcr-Abl or c-Abl increased GPx1 levels and possibly other antioxidant proteins [265]. The data from the previous study (Chapter 2) were surprising, as it did not follow the expectation that inhibition of Bcr-Abl would decrease GPx activity. This initial hypothesis had been based on the observation that GPx1 is directly phosphorylated by c-Abl or Arg in HEK293, SHSY5Y and mouse embryo fibroblasts [232]. In this study, imatinib treatment of HEK293 and SHSY5Y resulted in inhibition of GPx activity and it was also previously reported that catalase was bound and phosphorylated by c-Abl [232,276]. Both GPx1 and catalase were stimulated by H₂O₂ and inhibited apoptotic cell death only in the presence of c-Abl or Arg. Hence, the induction of GPx activity following imatinib treatment was surprising, and warranted further investigation, especially as it could potentially result in the description of an as yet unknown regulation of GPx1 and other antioxidant proteins.

1. Inhibition of Bcr-Abl by imatinib increases protein and activity levels of multiple antioxidant proteins

Because the initial observation that GPx induction occurred in several CML patients, the effect of imatinib on GPx1 protein and activity levels was measured in the CML-derived KU812 Bcr-Abl-positive cell line. KU812 cells were subcloned to provide a homogeneous population in which to begin studying the effects of Bcr-Abl inhibition on GPx1. Initially, the response to imatinib of the clonal cell line KU812a was compared to parental KU812 in order to determine the maximal dose of imatinib for treatment (Fig. 3). Both cell lines

responded to imatinib treatment in a similar manner, reaching a maximal cytostatic dose of 250 nM, with similar growth rates in the two untreated populations. The cytostatic dose of 250 nM imatinib was within the expected range of doses as predicted from previously conducted studies utilizing KU812, which ranged from 100 nM–1000 nM in most studies [277-280]. Because the 250 nM was the maximal dose at which imatinib did not kill KU812a, a lower dose of 150 nM was selected for studies of the effect of imatinib on antioxidants in KU812a. The additional CML cell line MEG-01 was found to be growth-inhibited at a dose of 300 nM, which was again within the range of previously utilized imatinib doses in MEG-01 of 200 nM to 1000 nM [281-283]. Treatment of the Bcr-Abl-positive KU812a and MEG-01 cell lines with imatinib for 7 days increased GPx1, MnSOD and TrxR1 protein levels, but not GPx4, or catalase, whose levels were lowered by treatment (Fig. 4, 7, 10-11). Additionally, GPx1 and MnSOD enzyme activity was significantly increased (Fig. 4, 7, 10). The inhibition of catalase in KU812a in response to imatinib treatment could indicate that c-Abl phosphorylates and increases catalase levels, as was shown in MCF7 and mouse embryo fibroblast cells [276].

a. Steady-state mRNA levels of glutathione peroxidase 1 and manganese superoxide dismutase are not altered by Bcr-Abl inhibition

The induction of GPx1 and MnSOD could have been a result of increased transcription; both MnSOD and GPx1 transcription are regulated by oxidative response proteins such as p53, NF- κ B and AP-1, while the transcription of TrxR1 is regulated by Oct-1, Sp1, Sp3 and Nrf2 [234-237,284-287]. Both these transcription factors and the post-translational regulation of redox sites on the enzymes themselves regulate much of the antioxidant response, so an induction of transcription would be expected following imatinib treatment. However,

neither GPx1 nor MnSOD steady-state transcript levels were altered following imatinib treatment of the KU812a cell line (Fig. 6 and 10). Glutathione peroxidase 1 and MnSOD share multiple common transcription factors with catalase; however, catalase levels were inhibited following imatinib treatment, indicating that if Bcr-Abl inhibition altered transcription of these antioxidants, catalase levels would have been expected to increase as well [236,238,239,288]. The transcriptional regulation of GPx4 is complex: a single gene encodes for three isoforms with two independent transcription start sites [289,290]. Because transcription does not appear to be the mode through which GPx1, MnSOD and TrxR1 are increased following Bcr-Abl inhibition by imatinib treatment, it is expected that the induction of these proteins is post-transcriptional.

b. Inhibition of Bcr-Abl by imatinib increases antioxidant protein levels post-transcriptionally

Transcript stability and translation are two ways in which GPx1, MnSOD and TrxR1 levels could be enhanced by Bcr-Abl inhibition. GPx1 is sensitive to nonsense-mediated decay in low-selenium conditions when the in-frame UGA codon is not recoded to a Sec [132]. Thioredoxin reductase 1 could also potentially be susceptible to this mechanism of regulation; however, the location of the UGA codon immediately prior to the stop codon in the coding sequence generally protects this transcript from decay [291,292]. Manganese superoxide dismutase is also susceptible to mRNA decay in a redox-dependent manner as a result of inhibited import of the immature polypeptide chain [293,294]. Additionally, the MnSOD transcript is bound by an as yet undetermined RNA-binding protein at a translational enhancer element in the 3'-UTR, which may be a component in translation initiation [295-297]. However, comparison of GPx1, MnSOD and TrxR1 transcript sequences by alignment reveals little to no homology among all three transcripts, limiting the likelihood that the increase in these proteins is

through transcript stability or by the regulation of a common RNA binding protein (Appendix B) [298,299]. However, MnSOD and TrxR1 did have several regions of homology in their transcripts, but not within the same regions of mRNA, as the regions of homology in TrxR1 were found within the open reading frame and MnSOD in the 3'-UTR.

The post-transcriptional up-regulation of MnSOD via translation enhancement and an RNA-binding protein could indicate that not all three antioxidant proteins are up-regulated by imatinib treatment; instead, MnSOD alone may be enhanced by Bcr-Abl inhibition. This induction of MnSOD by Bcr-Abl inhibition following imatinib treatment could then lead to an induction of GPx1 and TrxR1 levels. The overexpression of MnSOD *in vitro* has mixed effects on the levels of other antioxidant proteins; some studies have shown no effect on GPx1 levels, but others have shown that increased MnSOD levels lead to an induction of GPx1. For example, overexpression of MnSOD in clonal line of NIH 3T3 mouse fibroblasts resulted in a 1.8-fold increase in MnSOD activity and a 1.5-fold increase in GPx activity, which was hypothesized to be an adaptive response to increased H₂O₂ production by MnSOD [24]. Other NIH 3T3 clones which overexpress MnSOD instead adapted to increased ROS levels through decreased Cu/ZnSOD levels. The increase in GPx activity following MnSOD overexpression indicates that the induction of one antioxidant may lead to the induction of another; however, overexpression of MnSOD in MCF7 breast cancer cells, U118 human glioma, and the A172R rat glioma cell line did not increase either GPx1 or catalase levels [25,26,300]. A similar result was obtained in C3H10T1/2 mouse cells overexpressing MnSOD [301]. However, subclones of U118 all showed increased GPx activity following MnSOD overexpression, which could be a result of the selection of a clone with differing endogenous antioxidant levels prior to transfection [25]. Thus,

it is unclear if increased MnSOD eventually results in the induction of GPx1, possibly as an adaptive response.

Altering MnSOD levels has no clear effect on the induction of other antioxidant proteins, such as GPx1. Similarly, deletion of GPx1 has no effect on MnSOD levels while overexpression of GPx1 in glioma cells which already overexpress MnSOD can overcome MnSOD-induced growth suppression, providing further evidence against the possibility that induction of one antioxidant following imatinib treatment can lead to subsequent induction of additional antioxidants [302,303]. Co-overexpression of GPx1 and MnSOD in pancreatic cancer cells resulted in significantly greater inhibition of cell growth than either protein alone and increased xenografted animal survival [304]. These data indicate that GPx1 and MnSOD are more likely to be induced simultaneously. Finally, overexpression of TrxR1 decreases GPx1 *in vitro*, and an increase in GPx1 is correlated with a decrease in TrxR1 in lactating dairy cows [305,306]. It is unlikely that the induction of only GPx1, MnSOD or TrxR1 by Bcr-Abl inhibition results in an induction of the other antioxidant proteins, as alterations in these proteins have not been shown to correlate previously.

Multiple signal transduction pathways alter translational regulation. Interferons and the Janus kinase (JAK) signal transducer and activator of transcription (STAT) pathway provide a potential common post-transcriptional regulatory pathway among GPx1, MnSOD, and TrxR1. The construction of a cDNA library of BT-20 breast cancer cells treated with β -interferon combined with retinoic acid showed that TrxR1 protein and activity levels increased, but steady-state mRNA levels did not [307]. Treatment of rat hepatocytes with α -interferon also increased MnSOD and GPx1 in a dose-dependent manner; where treatment significantly increased the protein levels of MnSOD and enzyme activity of both GPx1 and MnSOD; GPx1 protein was not

measured in that study [308]. The induction of these antioxidant proteins by interferons indicates a potential route through which these proteins may be induced by Bcr-Abl inhibition.

c. **Increased glutathione peroxidase 1 levels are not a result of decreased rates of protein decay**

The induction of MnSOD, GPx1, and TrxR1 protein levels following inhibition of Bcr-Abl could be as a result of increased protein stability following imatinib treatment. The antibiotic cycloheximide blocks translation by inhibiting the translocation of tRNA during elongation within the ribosomal complex [309,310]. The half-life of GPx1 was experimentally determined to be 72 hours in KU812a following cycloheximide treatment. The rate of GPx1 decay following translation inhibition was determined in the presence or absence of imatinib for a period up to 96 hours. There was no evident increase of protein stability in the presence of imatinib, as the rate of decay between 72 and 96 hours was similar to that found in the absence of imatinib (Fig. 6).

d. **Evidence that post-translational modifications also affect glutathione peroxidase 1 and manganese superoxide dismutase activity**

It is likely that post-translational modifications regulate the activity of GPx1 and MnSOD following inhibition of Bcr-Abl. The degree of protein and activity induction was not equal between in GPx1 and MnSOD following imatinib treatment, with protein induction exceeding activity induction. GPx1 protein levels were enhanced 7-fold and 4-fold in KU812a and MEG-01, but activity only increased respectively 2.5-fold and 1.6-fold (Fig. 4 and 7). Similarly, MnSOD protein increased 4-fold in both CML cell lines (KU812a and MEG-01), but activity increased 2.5-fold (Fig. 10). This indicates that an additional level of regulation is

limiting the activity of these proteins, despite the increased protein levels. Both MnSOD and GPx1 are modified by phosphate- or acetyl-functional groups, and these modifications could be limiting the degree of induction of the activity of these proteins [29,233,252,311]. MnSOD has at least two phosphorylation sites, one of which is modified by calcium availability, where increases in calcium levels result in de-phosphorylation of the protein and an increase in activity [311]. An activating phosphorylation of MnSOD is predicted on serine (Ser)-106, the phosphorylation of which is regulated by cyclin B1/Cdk1 as a stress response [29]. The activity of Cdk1 may be inhibited by imatinib [312], limiting the activation of MnSOD by phosphorylation. While phosphorylation by Cdk1 is a viable candidate for the regulation of MnSOD, there does not appear to be a Cdk1-responsive phosphorylation site on GPx1; however, there is a potential site for Cdk2 phosphorylation (Appendix C) [313]. The enzymatic activity of both GPx1 and MnSOD are potentially inhibited by acetylation, and their deacetylation may be dependent on the mitochondrial isoform of the sirtuin family, Sirt3, a stress-responsive histone deacetylase [31,233,252,314,315]. The potential of a shared regulation of MnSOD and GPx1 by inhibition of Sirt3 provides a potential route through which both of these enzymes may be partially inhibited by imatinib in Bcr-Abl-positive cells.

e. **Increased antioxidant protein levels following imatinib treatment are Bcr-Abl dependent**

Imatinib was designed to specifically target and inhibit the kinase region of c-Abl and Bcr-Abl, however, it does bind and inhibit other proteins, such as c-KIT, PDGFR and NADPH-quinone oxidoreductase (NQO2) [257,258,316]. c-KIT and PDGFR are both receptor tyrosine kinases, and the imatinib IC₅₀ (the dose at which phosphorylation or kinase activity reaches 50% of untreated samples) ranges from 0.2-0.3 μ M, which is the same as for

Bcr-Abl and c-Abl [257,258]. The IC_{50} for imatinib binding to NQO2 is 1.0 μ M, which could partly be attributed to the fact that imatinib must adopt a bent conformation in order to bind the active site of NQO2 [316,317]. The binding of imatinib to multiple proteins could indicate that, despite GPx1, MnSOD and TrxR1 induction in Bcr-Abl-positive cell lines, it could be the inhibition of one of these other proteins that increases GPx1, MnSOD and TrxR1. However, treatment of cells which do not carry the Bcr-Abl translocation (LNCaP) and the immortalized B-lymphocyte line (GM10832) with imatinib did not alter protein or enzyme activity for GPx1, MnSOD and TrxR1 (Fig. 8, 12). If c-Abl, c-KIT, PDGFR, or NQO2 were involved in the regulation of these antioxidant proteins, it would be expected that GPx1, MnSOD and TrxR1 levels would have also increased after imatinib treatment in the absence of Bcr-Abl. Additionally, transfection of a vector containing the Bcr-Abl transcript into LNCaP significantly decreased GPx1 protein and enzyme activity, but not the protein levels of either MnSOD or TrxR1 (Fig. 9 and 13). The inhibition of GPx1 following expression of ectopic Bcr-Abl demonstrates the probability that Bcr-Abl may inhibit GPx1 protein levels, but that MnSOD and TrxR1 are not directly inhibited by Bcr-Abl expression. Increased levels of these two antioxidant proteins may be a response of the cell in order to counteract the induction of apoptosis by imatinib. Imatinib treatment induces apoptosis in CML cells by activation of caspases via the depolarization of the mitochondrial membrane, and the increases in MnSOD and TrxR1 levels could counter apoptosis induced by imatinib treatment, as both of these proteins can inhibit apoptosis [29,114,318].

2. Inhibition of mTOR by rapamycin increases the protein levels of specific selenoproteins

a. Increased selenoprotein levels following mTOR inhibition are independent of Bcr-Abl

The Bcr-Abl kinase up-regulates multiple signal transduction pathways, including the PI3K-Akt-mTOR translation pathway [261,273]. Because the imatinib-induced increase in GPx1, MnSOD, and TrxR1 is post-transcriptional, these proteins are likely induced by translational regulation. The phosphorylation of p70S6 kinase (p70S6K) and eukaryotic translation initiation factor 4E-binding protein 1 (4EBP1) is regulated by mTOR, which results in the phosphorylation of the ribosomal complex protein S6 and the activation of the initiation factor eIF4E [274,275]. There are multiple inhibitors of mTOR, such as rapamycin/sirolimus, everolimus, and temsirolimus; however, most of these compounds inhibit total mTOR activity, whereas rapamycin directly inhibits only mTOR directed translation [319]. Treatment of KU812a, MEG-01, GM10832 and LNCaP cells with 1 ng/mL rapamycin for a period of 72 hours resulted in a significant increase in GPx1 protein and activity levels (Fig. 14 and 16). GPx4 was also increased in GM10832 and LNCaP, while TrxR1 was increased only in GM10832 (Fig. 17). Surprisingly, MnSOD protein was unaltered by rapamycin treatment in all cell lines examined, but MnSOD enzyme activity was increased in KU812a and LNCaP (Fig. 18). The dose of 1 ng/mL rapamycin was selected because it was the lowest cytostatic dose for all cell lines and within the range of cytostatic doses utilized in previous studies (0.1-10 ng/mL) [320,321]. Rapamycin inhibition of mTOR induces severe alterations in mitochondrial membrane potential and decreases ATP production and oxygen consumption via the inhibition of the mTOR-mediated biogenesis and maintenance of mitochondria [322,323]. The increase of MnSOD

activity following treatment with rapamycin could be in response to changes in the mitochondria as a result of altered phosphorylation or acetylation of MnSOD [322]. The lack of response to mTOR inhibition by GPx4 and TrxR1 in the CML cell lines and for TrxR1 in LNCaP could be attributed to the fact that all of the cell lines utilized have numerous mutations and deletions of key proteins, which confer their cancer or immortalized phenotype [270-272,324]. It would be nearly impossible to characterize the differences inherent in all of these lines, so the differential induction of GPx4 and TrxR1 as compared to GPx1 may be a result of the cell lines' genetic complexity. The increase in GPx1 levels was not a result of altered transcription, as steady-state levels were not altered following inhibition of mTOR.

The post-transcriptional increase in GPx1 following rapamycin treatment supports data from the previous imatinib study, and supports that GPx1 may be regulated via the PI3K-Akt-mTOR pathway, both in the presence and absence of Bcr-Abl. The induction of the selenoproteins GPx4 and TrxR1 in LNCaP or GM10832 following mTOR inhibition could indicate that inhibition of mTOR results in a more generalized up-regulation of multiple selenoproteins. Additionally, the induction of GPx1, GPx4, and TrxR1 in GM10832 (the only non-cancer cell line utilized in this study) supports that these selenoproteins may be commonly regulated by mTOR.

b. Increased glutathione peroxidase 1 levels by inhibition of mTOR may be independent of PI3K regulation.

The functionality of mTOR is dependent upon the formation of regulatory complexes (mTORC); rapamycin specifically inhibits the phosphorylation of p70S6K by mTORC1 with only partial inhibition of the 4EBP1 signaling arm [325-327]. Thus, it is probable that the inhibition of p70S6K increases selenoprotein levels. However, prolonged

treatment of cells with rapamycin also eventually results in the inhibition of mTORC2 which phosphorylates and activates Akt [328]. The inhibition of mTORC2 could also increase selenoprotein levels following the inhibition of Akt, which is downstream of PI3K, signaling to an alternative mTORC1-independent pathway. Indeed, the inhibition of PI3K by LY294002 in KU812a significantly decreased GPx activity, which was opposite of the expected increase of GPx activity following PI3K inhibition. The combined treatment of KU812a with LY294002 and imatinib further decreased GPx activity, while combined treatment with LY294002 and rapamycin rescued GPx activity to basal levels (Fig. 20). The inhibition of GPx activity following inhibition of PI3K indicates that the PI3K pathway could induce GPx1 levels. The PI3K pathway is pro-survival; in addition to regulating mTOR, it also regulates transcription factors such as NF- κ B, which regulates the transcription of GPx1 [236,329,330]. Glutathione peroxidase 1 mRNA levels were not measured following treatment of KU812a with LY294002. Inhibition of PI3K thus could have decreased transcription of GPx1, which was enhanced by the Bcr-Abl inhibition of GPx1 protein via mTOR.

The post-transcriptional regulation of the selenoproteins GPx1, GPx4 and TrxR1 is likely dependent on mTOR, but not via the signaling of PI3K-Akt because inhibition of PI3K reduces GPx activity. The Tsc1/Tsc2 protein complex inhibits mTOR activity by the inhibition of the protein Ras homolog enriched in brain (RHEB), a necessary component in the activation and assembly of mTORC1, and Tsc1/Tsc2 activity is inhibited by Akt phosphorylation following activation by PI3K [331-334]. The Erk component of the MAPK pathway also activates mTOR by the inhibition of Tsc1/Tsc2, removing RHEB inhibition and activating mTOR. Thus, the regulation of mTOR by Tsc1/Tsc2 is via a shared pathway between PI3K and MAPK [334]. The potential that GPx1 and potentially other selenoproteins is regulated via the MAPK pathway and

mTOR is suggested in *Saccharomyces cerevisiae* following deletion of Ras, which results in an increase of protein levels of the yeast homolog of GPx1 [335]. Inhibition of target of rapamycin (TOR) in *S. cerevisiae* by rapamycin also induces *GPX1* gene expression. Target of rapamycin in yeast regulates both transcription and translation; therefore, the induction of *GPX1* instead of protein by TOR inhibition is not surprising. As evidenced by the regulation of mTOR by both the MAPK and PI3K signal transduction pathways, there is much crosstalk between these two pathways [331-334]. This makes it difficult to predict which of these pathways is responsible for the increased levels of GPx1, GPx4 and TrxR1 following mTOR inhibition. However, the regulation of mTOR activity by the MAPK signal transduction pathway coupled with evidence that inhibition of PI3K decreases GPx activity presents a plausible route by which GPx1, GPx4 and TrxR1 are induced.

c. **Increased glutathione peroxidase 1 levels following inhibition of mTOR are not dependent on the selenocysteine insertion sequence element for UGA recoding**

Glutathione peroxidase 1, GPx4 and TrxR1 are all members of the selenoprotein family, all of which encode an in-frame UGA for selenocysteine insertion [95,96]. The translation of selenoproteins requires a stem-loop structure in the 3'-UTR, the selenocysteine-insertion sequence (SECIS), in order to recode the UGA from a stop codon into a selenocysteine codon [134]. This process requires multiple accessory proteins, such as SBP2, EFSec, Sec synthase, and others, to bind the SECIS, synthesize the Sec on the tRNA, and bring both complexes to the ribosomal machinery [336]. The recoding of the UGA via the SECIS element is a potential route by which GPx1, GPx4, and TrxR1 may be regulated by mTOR-sensitive proteins. A luciferase reporter construct containing an in-frame UGA and the GPx1

SECIS sequence was used to measure the effect of rapamycin on SECIS-dependent UGA recoding. Inhibition of mTOR by rapamycin did not alter luminescence produced by the SECIS reporter construct, which indicates the probability that regulation of GPx1 protein levels by mTOR is not by UGA recoding.

d. Mammalian target of rapamycin may alter levels of glutathione peroxidase 1 and other selenoproteins by altering translation initiation or elongation

As with all proteins, selenoproteins are also susceptible to regulation of translation initiation and elongation of the polypeptide chain. Because the recoding of the UGA by the GPx1 SECIS element is not altered following mTOR inhibition, it is probable that the observed induction of GPx1 protein occurs at initiation or elongation. Glutathione peroxidase 4 translation is regulated by the binding of guanine-rich sequence-binding factor 1 (GRSF-1) to the GPx4 5'-UTR at an A(G)₄A motif [337]. Binding of GRSF-1 to the GPx4 transcript increases GPx4 protein levels, either through increased Sec insertion efficiency or by an increase in ribosomal binding to the transcript. However, it is unlikely that GRSF-1 also regulates the translation of GPx1 and TrxR1 because neither of the transcripts contain the GRSF-1 binding motif, as determined by BLAST nucleotide sequence analysis [298,299]. The antioxidant protein DJ-1, which reduces H₂O₂ by the oxidation of cysteine at its active site, also binds GPx2, GPx3, SelW, SepS, and GPx4 mRNA [338-340]. The translation of GPx4 is inhibited when DJ-1 is bound to its 5'-UTR [338]. Oxidation of DJ-1 releases the protein from the GPx4 transcript and results in a post-transcriptional increase in GPx4 levels. Increased expression of DJ-1 also increases mTOR activity, especially in response to hypoxic conditions [341]. The release of DJ-

1 from the 5'-UTR of selenoproteins may occur in cooperation with mTOR inhibition by rapamycin and contribute to the regulation of GPx1, GPx4 and TrxR1.

Selenoprotein translation is inefficient; ribosomal loading is approximately one-fifth that expected for the length of a given selenoprotein transcript [342]. Actively translated mRNAs are predicted to have a ribosomal complex every 80-100 nucleotides, which for GPx4 would predict 5-6.5 ribosomal complexes [343,344]. Instead, the GPx4 transcript is found to have 1-2 complexes bound to the transcript, which correspond to the length of the transcript up to the UGA codon. Mutation of the Sec to a cysteine (Cys) increases translation efficiency 100 times and increases ribosomal loading to predicted levels. Selenoprotein translation is dependent on a balance between termination factors that will result in premature termination at the UGA and the UGA recoding elements; the balance of termination and recoding alters the efficiency of Sec insertion [345-347]. It is possible that the regulation of GPx1, GPx4 and TrxR1 by mTOR inhibition is via the efficiency of Sec incorporation, independent of the presence and activity of the SECIS and its associated proteins. Both initiation and elongation are viable mechanisms for the mTOR-directed translational regulation of GPx1, GPx4 and TrxR1.

IV. CONCLUSIONS AND FUTURE DIRECTIONS

The post-transcriptional regulation of antioxidant enzymes is one route by which the redox state of the cell is maintained. Unfortunately, we have a very limited understanding of the mechanisms that control the regulation of antioxidant protein translation and activation for many of these proteins, especially selenoprotein antioxidants like GPx1 [120]. Knowledge of the post-transcriptional regulation of these proteins will aid in better understanding their other roles within the cell, such as apoptosis, cellular proliferation, fertility, and the onset of cancer, diabetes, and other disease states [80].

The observation that treatment of CML patients with imatinib increased GPx activity in a subset of samples revealed a potential mechanism by which GPx1 and other antioxidants may be regulated by Bcr-Abl. We were unable to determine if there was an association between increased GPx activity and patient outcome since only one of the patients studied failed to respond to imatinib treatment. Longer-term follow-up in these patients and a greater sample set could reveal the impact of increased GPx activity in these patients and what proportion of the CML population responds to imatinib treatment with an increase in GPx activity. The *in vivo* observation of an imatinib-induced increase in GPx activity also occurred *in vitro* in two separate CML cell lines; unexpectedly, MnSOD and TrxR1 proteins were also increased. The induction of these antioxidant proteins by imatinib treatment and inhibition of Bcr-Abl was limited to the CML lines, and only GPx1 was susceptible to inhibition by ectopic expression of Bcr-Abl in LNCaP human prostate cancer cells. The suppression of GPx1 by overexpression of Bcr-Abl may indicate that GPx1 protein is inhibited by Bcr-Abl and in CML and its inhibition could be a factor in disease initiation and early progression by the loss of a major antioxidant enzyme [348]. If GPx1 is inhibited by Bcr-Abl, it may be a contributing factor to the increase in ROS levels

observed in some CML patients [349]. The suppression of GPx1 by Bcr-Abl suggests that GPx1 could be utilized as an additional target in the treatment of CML. The biological impact of the decrease in GPx1 by Bcr-Abl nor the impact of the release of suppression by imatinib was not investigated in this study, thus further studies are necessary on the biological implications of GPx1 suppression and its induction in treatment. The increased levels of MnSOD and TrxR1 protein could have been induced by the cell in order to counter the effects of imatinib treatment and the induction of apoptosis. The levels of MnSOD and TrxR1 were increased in the CML cell lines following imatinib treatment but ectopic expression of Bcr-Abl in LNCaP human prostate cancer cells did not inhibit either of these proteins. Increased antioxidant capacity during imatinib treatment could have negative connotations on treatment efficacy if it counteracts apoptotic signaling and thus, could be a contributing factor in the onset of imatinib resistance, which occurs in the majority of CML cases treated for prolonged periods with imatinib [318].

The Bcr-Abl-dependent imatinib induction of GPx1 and other antioxidant proteins revealed a mechanism by which these proteins could be regulated post-transcriptionally and/or post-translationally. The regulation of translation by mTOR provided a prime candidate to investigate the Bcr-Abl-dependent effects on GPx1 levels. Inhibition of mTOR by rapamycin increased GPx1 levels as expected, but surprisingly, two additional selenoproteins, TrxR1 and GPx4, were also altered by mTOR inhibition. Further analysis of GPx1 protein revealed that, while inhibition of mTOR by rapamycin increased GPx1, the inhibition was most likely not propagated via the PI3K pathway because direct inhibition of PI3K resulted in a significant decrease in GPx activity, which rapamycin could recover. These two experiments revealed a complex regulation of GPx1, which requires further investigation. The PI3K pathway may be

inducing *GPX1* expression while mTOR via the MAPK pathway is inhibiting its translation, as shown in Fig. 21. In order to determine if the proposed pathway is correct, mRNA levels for GPx1 should be assessed following PI3K inhibition, as should protein and activity levels following MAPK inhibition.

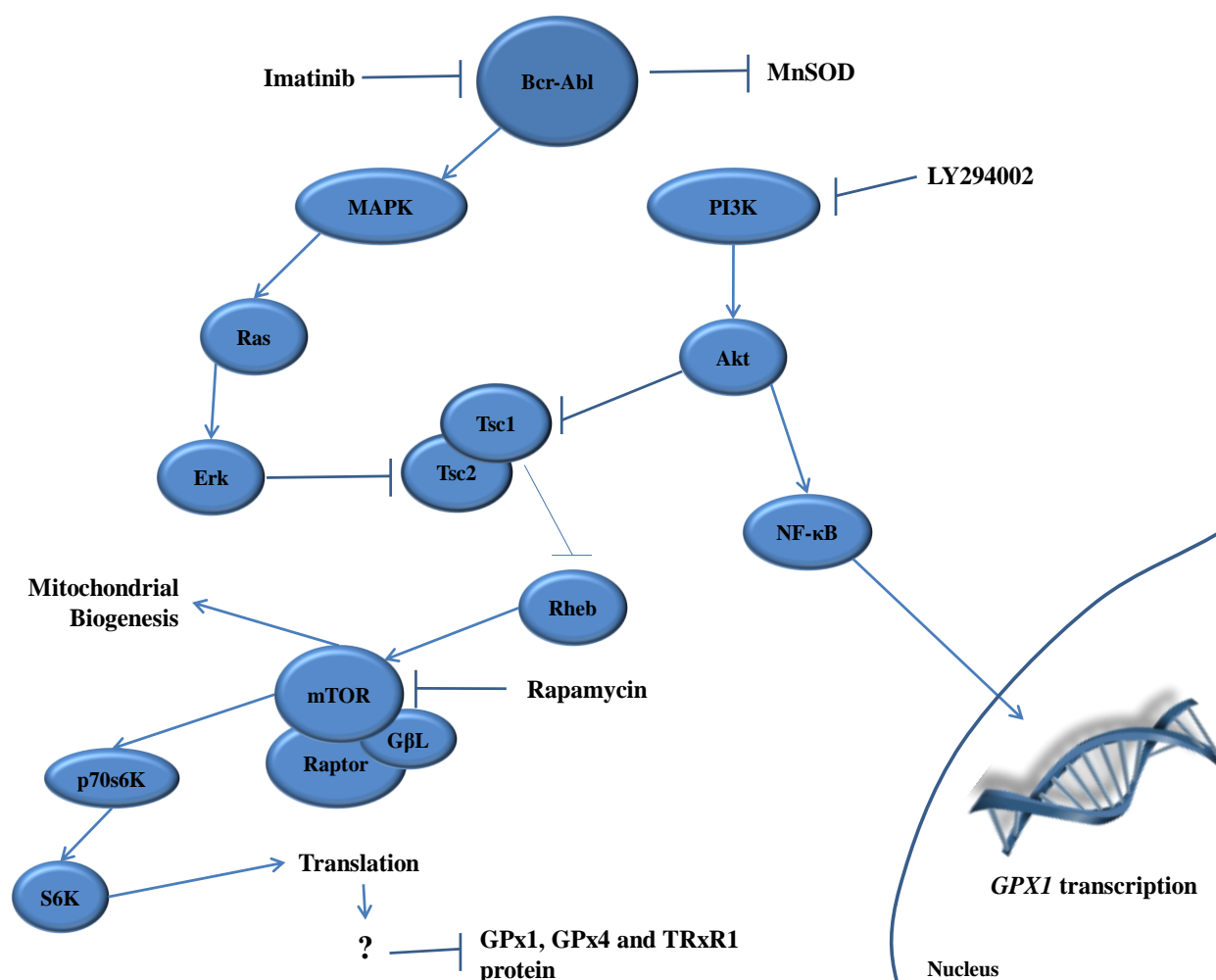


Figure 21. Proposed signaling cascade for the regulation of GPx1 transcription and translation.

The observation that the SECIS-dependent readthrough of the selenocysteine codon was unaffected by mTOR inhibition indicates that the SECIS element is not necessary for this post-transcriptional regulation of GPx1. It is likely, instead, that this regulation is via translation initiation and elongation. The mTOR inhibitor rapamycin predominately targets the p70S6K arm of the mTOR translation pathway, with only partial inhibition of the activity of eIF4E via 4EBP1 [325-327]. It is potentially through the p70S6K-regulated initiation of translation that an as yet unspecified protein is translated which may inhibit subsequent translation of GPx1 and other selenoproteins. Alternatively, because p70S6K and S6 regulate translation initiation, the observation that GPx1 and other selenoprotein levels are increased by the inhibition of p70S6K may reveal a mechanism by which p70S6K inhibits translation of specific proteins such as selenoproteins. The inefficiency of selenoprotein translation could be partially attributed to the competition between the SECIS element and translational termination at the UGA codon [342,345,346]. The S6-directed assembly of the ribosomal complex on GPx1 mRNA could potentially be a factor in the efficiency of the translation of the transcript, as could the competition between termination and SECIS recoding at the UGA, which can be overcome by the mutation of Sec to Cys. Further investigation into which of these two routes, if not both, may inhibit GPx1 translation is warranted.

Treatment of CML cells with imatinib revealed an additional mechanism by which protein activity levels may be altered in treatment. The induction of GPx1 and MnSOD protein was more robust than the induction of their activity. Both GPx1 and MnSOD have been shown to be acetylated, and their activation may be dependent on deacetylation via Sirt3; the moderate induction of activity by imatinib could indicate that imatinib alters the acetylome [31,252,314,315]. In fact, the hyperacetylation of multiple proteins occurs in the presence of

imatinib, and this could indicate the mechanism by which GPx1 and MnSOD activity fails to correlate with their protein levels following imatinib treatment.

Ultimately, the data presented in this dissertation demonstrate that multiple antioxidant proteins are regulated in a post-transcriptional manner in the presence of Bcr-Abl. Also, regulation of GPx1 and other selenoprotein levels may be via mTOR translational control, which is independent of the presence of Bcr-Abl. Additionally, the inhibition of GPx activity by PI3K inhibition could potentially reveal a mechanism by which GPx1 transcription is regulated via NF- κ B, a known transcriptional regulator of GPx1 [236]. If the proposed model is correct, it would reveal a previously undescribed mechanism by which GPx1 and potentially other selenoproteins are regulated, independent of selenium availability and the 3'-UTR SECIS element. Better understanding of the post-transcriptional control of antioxidants will provide further insight into the delicate balance between antioxidants and ROS, and how selenoproteins particularly affect this balance.

APPENDICES

APPENDIX A

Raw densitometry data for protein analysis

TABLE II. BAND INTENSITY AS DETERMINED BY DENSITOMETRY INDICATING THE EFFECT OF IMATINIB TREATMENT OF KU812A ON SELECTED ANTIOXIDANT PROTEINS

Cell line	Target	Treatment	Target Density (calibrated units)	Actin Density (calibrated units)	Normalization	Average Densitometry	Standard Deviation	Fold Change	Average of fold change	Standard Deviation	T-Test P-value
KU812a	GPx1	0 nM Imatinib	4159.10	7251.38	0.57	0.25	0.28	2.28	1.00	1.11	0.02
			729.92	9813.55	0.07			0.30			
			703.36	6610.71	0.11			0.42			
		150 nM Imatinib	15326.78	8222.96	1.86	2.32	0.91	7.41	9.24	3.63	
			17189.00	5095.38	3.37			13.42			
			8739.05	5052.54	1.73			6.88			
KU812a	GPx1	0 nM Imatinib	1022.36	9481.45	0.11			1.00			
		100 nM Imatinib	4307.33	9170.98	0.47			4.36			
		150 nM Imatinib	9396.81	10006.62	0.94			8.71			
KU812a	GPx1	0 day	1906.42	9636.18	0.20			1.00			
		3 day	4588.39	6346.83	0.72			3.65			
		7 day	4744.84	5054.69	0.94			4.74			
KU812a	MnSOD	0 nM Imatinib	3373.50	10871.18	0.31	0.35	0.09	0.88	1.00	0.26	0.004
			1865.50	6483.69	0.29			0.82			
			2892.95	6295.34	0.46			1.30			
		150 nM Imatinib	7733.77	7430.96	1.04	1.09	0.20	2.95	3.08	0.56	
			11358.89	8711.12	1.30			3.70			
			7517.60	8217.95	0.91			2.59			
KU812a	Catalase	0 nM Imatinib	8409.59	8614.60	0.98	0.76	0.25	1.28	1.00	0.33	0.24
			6591.69	7992.93	0.82			1.08			
			6031.48	12410.00	0.49			0.64			
		150 nM Imatinib	7682.35	12161.58	0.63	0.56	0.07	0.83	0.73	0.09	
			6331.99	11670.37	0.54			0.71			
			4510.93	9030.73	0.50			0.66			
KU812a	GPx4	0 nM Imatinib	11911.61	13109.08	0.91	0.97	0.57	0.94	1.00	0.59	0.34
			5414.95	12644.47	0.43			0.44			
			9280.10	5911.40	1.57			1.62			
		150 nM Imatinib	5108.31	16378.95	0.31	0.56	0.31	0.32	0.58	0.32	
			9313.76	10325.02	0.90			0.93			
			10219.37	21879.37	0.47			0.48			
KU812a	TrxR1	0 nM Imatinib	4660.40	10913.62	0.43	0.56	0.12	0.76	1.00	0.21	0.01
			6231.21	10107.21	0.62			1.09			
			6938.03	10684.67	0.65			1.15			
		150 nM Imatinib	16433.64	7566.96	2.17	1.48	0.73	3.85	2.63	1.29	
			12552.05	8061.43	1.56			2.76			
			3324.38	4637.72	0.72			1.27			

APPENDIX A (continued)

TABLE III. BAND INTENSITY AS DETERMINED BY DENSITOMETRY INDICATING THE EFFECT OF CYCLOHEXIMIDE \pm IMATINIB TREATMENT OF KU812A PROTEIN DECAY RATE OF GPX1

Cell line	Target	Treatment	Target Density (calibrated units)	Actin Density (calibrated units)	Normalization
KU812a	GPx1	Control	21391.66	21618.66	0.989499812
		150 nM Imatinib	9003.861	9896.933	0.909762752
72 hour		25 ug/ml cycloheximide	9161.953	10870.066	0.842860844
		Imatinib + cycloheximide	14099.832	14260.652	0.988722816
		150 nM Imatinib	15794.518	14272.066	1.106673554
96 hour		25 ug/ml cycloheximide	4583.74	10137.773	0.452144667
		Imatinib + cycloheximide	1180.841	6608.882	0.17867485

APPENDIX A (continued)

TABLE IV. BAND INTENSITY AS DETERMINED BY DENSITOMETRY INDICATING THE EFFECT OF IMATINIB TREATMENT OF MEG-01 ON SELECTED ANTIOXIDANT PROTEINS

Cell line	Target	Treatment	Target Density (calibrated units)	Actin Density (calibrated units)	Normalization	Average Densitometry	Standard Deviation	Fold Change	Average of fold change	Standard Deviation	T-Test P- value
MEG01	GPx1	0 nM Imatinib	2517.91	21585.92	0.12	0.12	0.01	0.97	1.00	0.09	0.03
			3073.91	27684.69	0.11			0.93			
			3791.81	28800.99	0.13			1.10			
		300 nM Imatinib	19393.28	26873.11	0.72	0.50	0.20	6.02	4.14	1.67	
			9777.71	28594.99	0.34			2.85			
			12833.61	30166.96	0.43			3.55			
MEG01	MnSOD	0 nM Imatinib	1434.65	8603.74	0.17	0.23	0.09	0.73	1.00	0.40	0.002
			873.23	4729.81	0.18			0.81			
			1677.86	5075.54	0.33			1.45			
		300 nM Imatinib	3797.75	5606.21	0.68	0.82	0.12	2.98	3.59	0.53	
			5806.97	6577.90	0.88			3.88			
			3774.13	4245.23	0.89			3.91			
MEG01	Catalase	0 nM Imatinib	3447.96	6527.40	0.53	0.40	0.16	1.34	1.00	0.42	0.88
			2481.74	5553.21	0.45			1.13			
			1175.06	5563.33	0.21			0.53			
		300 nM Imatinib	3354.00	7094.38	0.47	0.38	0.08	1.20	0.96	0.21	
			2157.13	6762.05	0.32			0.81			
			1510.69	4407.15	0.34			0.87			
MEG01	GPx4	0 nM Imatinib	6315.57	5749.21	1.10	1.12	0.25	0.98	1.00	0.22	0.16
			4986.20	5598.21	0.89			0.79			
			7634.50	5511.86	1.39			1.23			
		300 nM Imatinib	2267.36	7014.21	0.32	0.71	0.33	0.29	0.63	0.30	
			6364.45	6821.35	0.93			0.83			
			4180.31	4833.35	0.86			0.77			
MEG01	TrxR1	0 nM Imatinib	358.08	10278.98	0.03	0.03	0.01	1.08	1.00	0.15	0.0004
			262.80	9886.21	0.03			0.82			
			352.11	9882.38	0.04			1.10			
		300 nM Imatinib	7433.86	9212.96	0.81	0.82	0.11	24.94	25.21	3.42	
			10095.62	10849.08	0.93			28.77			
			6354.57	8954.84	0.71			21.94			

APPENDIX A (continued)

TABLE V. BAND INTENSITY AS DETERMINED BY DENSITOMETRY INDICATING THE EFFECT OF IMATINIB TREATMENT OF GM10832 ON SELECTED ANTIOXIDANT PROTEINS

Cell line	Target	Treatment	Target Density (calibrated units)	Actin Density (calibrated units)	Normalization	Average Densitometry	Standard Deviation	Fold Change	Average of fold change	Standard Deviation	T-Test <i>P</i> -value
GM10832	GPx1	0 nM Imatinib	8278.33	7593.03	1.09	1.09	0.13	1.00	1.00	0.12	0.17 ^a
			10578.69	8626.05	1.23			1.12			0.08 ^b
			8139.98	8434.67	0.97			0.88			
		150 nM Imatinib	7189.15	7274.40	0.99	0.96	0.03	0.90	0.88	0.02	
			7315.26	7805.93	0.94			0.86			
			8564.84	8854.05	0.97			0.88			
		300 nM Imatinib	8809.79	9023.10	0.98	0.90	0.07	0.89	0.82	0.06	
			7481.84	8819.71	0.85			0.78			
			6301.55	7252.50	0.87			0.79			
GM10832	MnSOD	0 nM Imatinib	4179.77	4709.52	0.89	1.04	0.33	0.86	1.00	0.32	0.13 ^a
			8985.79	6376.47	1.41			1.36			0.08 ^b
			4248.77	5255.38	0.81			0.78			
		150 nM Imatinib	5220.48	6428.28	0.81	0.57	0.26	0.78	0.55	0.26	
			1725.94	6021.67	0.29			0.28			
			3476.38	5786.81	0.60			0.58			
		300 nM Imatinib	9653.55	6547.13	1.47	1.53	0.18	1.42	1.48	0.18	
			9324.72	6774.13	1.38			1.33			
			12970.62	7492.40	1.73			1.67			
GM10832	Catalase	0 nM Imatinib	6060.13	8166.33	0.74	0.76	0.02	0.98	1.00	0.02	0.09 ^a
			7152.01	9531.69	0.75			0.99			0.05^b
			7403.50	9543.21	0.78			1.03			
		150 nM Imatinib	5914.21	8053.93	0.73	0.67	0.06	0.97	0.89	0.08	
			5888.55	8761.00	0.67			0.89			
			6210.55	10201.54	0.61			0.81			
		300 nM Imatinib	3585.55	10164.21	0.35	0.46	0.18	0.47	0.61	0.24	
			3132.55	8831.35	0.35			0.47			
			3571.89	5319.81	0.67			0.89			
GM10832	GPx4	0 nM Imatinib	17155.68	7140.64	2.40	2.70	0.42	0.89	1.00	0.16	0.48
			14963.18	4982.69	3.00			1.11			
		150 nM Imatinib	14204.42	5241.66	2.71	2.16	0.78	1.00	0.80	0.29	
			13576.81	8445.74	1.61			0.59			
GM10832	TrxR1	0 nM Imatinib	5327.56	2751.23	1.94	1.27	0.58	1.53	1.00	0.46	0.31
			6477.33	7128.62	0.91			0.72			
			8671.45	9099.23	0.95			0.75			
		150 nM Imatinib	6118.26	8895.86	0.69	0.76	0.07	0.54	0.60	0.05	
			8056.96	10285.79	0.78			0.62			
			4191.50	5132.78	0.82			0.65			

^a *P*-value calculated between 0 nM imatinib and 150 nM imatinib

^b *P*-value calculated between 0 nM imatinib and 300 nM imatinib

APPENDIX A (continued)

TABLE VI. BAND INTENSITY AS DETERMINED BY DENSITOMETRY INDICATING THE EFFECT OF IMATINIB TREATMENT OF LNCAP ON SELECTED ANTIOXIDANT PROTEINS

Cell line	Target	Treatment	Target Density (calibrated units)	Actin Density (calibrated units)	Normalization	Average Densitometry	Standard Deviation	Fold Change	Average of fold change	Standard Deviation	T-Test P- value
LNCaP	GPx1	0 nM Imatinib	7073.91	5807.08	1.22	1.08	0.51	1.12	1.00	0.47	0.45
			9780.50	6463.23	1.51			1.40			
			5515.69	10620.21	0.52			0.48			
		500 nM Imatinib	6423.35	6988.38	0.92	0.83	0.16	0.85	0.76	0.15	
			7953.23	8637.81	0.92			0.85			
			4595.74	7170.91	0.64			0.59			
LNCaP	MnSOD	0 nM Imatinib	6300.33	5521.21	0.73	0.67	0.06	1.09	1.00	0.09	0.13
			9818.23	9384.98	0.67			1.00			
			4906.08	8439.08	0.61			0.91			
		500 nM Imatinib	3695.91	8362.01	0.35	0.46	0.18	0.53	0.68	0.27	
			8265.67	6013.77	0.35			0.53			
			6728.57	8081.67	0.67			1.00			
LNCaP	Catalase	0 nM Imatinib	5862.33	6439.84	0.91	0.84	0.21	1.08	1.00	0.24	0.70
			7829.08	7825.71	1.00			1.19			
			5864.38	9637.40	0.61			0.72			
		500 nM Imatinib	6678.98	7978.86	0.84	1.03	0.77	1.00	1.22	0.91	
			8418.03	4501.33	1.87			2.23			
			3316.23	8817.26	0.38			0.45			
LNCaP	GPx4	0 nM Imatinib	3919.13	7057.62	0.56	0.61	0.08	0.91	1.00	0.13	0.40
			5524.50	7858.59	0.70			1.15			
			5329.62	9264.98	0.58			0.94			
		500 nM Imatinib	5820.79	7766.52	0.75	1.07	0.83	1.23	1.75	1.36	
			8752.08	4344.21	2.01			3.30			
			3623.50	8197.26	0.44			0.72			

APPENDIX A (continued)

**TABLE VII. BAND INTENSITY AS DETERMINED BY DENSITOMETRY
INDICATING THE TRANSFECTION OF BCR-ABL INTO LNCAP ON
GPX1**

Cell line	Target	Treatment	Target Density (calibrated units)	Actin Density (calibrated units)	Normalization	Average Densitometry	Standard Deviation	Fold Change	Average of fold change	Standard Deviation	T-Test P- value
LNCaP	GPx1	Vector	6744.67	3495.01	1.93	1.68	0.29	1.15	1.00	0.17	0.006^a
			6362.62	3653.67	1.74			1.04			0.02^b
			7814.03	5710.23	1.37			0.81			
		KD Bcr-Abl ^c	5306.38	8918.10	0.60	0.73	0.11	0.35	0.43	0.07	
			3290.20	4139.81	0.79			0.47			
			5440.28	6905.79	0.79			0.47			
		Bcr-Abl	1552.91	4201.18	0.37	0.74	0.36	0.22	0.44	0.21	
			5071.21	4660.79	1.09			0.65			
			4728.06	6232.36	0.76			0.45			
LNCaP	MnSOD	Vector	8130.38	9235.45	0.88	1.23	0.53	0.72	1.00	0.43	0.8 ^a
			12167.62	6639.23	1.83			1.50			0.32 ^b
			9187.15	9536.62	0.96			0.79			
		KD Bcr-Abl ^c	10955.86	8674.33	1.26	1.31	0.04	1.03	1.07	0.03	
			9613.91	7299.45	1.32			1.07			
			8940.45	6680.03	1.34			1.09			
		Bcr-Abl	9173.91	6840.23	1.34	1.75	0.60	1.09	1.43	0.49	
			10923.45	4471.69	2.44			1.99			
			8101.31	5526.36	1.47			1.20			
LNCaP	TrxR1	Vector	6811.01	9482.79	0.72	0.93	0.25	0.77	1.00	0.27	0.11 ^a
			9028.96	7464.74	1.21			1.30			0.18 ^b
			8567.96	9972.86	0.86			0.92			
		KD Bcr-Abl ^c	11445.84	8926.64	1.28	1.30	0.19	1.38	1.40	0.21	
			8515.84	7640.62	1.11			1.20			
			9710.96	6479.57	1.50			1.61			
		Bcr-Abl	7905.60	7119.59	1.11	1.51	0.57	1.20	1.62	0.62	
			10116.84	4668.38	2.17			2.33			
			7280.89	5821.43	1.25			1.35			

^a P-value calculated for Vector compared to KD Bcr-Abl

^b P-value calculated for Vector compared to Bcr-Abl

^c KD Bcr-Abl = Kinase deficient Bcr-Abl vector

APPENDIX A (continued)

**TABLE VIII. BAND INTENSITY AS DETERMINED BY DENSITOMETRY
INDICATING THE EFFECT OF RAPAMYCIN TREATMENT OF
KU812A ON SELECTED ANTIOXIDANT PROTEINS**

Cell line	Target	Treatment	Target Density (calibrated units)	Actin Density (calibrated units)	Normalization	Average Densitometry	Standard Deviation	Fold Change	Average of fold change	Standard Deviation	T-Test <i>P</i> -value
KU812a	GPx1	0 ng/ml Rapamycin	3859.79	12331.52	0.31	0.35	0.03	0.90	1.00	0.09	0.05
			3696.81	10282.35	0.36			1.03			
			5319.88	14125.00	0.38			1.08			
		1 ng/ml Rapamycin	11661.59	16061.30	0.73	1.04	0.42	2.08	2.96	1.21	
			10637.62	12270.54	0.87			2.48			
			11260.52	7419.13	1.52			4.34			
KU812a	MnSOD	0 ng/ml Rapamycin	3501.90	2785.03	1.26	1.15	0.24	1.09	1.00	0.21	0.23
			4521.69	5144.54	0.88			0.76			
			4327.72	3286.93	1.32			1.14			
		1 ng/ml Rapamycin	5199.03	2752.95	1.89	2.58	1.71	1.64	2.24	1.48	
			4849.67	1073.53	4.52			3.92			
			8700.64	6595.10	1.32			1.15			
KU812a	GPx4	0 ng/ml Rapamycin	9400.40	10268.59	0.92	0.90	0.03	1.02	1.00	0.03	0.10
			7066.15	7756.03	0.91			1.02			
			9517.88	11068.32	0.86			0.96			
		1 ng/ml Rapamycin	13201.97	10585.40	1.25	1.33	0.35	1.39	1.49	0.39	
			10666.28	6217.81	1.72			1.92			
			10945.59	10594.30	1.03			1.15			
KU812a	TrxR1	0 ng/ml Rapamycin	6929.13	8737.50	0.79	0.75	0.05	1.06	1.00	0.06	0.21
			5303.67	7582.38	0.70			0.93			
			7205.91	9561.40	0.75			1.01			
		1 ng/ml Rapamycin	9402.35	10840.69	0.87	1.04	0.38	1.16	1.39	0.51	
			8631.23	11037.10	0.78			1.04			
			7968.03	5385.85	1.48			1.98			

APPENDIX A (continued)

TABLE IX. BAND INTENSITY AS DETERMINED BY DENSITOMETRY INDICATING THE EFFECT OF RAPAMYCIN TREATMENT OF MEG-01 ON SELECTED ANTIOXIDANT PROTEINS

Cell line	Target	Treatment	Target Density (calibrated units)	Actin Density (calibrated units)	Normalization	Average Densitometry	Standard Deviation	Fold Change	Average of fold change	Standard Deviation	T-Test P- value
MEG01	GPx1	0 ng/ml Rapamycin	8987.86	13628.40	0.66	0.69	0.05	0.95	1.00	0.07	0.05
			12322.71	16486.18	0.75			1.08			
			10668.88	15976.05	0.67			0.97			
		1 ng/ml Rapamycin	10344.02	13148.98	0.79	0.88	0.11	1.14	1.28	0.16	
			15453.76	15371.05	1.01			1.45			
			13863.49	16067.69	0.86			1.25			
MEG01	MnSOD	0 ng/ml Rapamycin	7459.59	10944.33	0.68	0.79	0.09	0.87	1.00	0.12	0.47
			12272.44	14465.86	0.85			1.08			
			11141.98	13493.23	0.83			1.05			
		1 ng/ml Rapamycin	8286.74	14105.59	0.59	0.71	0.14	0.75	0.90	0.17	
			10962.25	12796.18	0.86			1.09			
			7968.33	11670.93	0.68			0.87			
MEG01	GPx4	0 ng/ml Rapamycin	8580.57	8681.35	0.99	1.04	0.07	0.95	1.00	0.07	0.37
			10032.86	8912.35	1.13			1.08			
			10837.64	10753.40	1.01			0.97			
		1 ng/ml Rapamycin	7721.62	8297.64	0.93	5.43	7.50	0.89	5.22	7.20	
			9532.28	7439.54	1.28			1.23			
			2245.45	159.39	14.09			13.54			
MEG01	TrxR1	0 ng/ml Rapamycin	2001.42	6355.32	0.31	0.37	0.05	0.84	1.00	0.14	0.19
			2610.01	6228.50	0.42			1.12			
			2998.13	7720.45	0.39			1.04			
		1 ng/ml Rapamycin	2536.89	7883.15	0.32	0.29	0.02	0.86	0.79	0.07	
			2704.01	9464.62	0.29			0.76			
			1988.18	7242.13	0.27			0.73			

APPENDIX A (continued)

TABLE X. BAND INTENSITY AS DETERMINED BY DENSITOMETRY INDICATING THE EFFECT OF RAPAMYCIN TREATMENT OF GM10832 ON SELECTED ANTIOXIDANT PROTEINS

Cell line	Target	Treatment	Target Density (calibrated units)	Actin Density (calibrated units)	Normalization	Average Densitometry	Standard Deviation	Fold Change	Average of fold change	Standard Deviation	T-Test P- value
GM10832	GPx1	0 ng/ml Rapamycin	8248.43	4971.28	1.66	1.41	0.56	1.18	1.00	0.39	0.04
			10159.03	5671.88	1.79			1.27			
			3845.13	4992.74	0.77			0.55			
		1 ng/ml Rapamycin	16475.76	5660.35	2.91	2.53	0.33	2.07	1.80	0.24	
			13826.52	5807.73	2.38			1.69			
			13945.56	6087.10	2.29			1.63			
GM10832	MnSOD	0 ng/ml Rapamycin	8528.66	5080.10	1.68	1.02	0.61	1.65	1.00	0.60	0.79
			9283.40	10505.90	0.88			0.87			
			4861.21	10065.90	0.48			0.48			
		1 ng/ml Rapamycin	12493.64	15188.02	0.82	0.88	0.55	0.81	0.87	0.54	
			15322.23	10527.92	1.46			1.43			
			2644.23	7141.62	0.37			0.36			
GM10832	GPx4	0 ng/ml Rapamycin	3429.55	7156.64	0.48	0.49	0.43	0.97	1.00	0.88	0.05
			7194.21	7707.90	0.93			1.90			
			304.26	4681.39	0.06			0.13			
		1 ng/ml Rapamycin	15841.40	4480.28	3.54	2.33	1.05	7.18	4.74	2.12	
			9047.15	4961.23	1.82			3.70			
			12303.87	7513.41	1.64			3.32			
GM10832	TrxR1	0 ng/ml Rapamycin	4657.84	5970.84	0.78	0.76	0.06	1.02	1.00	0.08	0.002
			6046.96	8660.81	0.70			0.91			
			6556.08	8038.10	0.82			1.07			
		1 ng/ml Rapamycin	11457.33	8266.91	1.39	1.53	0.16	1.81	2.00	0.21	
			12170.86	8122.98	1.50			1.96			
			9785.23	5757.68	1.70			2.22			

APPENDIX A (continued)

TABLE XI. BAND INTENSITY AS DETERMINED BY DENSITOMETRY INDICATING THE EFFECT OF RAPAMYCIN TREATMENT OF LNCAP ON SELECTED ANTIOXIDANT PROTEINS

Cell line	Target	Treatment	Target Density (calibrated units)	Actin Density (calibrated units)	Normalization	Average Densitometry	Standard Deviation	Fold Change	Average of fold change	Standard Deviation	T-Test P- value
LNCaP	GPx1	0 ng/ml Rapamycin	6171.84	7417.62	0.83	0.73	0.12	1.14	1.00	0.16	0.02
			5852.45	7663.52	0.76			1.04			
			4221.26	7006.52	0.60			0.82			
		1 ng/ml Rapamycin	7580.33	5320.98	1.42	1.22	0.18	1.94	1.67	0.25	
			9513.50	8861.35	1.07			1.47			
			9661.21	8268.67	1.17			1.59			
LNCaP	MnSOD	0 ng/ml Rapamycin	4770.86	9531.33	0.50	0.49	0.09	1.01	1.00	0.18	0.28
			6657.81	11527.69	0.58			1.17			
			5104.45	12621.50	0.40			0.82			
		1 ng/ml Rapamycin	3200.91	9662.57	0.33	0.37	0.14	0.67	0.75	0.29	
			5875.15	11004.23	0.53			1.08			
			1908.08	7515.90	0.25			0.51			
LNCaP	GPx4	0 ng/ml Rapamycin	1231.50	9539.67	0.13	0.17	0.07	0.75	1.00	0.43	0.02
			1234.06	9583.64	0.13			0.75			
			760.53	2960.55	0.26			1.50			
		1 ng/ml Rapamycin	13835.09	7595.61	1.82	1.48	0.60	10.62	8.61	3.48	
			8204.45	10417.90	0.79			4.59			
			7526.86	4134.37	1.82			10.61			

APPENDIX B

NCBI BLAST Alignment for sequence homology between GPx1, MnSOD and TrxR1.

GPx1 vs. MnSOD

BLAST® Basic Local Alignment Search Tool

Home Recent Results Saved Strategies Help

My NCBI [Sign In] [Register]

NCBI/BLAST/blastn suite-2sequences/ Formatting Results - F9DS010C114

[Edit and Resubmit](#) [Save Search Strategies](#) [Formatting options](#) [Download](#)

[You Tube](#) [Learn about the enhanced report](#) [Blast report description](#)

[Change the result display back to traditional format](#)

Blast 2 sequences

GPx1 vs MnSOD

Query ID	Id 15123	Subject ID	15125
Description	None	Description	None
Molecule type	nucleic acid	Molecule type	nucleic acid
Query Length	921	Subject Length	1593
		Program	BLASTN 2.2.27+ Citation

No significant similarity found. For reasons why, click here

Other reports: [Search Summary](#) [Taxonomy reports](#)

BLAST is a registered trademark of the National Library of Medicine.

Copyright | Disclaimer | Privacy | Accessibility | Contact | Send feedback

NCBI | NLM | NIH | DHHS

GPx1 vs. TrxR1

BLAST® Basic Local Alignment Search Tool

Home Recent Results Saved Strategies Help

My NCBI [Sign In] [Register]

NCBI/BLAST/blastn suite-2sequences/ Formatting Results - F9EAD984114

[Edit and Resubmit](#) [Save Search Strategies](#) [Formatting options](#) [Download](#)

[You Tube](#) [Learn about the enhanced report](#) [Blast report description](#)

[Change the result display back to traditional format](#)

Blast 2 sequences

GPx1 vs TrxR1

Query ID	Id 57191	Subject ID	57193
Description	None	Description	None
Molecule type	nucleic acid	Molecule type	nucleic acid
Query Length	921	Subject Length	3846
		Program	BLASTN 2.2.27+ Citation

No significant similarity found. For reasons why, click here

Other reports: [Search Summary](#) [Taxonomy reports](#)

BLAST is a registered trademark of the National Library of Medicine.

Copyright | Disclaimer | Privacy | Accessibility | Contact | Send feedback

NCBI | NLM | NIH | DHHS

APPENDIX B (continued)

MnSOD vs TrxR1

BLAST Basic Local Alignment Search Tool

Home Recent Results Saved Strategies Help

My NCBI [Sign In] [Register]

NCBI/ BLAST/ blastn suite-2sequences/ Formatting Results - F9ECX3E6114

[Edit and Resubmit](#) [Save Search Strategies](#) [Formatting options](#) [Download](#) [Change the result display back to traditional format](#)

[YouTube](#) [Learn about the enhanced report](#) [Blast report description](#)

Blast 2 sequences

MnSOD vs TrxR1

Query ID: lcl|11807
Description: None
Molecule type: nucleic acid
Query Length: 1593

Subject ID: 11809
Description: None
Molecule type: nucleic acid
Subject Length: 3846
Program: BLASTN 2.2.27+ [Citation](#)

Other reports: [Search Summary](#) [Taxonomy reports](#)

[Graphic Summary](#)

[Dot Matrix View](#)

[Descriptions](#) [Provide feedback on the new report](#)

Sequences producing significant alignments:

Select: [All](#) [None](#) Selected: 0

[Alignments](#) [Download](#) [Graphics](#)

	Description	Max score	Total score	Query cover	E value	Max ident	Accession
<input type="checkbox"/>	None provided	26.5	70.6	2%	0.062	100%	11809

[Alignments](#) [Provide feedback on the new report](#)

[Download](#) [Graphics](#) sort by: Query start position

Sequence ID: lcl|11809 Length: 3846 Number of Matches: 3

Range 1: 3597 to 3610 [Graphics](#) [Next Match](#) [Previous Match](#)

Score	Expect	Identities	Gaps	Strand
26.5 bits(28)	0.062	14/14(100%)	0/14(0%)	Plus/Minus

Query 743 AGGCCTGATTATCT 756
|||||
Sbjct 3610 AGGCCTGATTATCT 3597

Range 2: 707 to 717 [Graphics](#) [Next Match](#) [Previous Match](#) [First Match](#)

Score	Expect	Identities	Gaps	Strand
21.1 bits(22)	2.6	11/11(100%)	0/11(0%)	Plus/Minus

Query 1103 TTCCATCCATA 1113
|||||
Sbjct 717 TTCCATCCATA 707

Range 3: 3520 to 3541 [Graphics](#) [Next Match](#) [Previous Match](#) [First Match](#)

Score	Expect	Identities	Gaps	Strand
22.9 bits(24)	0.76	18/22(82%)	0/22(0%)	Plus/Minus

Query 1194 TTAATAATAAATAAATAAATAA 1215
|||||
Sbjct 3541 TTAATAATAAATAAATAAATAA 3520

[Related Information](#)

APPENDIX C

Potential sites of post-translational modification- Phosphorylation of GPx1 #1

1/10/13

Motif Scan

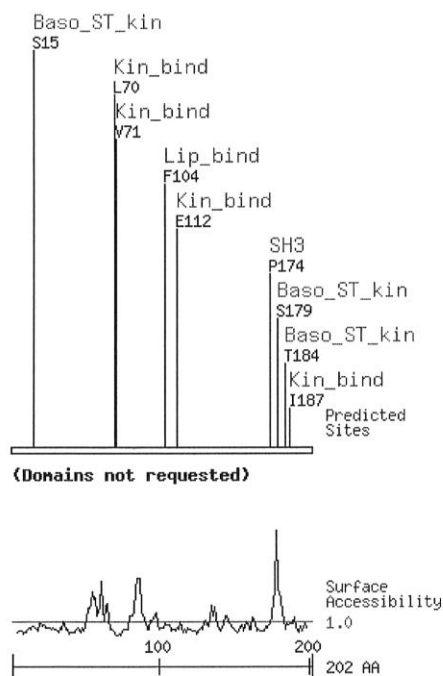
Motif Scan Graphic Results: GPX1

Description: User-entered sequence

Motifs scanned: All

Stringency: Medium

Show domains: No



Src homology 3 group (SH3)

Intersectin SH3A

Gene Card [ITSN](#)

Site	Score	Percentile	Sequence	SA
P174	<u>0.6979</u>	0.962 %	<u>LVGPDGVPLRRYSRR</u>	0.823

Basophilic serine/threonine kinase group (Baso_ST_kin)

Calmodulin dependent

Gene Card [CAMK2G](#)

Kinase 2

Site	Score	Percentile	Sequence	SA
T184	<u>0.3853</u>	0.045 %	<u>RYSRRFQTIDIEPDI</u>	0.407

APPENDIX C (continued)

Potential sites of post-translational modification- Phosphorylation of GPx1 #2

1/10/13

Motif Scan

Protein Kinase A

Gene Card **PRKACG**

Site	Score	Percentile	Sequence	SA
S179	<u>0.4094</u>	0.463 %	<u>GVPLRRYSRRFQTID</u>	3.131

PKC delta

Gene Card **PRKCD**

Site	Score	Percentile	Sequence	SA
S15	<u>0.4323</u>	0.479 %	<u>AAAAAAQSVYAFSAR</u>	0.631

Protein Kinase A

Gene Card **PRKACG**

Site	Score	Percentile	Sequence	SA
T184	<u>0.4561</u>	0.740 %	<u>RYSRRFQTIDIEPDI</u>	0.407

Akt Kinase

Gene Card **AKT1**

Site	Score	Percentile	Sequence	SA
T184	<u>0.5604</u>	0.599 %	<u>RYSRRFQTIDIEPDI</u>	0.407

Kinase binding site group (Kin_bind)

Erk D-domain

Gene Card **MAPK1**

Site	Score	Percentile	Sequence	SA
L70	<u>0.5846</u>	0.201 %	<u>RRLGPRGLVVLGFPC</u>	0.166

PDK1 Binding

Gene Card **PDPK1**

Site	Score	Percentile	Sequence	SA
E112	<u>0.6079</u>	0.769 %	<u>EPNFMLFEKCEVNGA</u>	0.526

Erk D-domain

Gene Card **MAPK1**

Site	Score	Percentile	Sequence	SA
V71	<u>0.6735</u>	0.826 %	<u>RLGPRGLVVLGFPCN</u>	0.084

Erk D-domain

Gene Card **MAPK1**

Site	Score	Percentile	Sequence	SA
I187	<u>0.5062</u>	0.051 %	<u>RRFQTIDIEPDIEAL</u>	0.841

Lipid binding group (Lip_bind)

PIP3-binding PH

Gene Card **PIP3-E**

Site	Score	Percentile	Sequence	SA
F104	<u>0.7409</u>	0.862 %	<u>YVRPGGGFEPNFMLE</u>	0.869

Repeat Scan at High StringencyRepeat Scan at Low Stringency**Scan Another Protein**

APPENDIX C (continued)**Potential sites of post-translational modification- Phosphorylation of GPx1 #3**

1/10/13

Motif Scan

DISCLAIMER: These predictions are purely speculative and should be used with EXTREME CAUTION because they are based on the assumption that the peptide library data is correct and sufficient to predict a site.

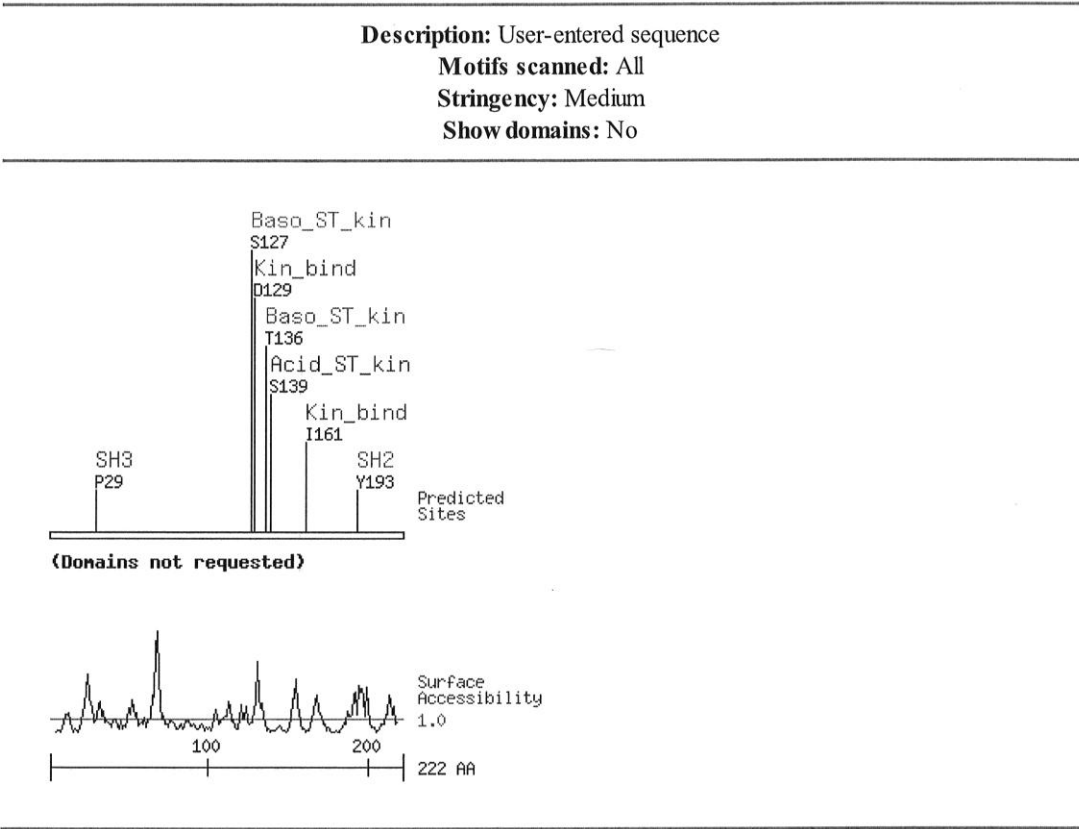
APPENDIX C (continued)

Potential sites of post-translational modification- Phosphorylation of MnSOD #1

1/10/13

Motif Scan

Motif Scan Graphic Results: MNSOD



Src homology 2 group (SH2)					
Grb2 SH2			Gene Card GRB2		
Site	Score	Percentile	Sequence	SA	
Y193	<u>0.5132</u>	0.718 %	<u>EHAYYLOQYKNVRPDY</u>	1.271	
Src homology 3 group (SH3)					
Grb2 SH3			Gene Card GRB2		
Site	Score	Percentile	Sequence	SA	
P29	<u>0.5038</u>	0.496 %	<u>SRQKHSLPDLPYDYG</u>	0.834	
Basophilic serine/threonine kinase group (Baso_ST_kin)					
PKC epsilon			Gene Card PRKCE		
Site	Score	Percentile	Sequence	SA	
T136	<u>0.4275</u>	0.538 %	<u>DKFKEKLTAASVGVO</u>	0.746	
PKC zeta			Gene Card PRKCZ		

APPENDIX C (continued)

Potential sites of post-translational modification- Phosphorylation of MnSOD #2

1/10/13

Motif Scan

<u>Site</u>	<u>Score</u>	<u>Percentile</u>	<u>Sequence</u>	<u>SA</u>
S127	<u>0.4454</u>	0.097 %	<u>AIKRDFGSFDKFKEK</u>	0.761
PKC zeta		Gene Card <u>PRKCZ</u>		
<u>Site</u>	<u>Score</u>	<u>Percentile</u>	<u>Sequence</u>	<u>SA</u>
T136	<u>0.5373</u>	0.910 %	<u>DKFKEKLTAASVGVO</u>	0.746
Acidophilic serine/threonine kinase group (Acid_ST_kin)		Gene Card <u>CSNK1G2</u>		
Casein Kinase 1		Gene Card <u>CSNK1G2</u>		
<u>Site</u>	<u>Score</u>	<u>Percentile</u>	<u>Sequence</u>	<u>SA</u>
S139	<u>0.3958</u>	0.321 %	<u>KEKLTAASVGVOGSG</u>	0.171
Kinase binding site group (Kin_bind)		Gene Card <u>PDPK1</u>		
PDK1 Binding		Gene Card <u>PDPK1</u>		
<u>Site</u>	<u>Score</u>	<u>Percentile</u>	<u>Sequence</u>	<u>SA</u>
D129	<u>0.5784</u>	0.439 %	<u>KRDFGSFDKFKEKLT</u>	1.538
Erk D-domain		Gene Card <u>MAPK1</u>		
<u>Site</u>	<u>Score</u>	<u>Percentile</u>	<u>Sequence</u>	<u>SA</u>
I161	<u>0.6461</u>	0.533 %	<u>KERGHLOIAACPNOQD</u>	0.126

[Repeat Scan at High Stringency](#)

[Repeat Scan at Low Stringency](#)



[Scan Another Protein](#)

DISCLAIMER: These predictions are purely speculative and should be used with EXTREME CAUTION because they are based on the assumption that the peptide library data is correct and sufficient to predict a site.

APPENDIX C (continued)

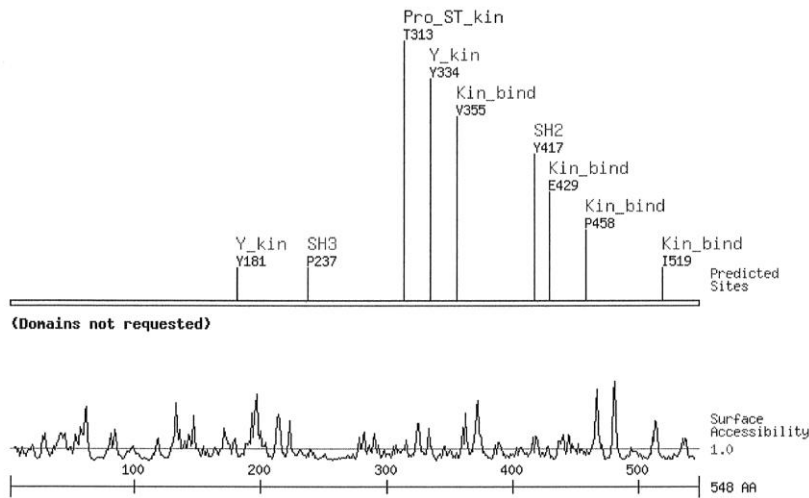
Potential sites of post-translational modification- Phosphorylation of TrxR1 #1

1/10/13

Motif Scan

Motif Scan Graphic Results: TRXR1

Description: User-entered sequence
Motifs scanned: All
Stringency: Medium
Show domains: No



Tyrosine kinase group (Y_kin)					
Src Kinase			Gene Card <u>SRC</u>		
Site	Score	Percentile	Sequence	SA	
Y181	<u>0.5042</u>	0.639 %	<u>KVVYENAYGQFIGPH</u>	0.899	
Insulin Receptor Kinase			Gene Card <u>INSR</u>		
Site	Score	Percentile	Sequence	SA	
Y334	<u>0.6204</u>	0.761 %	<u>EEIIEGEYNTVMLAI</u>	1.101	
Src homology 2 group (SH2)					
Fgr SH2			Gene Card <u>FGR</u>		
Site	Score	Percentile	Sequence	SA	
Y417	<u>0.4373</u>	0.324 %	<u>GSTVKCDYENVPTTV</u>	0.690	
Grb2 SH2			Gene Card <u>GRB2</u>		
Site	Score	Percentile	Sequence	SA	
Y417	<u>0.4615</u>	0.343 %	<u>GSTVKCDYENVPTTV</u>	0.690	
Abl SH2			Gene Card <u>ABL1</u>		
Site	Score	Percentile	Sequence	SA	
Y417	<u>0.4881</u>	0.992 %	<u>GSTVKCDYENVPTTV</u>	0.690	
Src homology 3 group (SH3)					
Abl SH3			Gene Card <u>ABL1</u>		

APPENDIX C (continued)

Potential sites of post-translational modification- Phosphorylation of TrxR1 #2

1/10/13

Motif Scan				
Site	Score	Percentile	Sequence	SA
P237	<u>0.4855</u>	0.840 %	<u>SDDLFLPYCPGKTL</u>	0.509
Proline-dependent serine/threonine kinase group (Pro_ST_kin)				
Cdk5 Kinase Gene Card CDK5				
Site	Score	Percentile	Sequence	SA
T313	<u>0.4746</u>	0.652 %	<u>VEQIEAGTPGRLRVV</u>	0.991
Cdc2 Kinase Gene Card CDC2				
Site	Score	Percentile	Sequence	SA
T313	<u>0.5227</u>	0.751 %	<u>VEQIEAGTPGRLRVV</u>	0.991
Kinase binding site group (Kin_bind)				
PDK1 Binding Gene Card PDPK1				
Site	Score	Percentile	Sequence	SA
E429	<u>0.5781</u>	0.436 %	<u>TTVFTPLEYGACGLS</u>	0.793
Erk1 Binding Gene Card MAPK3				
Site	Score	Percentile	Sequence	SA
P458	<u>0.6159</u>	0.595 %	<u>VYHSYFWPLEWTIPS</u>	0.485
Erk D-domain Gene Card MAPK1				
Site	Score	Percentile	Sequence	SA
V355	<u>0.6328</u>	0.436 %	<u>RKIGLETGVKINEK</u>	0.624
Erk D-domain Gene Card MAPK1				
Site	Score	Percentile	Sequence	SA
I519	<u>0.6036</u>	0.273 %	<u>KKQLDSTIGIHPVCA</u>	0.293

[Repeat Scan at High Stringency](#)

[Repeat Scan at Low Stringency](#)



[Scan Another Protein](#)

DISCLAIMER: These predictions are purely speculative and should be used with EXTREME CAUTION because they are based on the assumption that the peptide library data is correct and sufficient to predict a site.

APPENDIX D

IRB- Protocols- Dr. Alan M. Diamond #1

UNIVERSITY OF ILLINOIS AT CHICAGO

Office for the Protection of Research Subjects (OPRS)
Office of the Vice Chancellor for Research (MC 672)
203 Administrative Office Building
1737 West Polk Street
Chicago, Illinois 60612-7227

Exemption Granted

November 21, 2009

Alan M. Diamond, PhD
Pathology
The Department of Pathology
840 S. Wood St., RM 130 CSN, M/C 847
Chicago, IL 60612
Phone: (312) 413-8747 / Fax: (312) 355-0042

RE: Research Protocol # 2009-1005
"Selenium as an Adjuvant to Imatinib Therapy"

PAF#: 2007-04733
Grant/Contract No: 5R21CA129590-02
Grant/Contract Title: Selenium as an Adjuvant to Imatinib Therapy
Sponsor: NCI - National Cancer Institute

Dear Dr. Diamond:

Your Claim of Exemption was reviewed on November 21, 2009 and it was determined that your research meets the criteria for exemption. You may now begin your research.

Your research may be conducted at UIC and with existing de-identified samples obtained from the Oregon Health and Sciences University.

Exemption Period: November 21, 2009 – November 20, 2012

The specific exemption category under 45 CFR 46.101(b) is:

(4) Research involving the collection or study of existing data, documents, records, pathological specimens, or diagnostic specimens, if these sources are publicly available or if the information is recorded by the investigator in such a manner that subjects cannot be identified, directly or through identifiers linked to the subjects.

Please note the Review History of this submission:

Receipt Date	Submission Type	Review Process	Review Date	Review Action
11/02/2009	Initial Review	Exempt	11/06/2009	Modifications Required
11/09/2009	Response to Modifications	Exempt	11/21/2009	Approved

You are reminded that investigators whose research involving human subjects is determined to be exempt from the federal regulations for the protection of human subjects still have responsibilities

Phone: 312-996-1711

<http://www.uic.edu/depts/ovcr/oprs/>

Fax: 312-413-2929

APPENDIX D (continued)

IRB protocols- Dr. Alan M. Diamond #2

2009-1005

Page 2 of 2

November 21, 2009

for the ethical conduct of the research under state law and UIC policy. Please be aware of the following UIC policies and responsibilities for investigators:

1. Amendments You are responsible for reporting any amendments to your research protocol that may affect the determination of the exemption and may result in your research no longer being eligible for the exemption that has been granted.
2. Record Keeping You are responsible for maintaining a copy all research related records in a secure location in the event future verification is necessary, at a minimum these documents include: the research protocol, the claim of exemption application, all questionnaires, survey instruments, interview questions and/or data collection instruments associated with this research protocol, recruiting or advertising materials, any consent forms or information sheets given to subjects, or any other pertinent documents.
3. Final Report When you have completed work on your research protocol, you should submit a final report to the Office for Protection of Research Subjects (OPRS).

Please be sure to:

→ Use your research protocol number (2009-1005) on any documents or correspondence with the IRB concerning your research protocol.

We wish you the best as you conduct your research. If you have any questions or need further help, please contact the OPRS office at (312) 996-1711 or me at (312) 355-2908. Please send any correspondence about this protocol to OPRS at 203 AOB, M/C 672.

Sincerely,

Charles W. Hoehne, CIP
Assistant Director, IRB # 2
Office for the Protection of Research Subjects

Enclosure(s): (1) Optional Form 310 - Protection of Human Subjects, Assurance
Identification/Certification/Declaration

cc: Frederick G. Behm, Pathology, M/C 847
OVCR Administration, M/C 672

APPENDIX D (continued)

IRB Protocols- Dr. Peter Gann #1

UNIVERSITY OF ILLINOIS AT CHICAGO

Office for the Protection of Research Subjects (OPRS)
Office of the Vice Chancellor for Research (MC 672)
203 Administrative Office Building
1737 West Polk Street
Chicago, Illinois 60612-7227

Approval Notice Continuing Review (Response To Modifications)

October 2, 2012

Peter Gann, MD, ScD
Pathology
1819 W. Polk Street, 446 C.M.W.
M/C 847
Chicago, IL 60612
Phone: (312) 355-3723 / Fax: (312) 996-4812

RE: **Protocol # 2005-0828**
"R01 CA90759: The Effects of Lycopene on High-Risk Prostatic Tissue"

Dear Dr. Gann:

Your Continuing Review (Response To Modifications) was reviewed and approved by the Expedited review process on October 1, 2012. You may now continue your research.

Please note the following information about your approved research protocol:

<u>Protocol Approval Period:</u>	October 1, 2012 - September 30, 2013
<u>Approved Subject Enrollment #:</u>	80 (22 subjects enrolled) limited to data analysis
<u>Additional Determinations for Research Involving Minors:</u>	These determinations have not been made for this study since it has not been approved for enrollment of minors.
<u>Performance Sites:</u>	Jesse Brown VAMC, UIC, Northwestern University
<u>Sponsor:</u>	National Institutes of Health
<u>PAF#:</u>	2006-03184
<u>Grant/Contract No:</u>	R01 CA90759-01A1
<u>Grant/Contract Title:</u>	The Effects of Lycopene on High-Risk Prostatic Tissue
<u>Research Protocol(s):</u>	
a) "Phase II Trial: The Effects of Lycopene on High Risk Prostatic Tissue, " (NIH Grant R01 CA90759-01A1), Version 2, 02/22/2006	

Your research meets the criteria for expedited review as defined in 45 CFR 46.110(b)(1) under the following specific category:

(8c) Continuing review of research previously approved by the convened IRB where the remaining research activities are limited to data analysis.

Phone: 312-996-1711

<http://www.uic.edu/depts/ovcr/oprs/>

FAX: 312-413-2929

APPENDIX D (continued)

IRB Protocols- Dr. Peter Gann #2

Page 2 of 2

Please note the Review History of this submission:

Receipt Date	Submission Type	Review Process	Review Date	Review Action
09/14/2012	Continuing Review	Expedited	09/17/2012	Modifications Required
09/26/2012	Response To Modifications	Expedited	10/01/2012	Approved

Please remember to:

→ Use your **research protocol number** (2005-0828) on any documents or correspondence with the IRB concerning your research protocol.

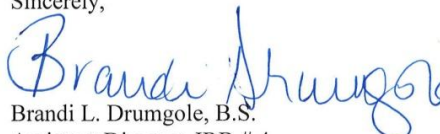
→ Review and comply with all requirements on the enclosure,
"UIC Investigator Responsibilities, Protection of Human Research Subjects"
"JBVAMC Investigator Responsibilities for Performing Research Involving Human Subjects"

Please note that the UIC IRB has the prerogative and authority to ask further questions, seek additional information, require further modifications, or monitor the conduct of your research and the consent process.

Please be aware that if the scope of work in the grant/project changes, the protocol must be amended and approved by the UIC IRB before the initiation of the change.

We wish you the best as you conduct your research. If you have any questions or need further help, please contact OPRS at (312) 996-1711 or me at (312) 996-0548. Please send any correspondence about this protocol to OPRS at 203 AOB, M/C 672.

Sincerely,



Brandi L. Drumgole, B.S.

Assistant Director, IRB # 4

Office for the Protection of Research Subjects

Enclosure(s):

1. **UIC Investigator Responsibilities, Protection of Human Research Subjects**
2. **JBVAMC Investigator Responsibilities for Performing Research Involving Human Subjects**

cc: Dorothy Sholeen-Modrzyk, Cancer Center, 237 MCA, MC 700
 Frederick G. Behm, Pathology, M/C 847
 Israel Rubinstein, M.D, JBVAMC, Mail Point 151, M/C 977
 OVCR Administration, M/C 672
 Northwestern University IRB Office
 Privacy Office, Health Information Management Department, M/C 772
 IDS, Pharmacy Practice, M/C 883

CITED LITERATURE

1. Harman D. Aging: a theory based on free radical and radiation chemistry. *J Gerontol.* 1956; 11(3):298-300.
2. Yuan H, Wang Z, Gao C, Chen W, Huang Q, Yee JK, Bhatia R, Chen W. BCR-ABL gene expression is required for its mutations in a novel KCL-22 cell culture model for acquired resistance of chronic myelogenous leukemia. *J Biol Chem.* 2010; 285(7):5085-96.
3. Palmer RM, Ashton DS, Moncada S. Vascular endothelial cells synthesize nitric oxide from L-arginine. *Nature.* 1988; 333(6174):664-6.
4. Palmer RM, Ferrige AG, Moncada S. Nitric oxide release accounts for the biological activity of endothelium-derived relaxing factor. *Nature.* 1987; 327(6122):524-6.
5. Flohe L, Loschen G, Gunzler WA, Eichele E. Glutathione peroxidase, V. The kinetic mechanism. *Hoppe Seylers Z Physiol Chem.* 1972; 353(6):987-99.
6. Loschen G, Gunzler WA, Flohe L. [Kinetic mechanism of glutathione:H₂O₂ - oxidoreductase]. *Hoppe Seylers Z Physiol Chem.* 1972; 353(5):733.
7. Takebe G, Yarimizu J, Saito Y, Hayashi T, Nakamura H, Yodoi J, Nagasawa S, Takahashi K. A comparative study on the hydroperoxide and thiol specificity of the glutathione peroxidase family and selenoprotein P. *J Biol Chem.* 2002; 277(43):41254-8.
8. Zhao Y, Lee MJ, Cheung C, Ju JH, Chen YK, Liu B, Hu LQ, Yang CS. Analysis of multiple metabolites of tocopherols and tocotrienols in mice and humans. *J Agric Food Chem.* 2010; 58(8):4844-52.
9. Han D, Antunes F, Canali R, Rettori D, Cadenas E. Voltage-dependent anion channels control the release of the superoxide anion from mitochondria to cytosol. *J Biol Chem.* 2003; 278(8):5557-63.
10. Dhar SK, St Clair DK. Manganese superoxide dismutase regulation and cancer. *Free Radic Biol Med.* 2012; 52(11-12):2209-22.
11. Weisiger RA, Fridovich I. Mitochondrial superoxide simutase. Site of synthesis and intramitochondrial localization. *J Biol Chem.* 1973; 248(13):4793-6.
12. Weisiger RA, Fridovich I. Superoxide dismutase. Organelle specificity. *J Biol Chem.* 1973; 248(10):3582-92.

13. Ravindranath SD, Fridovich I. Isolation and characterization of a manganese-containing superoxide dismutase from yeast. *J Biol Chem.* 1975; 250(15):6107-12.
14. Luk E, Yang M, Jensen LT, Bourbonnais Y, Culotta VC. Manganese activation of superoxide dismutase 2 in the mitochondria of *Saccharomyces cerevisiae*. *J Biol Chem.* 2005; 280(24):22715-20.
15. Bielski BH. Fast kinetic studies of dioxygen-derived species and their metal complexes. *Philos Trans R Soc Lond B Biol Sci.* 1985; 311(1152):473-82.
16. Wispe JR, Clark JC, Burhans MS, Kropp KE, Korfhagen TR, Whitsett JA. Synthesis and processing of the precursor for human mangano-superoxide dismutase. *Biochim Biophys Acta.* 1989; 994(1):30-6.
17. Shimoda-Matsubayashi S, Matsumine H, Kobayashi T, Nakagawa-Hattori Y, Shimizu Y, Mizuno Y. Structural dimorphism in the mitochondrial targeting sequence in the human manganese superoxide dismutase gene. A predictive evidence for conformational change to influence mitochondrial transport and a study of allelic association in Parkinson's disease. *Biochem Biophys Res Commun.* 1996; 226(2):561-5.
18. Lebovitz RM, Zhang H, Vogel H, Cartwright J, Jr., Dionne L, Lu N, Huang S, Matzuk MM. Neurodegeneration, myocardial injury, and perinatal death in mitochondrial superoxide dismutase-deficient mice. *Proc Natl Acad Sci U S A.* 1996; 93(18):9782-7.
19. Li Y, Huang TT, Carlson EJ, Melov S, Ursell PC, Olson JL, Noble LJ, Yoshimura MP, Berger C, Chan PH, Wallace DC, Epstein CJ. Dilated cardiomyopathy and neonatal lethality in mutant mice lacking manganese superoxide dismutase. *Nat Genet.* 1995; 11(4):376-81.
20. Copin JC, Gasche Y, Chan PH. Overexpression of copper/zinc superoxide dismutase does not prevent neonatal lethality in mutant mice that lack manganese superoxide dismutase. *Free Radic Biol Med.* 2000; 28(10):1571-6.
21. Parajuli N, Marine A, Simmons S, Saba H, Mitchell T, Shimizu T, Shirasawa T, Macmillan-Crow LA. Generation and characterization of a novel kidney-specific manganese superoxide dismutase knockout mouse. *Free Radic Biol Med.* 2011; 51(2):406-16.
22. Parajuli N, Macmillan-Crow LA. Role of reduced manganese superoxide dismutase in ischemia/reperfusion injury: a possible trigger for autophagy and mitochondrial biogenesis? *Am J Physiol Renal Physiol.* 2012.
23. Sarsour EH, Goswami M, Kalen AL, Goswami PC. MnSOD activity protects mitochondrial morphology of quiescent fibroblasts from age associated abnormalities. *Mitochondrion.* 2010; 10(4):342-9.

24. Li N, Oberley TD, Oberley LW, Zhong W. Inhibition of cell growth in NIH/3T3 fibroblasts by overexpression of manganese superoxide dismutase: mechanistic studies. *J Cell Physiol.* 1998; 175(3):359-69.
25. Zhong W, Oberley LW, Oberley TD, St Clair DK. Suppression of the malignant phenotype of human glioma cells by overexpression of manganese superoxide dismutase. *Oncogene.* 1997; 14(4):481-90.
26. Zhong W, Oberley LW, Oberley TD, Yan T, Domann FE, St Clair DK. Inhibition of cell growth and sensitization to oxidative damage by overexpression of manganese superoxide dismutase in rat glioma cells. *Cell Growth Differ.* 1996; 7(9):1175-86.
27. Wang JN, Shi N, Chen SY. Manganese superoxide dismutase inhibits neointima formation through attenuation of migration and proliferation of vascular smooth muscle cells. *Free Radic Biol Med.* 2012; 52(1):173-81.
28. Sarsour EH, Kalen AL, Xiao Z, Veenstra TD, Chaudhuri L, Venkataraman S, Reigan P, Buettner GR, Goswami PC. Manganese superoxide dismutase regulates a metabolic switch during the mammalian cell cycle. *Cancer Res.* 2012; 72(15):3807-16.
29. Candas D, Fan M, Nantajit D, Vaughan AT, Murley J, Woloschak G, Grdina DJ, Li JJ. CyclinB1/Cdk1 phosphorylates mitochondrial antioxidant MnSOD in cell adaptive response to radiation stress. *J Mol Cell Biol.* 2012.
30. Ozden O, Park SH, Kim HS, Jiang H, Coleman MC, Spitz DR, Gius D. Acetylation of MnSOD directs enzymatic activity responding to cellular nutrient status or oxidative stress. *Aging (Albany NY).* 2011; 3(2):102-7.
31. Tao R, Coleman MC, Pennington JD, Ozden O, Park SH, Jiang H, Kim HS, Flynn CR, Hill S, Hayes McDonald W, Olivier AK, Spitz DR, Gius D. Sirt3-mediated deacetylation of evolutionarily conserved lysine 122 regulates MnSOD activity in response to stress. *Mol Cell.* 2010; 40(6):893-904.
32. Tsai SM, Hou MF, Wu SH, Hu BW, Yang SF, Chen WT, Chai CY, Ma H, Tsai LY. Expression of manganese superoxide dismutase in patients with breast cancer. *Kaohsiung J Med Sci.* 2011; 27(5):167-72.
33. Martin RC, Li Y, Liu Q, Barker DF, Doll MA, Hein DW. Manganese superoxide dismutase expression as a function of genotype and lung cancer pathology. *Cancer Invest.* 2010; 28(8):813-9.
34. Dhar SK, Tangpong J, Chaiswing L, Oberley TD, St Clair DK. Manganese superoxide dismutase is a p53-regulated gene that switches cancers between early and advanced stages. *Cancer Res.* 2011; 71(21):6684-95.

35. Chen PM, Wu YH, Li MC, Cheng YW, Chen CY, Lee H. MnSOD promotes tumor invasion via upregulation of FoxM1-MMP2 axis and related with poor survival and relapse in Lung Adenocarcinomas. *Mol Cancer Res.* 2012.
36. Okado-Matsumoto A, Fridovich I. Subcellular distribution of superoxide dismutases (SOD) in rat liver: Cu,Zn-SOD in mitochondria. *J Biol Chem.* 2001; 276(42):38388-93.
37. Crapo JD, Oury T, Rabouille C, Slot JW, Chang LY. Copper,zinc superoxide dismutase is primarily a cytosolic protein in human cells. *Proc Natl Acad Sci U S A.* 1992; 89(21):10405-9.
38. Sturtz LA, Diekert K, Jensen LT, Lill R, Culotta VC. A fraction of yeast Cu,Zn-superoxide dismutase and its metallochaperone, CCS, localize to the intermembrane space of mitochondria. A physiological role for SOD1 in guarding against mitochondrial oxidative damage. *J Biol Chem.* 2001; 276(41):38084-9.
39. Banci L, Bertini I, Cramaro F, Del Conte R, Viezzoli MS. Solution structure of Apo Cu,Zn superoxide dismutase: role of metal ions in protein folding. *Biochemistry.* 2003; 42(32):9543-53.
40. Strange RW, Antonyuk S, Hough MA, Doucette PA, Rodriguez JA, Hart PJ, Hayward LJ, Valentine JS, Hasnain SS. The structure of holo and metal-deficient wild-type human Cu, Zn superoxide dismutase and its relevance to familial amyotrophic lateral sclerosis. *J Mol Biol.* 2003; 328(4):877-91.
41. McCord JM, Fridovich I. Superoxide dismutase. An enzymic function for erythrocuprein (hemocuprein). *J Biol Chem.* 1969; 244(22):6049-55.
42. Marklund SL. Extracellular superoxide dismutase in human tissues and human cell lines. *J Clin Invest.* 1984; 74(4):1398-403.
43. Marklund SL, Holme E, Hellner L. Superoxide dismutase in extracellular fluids. *Clin Chim Acta.* 1982; 126(1):41-51.
44. Antonyuk SV, Strange RW, Marklund SL, Hasnain SS. The structure of human extracellular copper-zinc superoxide dismutase at 1.7 Å resolution: insights into heparin and collagen binding. *J Mol Biol.* 2009; 388(2):310-26.
45. Folz RJ, Crapo JD. Extracellular superoxide dismutase (SOD3): tissue-specific expression, genomic characterization, and computer-assisted sequence analysis of the human EC SOD gene. *Genomics.* 1994; 22(1):162-71.
46. Kondo T, Reaume AG, Huang TT, Carlson E, Murakami K, Chen SF, Hoffman EK, Scott RW, Epstein CJ, Chan PH. Reduction of CuZn-superoxide dismutase activity

- exacerbates neuronal cell injury and edema formation after transient focal cerebral ischemia. *J Neurosci.* 1997; 17(11):4180-9.
47. Ohlemiller KK, McFadden SL, Ding DL, Flood DG, Reaume AG, Hoffman EK, Scott RW, Wright JS, Putcha GV, Salvi RJ. Targeted deletion of the cytosolic Cu/Zn-superoxide dismutase gene (Sod1) increases susceptibility to noise-induced hearing loss. *Audiol Neurotol.* 1999; 4(5):237-46.
 48. Reaume AG, Elliott JL, Hoffman EK, Kowall NW, Ferrante RJ, Siwek DF, Wilcox HM, Flood DG, Beal MF, Brown RH, Jr., Scott RW, Snider WD. Motor neurons in Cu/Zn superoxide dismutase-deficient mice develop normally but exhibit enhanced cell death after axonal injury. *Nat Genet.* 1996; 13(1):43-7.
 49. Schwartz PJ, Reaume A, Scott R, Coyle JT. Effects of over- and under-expression of Cu,Zn-superoxide dismutase on the toxicity of glutamate analogs in transgenic mouse striatum. *Brain Res.* 1998; 789(1):32-9.
 50. Elchuri S, Oberley TD, Qi W, Eisenstein RS, Jackson Roberts L, Van Remmen H, Epstein CJ, Huang TT. CuZnSOD deficiency leads to persistent and widespread oxidative damage and hepatocarcinogenesis later in life. *Oncogene.* 2005; 24(3):367-80.
 51. Carlsson LM, Jonsson J, Edlund T, Marklund SL. Mice lacking extracellular superoxide dismutase are more sensitive to hyperoxia. *Proc Natl Acad Sci U S A.* 1995; 92(14):6264-8.
 52. McPhail LC, Henson PM, Johnston RB, Jr. Respiratory burst enzyme in human neutrophils. Evidence for multiple mechanisms of activation. *J Clin Invest.* 1981; 67(3):710-6.
 53. Chambers DE, Parks DA, Patterson G, Roy R, McCord JM, Yoshida S, Parmley LF, Downey JM. Xanthine oxidase as a source of free radical damage in myocardial ischemia. *J Mol Cell Cardiol.* 1985; 17(2):145-52.
 54. Handler JA, Thurman RG. Catalase-dependent ethanol oxidation in perfused rat liver. Requirement for fatty-acid-stimulated H₂O₂ production by peroxisomes. *Eur J Biochem.* 1988; 176(2):477-84.
 55. Boveris A, Valdez LB, Zaobornyj T, Bustamante J. Mitochondrial metabolic states regulate nitric oxide and hydrogen peroxide diffusion to the cytosol. *Biochim Biophys Acta.* 2006; 1757(5-6):535-42.
 56. Makino N, Sasaki K, Hashida K, Sakakura Y. A metabolic model describing the H₂O₂ elimination by mammalian cells including H₂O₂ permeation through cytoplasmic and peroxisomal membranes: comparison with experimental data. *Biochim Biophys Acta.* 2004; 1673(3):149-59.

57. Bienert GP, Moller AL, Kristiansen KA, Schulz A, Moller IM, Schjoerring JK, Jahn TP. Specific aquaporins facilitate the diffusion of hydrogen peroxide across membranes. *J Biol Chem.* 2007; 282(2):1183-92.
58. Miller EW, Dickinson BC, Chang CJ. Aquaporin-3 mediates hydrogen peroxide uptake to regulate downstream intracellular signaling. *Proc Natl Acad Sci U S A.* 2010; 107(36):15681-6.
59. Baker MS, Gebicki JM. The effect of pH on yields of hydroxyl radicals produced from superoxide by potential biological iron chelators. *Arch Biochem Biophys.* 1986; 246(2):581-8.
60. Morena M, Delbosc S, Dupuy AM, Canaud B, Cristol JP. Overproduction of reactive oxygen species in end-stage renal disease patients: a potential component of hemodialysis-associated inflammation. *Hemodial Int.* 2005; 9(1):37-46.
61. Okayasu I. Development of ulcerative colitis and its associated colorectal neoplasia as a model of the organ-specific chronic inflammation-carcinoma sequence. *Pathol Int.* 2012; 62(6):368-80.
62. Samuelson DJ, Powell MB, Lloria-Prevatt M, Romagnolo DF. Transcriptional activation of the gp91phox NADPH oxidase subunit by TPA in HL-60 cells. *J Leukoc Biol.* 2001; 69(1):161-8.
63. Denu JM, Tanner KG. Specific and reversible inactivation of protein tyrosine phosphatases by hydrogen peroxide: evidence for a sulfenic acid intermediate and implications for redox regulation. *Biochemistry.* 1998; 37(16):5633-42.
64. Guo Z, Kozlov S, Lavin MF, Person MD, Paull TT. ATM activation by oxidative stress. *Science.* 2010; 330(6003):517-21.
65. Dandrea T, Bajak E, Warngard L, Cotgreave IA. Protein S-glutathionylation correlates to selective stress gene expression and cytoprotection. *Arch Biochem Biophys.* 2002; 406(2):241-52.
66. Barrett WC, DeGnore JP, Keng YF, Zhang ZY, Yim MB, Chock PB. Roles of superoxide radical anion in signal transduction mediated by reversible regulation of protein-tyrosine phosphatase 1B. *J Biol Chem.* 1999; 274(49):34543-6.
67. Ahn JH, Lee M. Tyrosine phosphorylation and Ras activation is required for hydrogen peroxide-mediated Raf-1 kinase activation. *Mol Cell Biochem.* 2008; 317(1-2):121-9.
68. Arora-Kuruganti P, Lucchesi PA, Wurster RD. Proliferation of cultured human astrocytoma cells in response to an oxidant and antioxidant. *J Neurooncol.* 1999; 44(3):213-21.

69. Burdon RH, Alliangana D, Gill V. Hydrogen peroxide and the proliferation of BHK-21 cells. *Free Radic Res.* 1995; 23(5):471-86.
70. Davicino R, Manuele MG, Ferraro G, Micalizzi B, Anesini C. Modulatory effect of hydrogen peroxide on tumoral lymphocytes proliferation. *Immunopharmacol Immunotoxicol.* 2009; 31(1):130-9.
71. Ibanez IL, Bracalente C, Notcovich C, Tropper I, Molinari BL, Policastro LL, Duran H. Phosphorylation and Subcellular Localization of p27Kip1 Regulated by Hydrogen Peroxide Modulation in Cancer Cells. *PLoS ONE.* 2012; 7(9):e44502.
72. Radisavljevic ZM, Gonzalez-Flecha B. Signaling through Cdk2, importin-alpha and NuMA is required for H₂O₂-induced mitosis in primary type II pneumocytes. *Biochim Biophys Acta.* 2003; 1640(2-3):163-70.
73. Brown MR, Miller FJ, Jr., Li WG, Ellingson AN, Mozena JD, Chatterjee P, Engelhardt JF, Zwacka RM, Oberley LW, Fang X, Spector AA, Weintraub NL. Overexpression of human catalase inhibits proliferation and promotes apoptosis in vascular smooth muscle cells. *Circ Res.* 1999; 85(6):524-33.
74. Zanetti M, Katusic ZS, O'Brien T. Adenoviral-mediated overexpression of catalase inhibits endothelial cell proliferation. *Am J Physiol Heart Circ Physiol.* 2002; 283(6):H2620-6.
75. Guzik TJ, West NE, Black E, McDonald D, Ratnatunga C, Pillai R, Channon KM. Vascular superoxide production by NAD(P)H oxidase: association with endothelial dysfunction and clinical risk factors. *Circ Res.* 2000; 86(9):E85-90.
76. McNally JS, Davis ME, Giddens DP, Saha A, Hwang J, Dikalov S, Jo H, Harrison DG. Role of xanthine oxidoreductase and NAD(P)H oxidase in endothelial superoxide production in response to oscillatory shear stress. *Am J Physiol Heart Circ Physiol.* 2003; 285(6):H2290-7.
77. Brand MD, Lehninger AL. H⁺/ATP ratio during ATP hydrolysis by mitochondria: modification of the chemiosmotic theory. *Proc Natl Acad Sci U S A.* 1977; 74(5):1955-9.
78. Vallyathan V, Shi X. The role of oxygen free radicals in occupational and environmental lung diseases. *Environ Health Perspect.* 1997; 105 Suppl 1:165-77.
79. Joosse A, De Vries E, van Eijck CH, Eggermont AM, Nijsten T, Coebergh JW. Reactive oxygen species and melanoma: an explanation for gender differences in survival? *Pigment Cell Melanoma Res.* 2010; 23(3):352-64.
80. Trachootham D, Lu W, Ogasawara MA, Nilsa RD, Huang P. Redox regulation of cell survival. *Antioxid Redox Signal.* 2008; 10(8):1343-74.

81. Morikawa S, Harada T. Immunohistochemical localization of catalase in mammalian tissues. *J Histochem Cytochem.* 1969; 17(1):30-5.
82. Kirkman HN, Gaetani GF. Catalase: a tetrameric enzyme with four tightly bound molecules of NADPH. *Proc Natl Acad Sci U S A.* 1984; 81(14):4343-7.
83. Hollinshead M, Meijer J. Immunocytochemical analysis of soluble epoxide hydrolase and catalase in mouse and rat hepatocytes demonstrates a peroxisomal localization before and after clofibrate treatment. *Eur J Cell Biol.* 1988; 46(3):394-402.
84. Reid TJ, 3rd, Murthy MR, Sicignano A, Tanaka N, Musick WD, Rossmann MG. Structure and heme environment of beef liver catalase at 2.5 Å resolution. *Proc Natl Acad Sci U S A.* 1981; 78(8):4767-71.
85. Shull S, Heintz NH, Periasamy M, Manohar M, Janssen YM, Marsh JP, Mossman BT. Differential regulation of antioxidant enzymes in response to oxidants. *J Biol Chem.* 1991; 266(36):24398-403.
86. Nagato AC, Bezerra FS, Lanzetti M, Lopes AA, Silva MA, Porto LC, Valenca SS. Time course of inflammation, oxidative stress and tissue damage induced by hyperoxia in mouse lungs. *Int J Exp Pathol.* 2012; 93(4):269-78.
87. Ho YS, Xiong Y, Ma W, Spector A, Ho DS. Mice lacking catalase develop normally but show differential sensitivity to oxidant tissue injury. *J Biol Chem.* 2004; 279(31):32804-12.
88. Takemoto K, Tanaka M, Iwata H, Nishihara R, Ishihara K, Wang DH, Ogino K, Taniuchi K, Masuoka N. Low catalase activity in blood is associated with the diabetes caused by alloxan. *Clin Chim Acta.* 2009; 407(1-2):43-6.
89. Wen JK, Osumi T, Hashimoto T, Ogata M. Molecular analysis of human acatalasemia. Identification of a splicing mutation. *J Mol Biol.* 1990; 211(2):383-93.
90. Goth L, Eaton JW. Hereditary catalase deficiencies and increased risk of diabetes. *Lancet.* 2000; 356(9244):1820-1.
91. Spector A, Yan GZ, Huang RR, McDermott MJ, Gascoyne PR, Pigiet V. The effect of H₂O₂ upon thioredoxin-enriched lens epithelial cells. *J Biol Chem.* 1988; 263(10):4984-90.
92. Kang SW, Baines IC, Rhee SG. Characterization of a mammalian peroxiredoxin that contains one conserved cysteine. *J Biol Chem.* 1998; 273(11):6303-11.
93. Zhong L, Arner ES, Holmgren A. Structure and mechanism of mammalian thioredoxin reductase: the active site is a redox-active selenolthiol/selenenylsulfide formed from the

- conserved cysteine-selenocysteine sequence. *Proc Natl Acad Sci U S A.* 2000; 97(11):5854-9.
94. Zhong L, Holmgren A. Essential role of selenium in the catalytic activities of mammalian thioredoxin reductase revealed by characterization of recombinant enzymes with selenocysteine mutations. *J Biol Chem.* 2000; 275(24):18121-8.
 95. Gladyshev VN, Jeang KT, Stadtman TC. Selenocysteine, identified as the penultimate C-terminal residue in human T-cell thioredoxin reductase, corresponds to TGA in the human placental gene. *Proc Natl Acad Sci U S A.* 1996; 93(12):6146-51.
 96. Tamura T, Stadtman TC. A new selenoprotein from human lung adenocarcinoma cells: purification, properties, and thioredoxin reductase activity. *Proc Natl Acad Sci U S A.* 1996; 93(3):1006-11.
 97. Cone JE, Del Rio RM, Davis JN, Stadtman TC. Chemical characterization of the selenoprotein component of clostridial glycine reductase: identification of selenocysteine as the organoselenium moiety. *Proc Natl Acad Sci U S A.* 1976; 73(8):2659-63.
 98. Lee SR, Bar-Noy S, Kwon J, Levine RL, Stadtman TC, Rhee SG. Mammalian thioredoxin reductase: oxidation of the C-terminal cysteine/selenocysteine active site forms a thioselenide, and replacement of selenium with sulfur markedly reduces catalytic activity. *Proc Natl Acad Sci U S A.* 2000; 97(6):2521-6.
 99. Cheng Q, Sandalova T, Lindqvist Y, Arner ES. Crystal structure and catalysis of the selenoprotein thioredoxin reductase 1. *J Biol Chem.* 2009; 284(6):3998-4008.
 100. Miller S, Walker SW, Arthur JR, Nicol F, Pickard K, Lewin MH, Howie AF, Beckett GJ. Selenite protects human endothelial cells from oxidative damage and induces thioredoxin reductase. *Clin Sci (Lond).* 2001; 100(5):543-50.
 101. Berggren MM, Mangin JF, Gasdaka JR, Powis G. Effect of selenium on rat thioredoxin reductase activity: increase by supranutritional selenium and decrease by selenium deficiency. *Biochem Pharmacol.* 1999; 57(2):187-93.
 102. May JM, Mendiratta S, Hill KE, Burk RF. Reduction of dehydroascorbate to ascorbate by the selenoenzyme thioredoxin reductase. *J Biol Chem.* 1997; 272(36):22607-10.
 103. Bjornstedt M, Odlander B, Kuprin S, Claesson HE, Holmgren A. Selenite incubated with NADPH and mammalian thioredoxin reductase yields selenide, which inhibits lipoxygenase and changes the electron spin resonance spectrum of the active site iron. *Biochemistry.* 1996; 35(26):8511-6.

104. Rigobello MP, Callegaro MT, Barzon E, Benetti M, Bindoli A. Purification of mitochondrial thioredoxin reductase and its involvement in the redox regulation of membrane permeability. *Free Radic Biol Med.* 1998; 24(2):370-6.
105. Lee SR, Kim JR, Kwon KS, Yoon HW, Levine RL, Ginsburg A, Rhee SG. Molecular cloning and characterization of a mitochondrial selenocysteine-containing thioredoxin reductase from rat liver. *J Biol Chem.* 1999; 274(8):4722-34.
106. Turanov AA, Su D, Gladyshev VN. Characterization of alternative cytosolic forms and cellular targets of mouse mitochondrial thioredoxin reductase. *J Biol Chem.* 2006; 281(32):22953-63.
107. Conrad M, Jakupoglu C, Moreno SG, Lippl S, Banjac A, Schneider M, Beck H, Hatzopoulos AK, Just U, Sinowatz F, Schmahl W, Chien KR, Wurst W, Bornkamm GW, Brielmeier M. Essential role for mitochondrial thioredoxin reductase in hematopoiesis, heart development, and heart function. *Mol Cell Biol.* 2004; 24(21):9414-23.
108. Jakupoglu C, Przemeck GK, Schneider M, Moreno SG, Mayr N, Hatzopoulos AK, de Angelis MH, Wurst W, Bornkamm GW, Brielmeier M, Conrad M. Cytoplasmic thioredoxin reductase is essential for embryogenesis but dispensable for cardiac development. *Mol Cell Biol.* 2005; 25(5):1980-8.
109. Sun QA, Kimnarsky L, Sherman S, Gladyshev VN. Selenoprotein oxidoreductase with specificity for thioredoxin and glutathione systems. *Proc Natl Acad Sci U S A.* 2001; 98(7):3673-8.
110. Sun QA, Su D, Novoselov SV, Carlson BA, Hatfield DL, Gladyshev VN. Reaction mechanism and regulation of mammalian thioredoxin/glutathione reductase. *Biochemistry.* 2005; 44(44):14528-37.
111. Su D, Novoselov SV, Sun QA, Moustafa ME, Zhou Y, Oko R, Hatfield DL, Gladyshev VN. Mammalian selenoprotein thioredoxin-glutathione reductase. Roles in disulfide bond formation and sperm maturation. *J Biol Chem.* 2005; 280(28):26491-8.
112. Arner ES. Focus on mammalian thioredoxin reductases--important selenoproteins with versatile functions. *Biochim Biophys Acta.* 2009; 1790(6):495-526.
113. Cadenas C, Franckenstein D, Schmidt M, Gehrmann M, Hermes M, Geppert B, Schormann W, Maccoux LJ, Schug M, Schumann A, Wilhelm C, Freis E, Ickstadt K, Rahnenfuhrer J, Baumbach JJ, Sickmann A, Hengstler JG. Role of thioredoxin reductase 1 and thioredoxin interacting protein in prognosis of breast cancer. *Breast Cancer Res.* 2010; 12(3):R44.

114. Iwasawa S, Yamano Y, Takiguchi Y, Tanzawa H, Tatsumi K, Uzawa K. Upregulation of thioredoxin reductase 1 in human oral squamous cell carcinoma. *Oncol Rep.* 2011; 25(3):637-44.
115. Zhu X, Huang C, Peng B. Overexpression of thioredoxin system proteins predicts poor prognosis in patients with squamous cell carcinoma of the tongue. *Oral Oncol.* 2011; 47(7):609-14.
116. Edes K, Cassidy P, Shami PJ, Moos PJ. JS-K, a nitric oxide prodrug, has enhanced cytotoxicity in colon cancer cells with knockdown of thioredoxin reductase 1. *PLoS ONE.* 2010; 5(1):e8786.
117. Honeggar M, Beck R, Moos PJ. Thioredoxin reductase 1 ablation sensitizes colon cancer cells to methylseleninate-mediated cytotoxicity. *Toxicol Appl Pharmacol.* 2009; 241(3):348-55.
118. Poerschke RL, Moos PJ. Thioredoxin reductase 1 knockdown enhances selenazolidine cytotoxicity in human lung cancer cells via mitochondrial dysfunction. *Biochem Pharmacol.* 2011; 81(2):211-21.
119. Yoo MH, Xu XM, Carlson BA, Gladyshev VN, Hatfield DL. Thioredoxin reductase 1 deficiency reverses tumor phenotype and tumorigenicity of lung carcinoma cells. *J Biol Chem.* 2006; 281(19):13005-8.
120. Lubos E, Loscalzo J, Handy DE. Glutathione peroxidase-1 in health and disease: from molecular mechanisms to therapeutic opportunities. *Antioxid Redox Signal.* 2011; 15(7):1957-97.
121. Singh S, Khan AR, Gupta AK. Role of glutathione in cancer pathophysiology and therapeutic interventions. *J Exp Ther Oncol.* 2012; 9(4):303-16.
122. Khalife KH, Lupidi G. Nonenzymatic reduction of thymoquinone in physiological conditions. *Free Radic Res.* 2007; 41(2):153-61.
123. Alvarez-Idaboy JR, Galano A. On the chemical repair of DNA radicals by glutathione: hydrogen vs electron transfer. *J Phys Chem B.* 2012; 116(31):9316-25.
124. Leier I, Jedlitschky G, Buchholz U, Center M, Cole SP, Deeley RG, Keppler D. ATP-dependent glutathione disulphide transport mediated by the MRP gene-encoded conjugate export pump. *Biochem J.* 1996; 314 (Pt 2):433-7.
125. Kryukov GV, Castellano S, Novoselov SV, Lobanov AV, Zehtab O, Guigo R, Gladyshev VN. Characterization of mammalian selenoproteomes. *Science.* 2003; 300(5624):1439-43.

126. Nguyen VD, Saaranen MJ, Karala AR, Lappi AK, Wang L, Raykhel IB, Alanen HI, Salo KE, Wang CC, Ruddock LW. Two endoplasmic reticulum PDI peroxidases increase the efficiency of the use of peroxide during disulfide bond formation. *J Mol Biol.* 2011; 406(3):503-15.
127. Tosatto SC, Bosello V, Fogolari F, Mauri P, Roveri A, Toppo S, Flohe L, Ursini F, Maiorino M. The catalytic site of glutathione peroxidases. *Antioxid Redox Signal.* 2008; 10(9):1515-26.
128. Low SC, Grundner-Culemann E, Harney JW, Berry MJ. SECIS-SBP2 interactions dictate selenocysteine incorporation efficiency and selenoprotein hierarchy. *Embo J.* 2000; 19(24):6882-90.
129. Kipp A, Banning A, van Schothorst EM, Meplan C, Schomburg L, Evelo C, Coort S, Gaj S, Keijer J, Hesketh J, Brigelius-Flohe R. Four selenoproteins, protein biosynthesis, and Wnt signalling are particularly sensitive to limited selenium intake in mouse colon. *Mol Nutr Food Res.* 2009; 53(12):1561-72.
130. Lei XG, Evenson JK, Thompson KM, Sunde RA. Glutathione peroxidase and phospholipid hydroperoxide glutathione peroxidase are differentially regulated in rats by dietary selenium. *J Nutr.* 1995; 125(6):1438-46.
131. Wingler K, Bocher M, Flohe L, Kollmus H, Brigelius-Flohe R. mRNA stability and selenocysteine insertion sequence efficiency rank gastrointestinal glutathione peroxidase high in the hierarchy of selenoproteins. *European Journal of Biochemistry.* 1999; 259:149-57.
132. Moriarty PM, Reddy CC, Maquat LE. Selenium deficiency reduces the abundance of mRNA for Se-dependent glutathione peroxidase 1 by a UGA-dependent mechanism likely to be nonsense codon-mediated decay of cytoplasmic mRNA. *Mol Cell Biol.* 1998; 18(5):2932-9.
133. Sun X, Moriarty PM, Maquat LE. Nonsense-mediated decay of glutathione peroxidase 1 mRNA in the cytoplasm depends on intron position. *Embo J.* 2000; 19(17):4734-44.
134. Berry MJ, Banu L, Chen Y, Mandel SJ, Kiefer JD, Harney JW, Larsen PR. Recognition of UGA as a selenocysteine codon in Type I deiodinase requires sequences in the 3' untranslated region. *Nature.* 1991; 353:273-76.
135. Copeland P, Fletcher J, BA C, Hatfield D, Driscoll D. A novel RNA binding protein, SBP2, is required for the translation of mammalian selenoprotein mRNAs. *EMBO J.* 2000; 19(2):306-14.

136. Tujebajeva R, Copeland P, Xu X-M, Carlson B, Harney J, Driscoll D, Hatfield D, Berry M. Decoding apparatus for eukaryotic selenocysteine insertion. *EMBO Rep.* 2000; 1(2):158-63.
137. Dumitrescu AM, Liao XH, Abdullah MS, Lado-Abeal J, Majed FA, Moeller LC, Boran G, Schomburg L, Weiss RE, Refetoff S. Mutations in SECISBP2 result in abnormal thyroid hormone metabolism. *Nat Genet.* 2005; 37(11):1247-52.
138. Budiman ME, Bubenik JL, Miniard AC, Middleton LM, Gerber CA, Cash A, Driscoll DM. Eukaryotic initiation factor 4a3 is a selenium-regulated RNA-binding protein that selectively inhibits selenocysteine incorporation. *Mol Cell.* 2009; 35(4):479-89.
139. Awasthi YC, Beutler E, Srivastava SK. Purification and properties of human erythrocyte glutathione peroxidase. *J Biol Chem.* 1975; 250(13):5144-9.
140. Ursini F, Maiorino M, Gregolin C. The selenoenzyme phospholipid hydroperoxide glutathione peroxidase. *Biochim Biophys Acta.* 1985; 839(1):62-70.
141. Takahashi K, Avissar N, Whitin J, Cohen H. Purification and characterization of human plasma glutathione peroxidase: a selenoglycoprotein distinct from the known cellular enzyme. *Arch Biochem Biophys.* 1987; 256(2):677-86.
142. Chu FF, Esworthy RS, Ho YS, Bermeister M, Swiderek K, Elliott RW. Expression and chromosomal mapping of mouse Gpx2 gene encoding the gastrointestinal form of glutathione peroxidase, GPX-GI. *Biomed Environ Sci.* 1997; 10(2-3):156-62.
143. Toppo S, Vanin S, Bosello V, Tosatto SC. Evolutionary and structural insights into the multifaceted glutathione peroxidase (Gpx) superfamily. *Antioxid Redox Signal.* 2008; 10(9):1501-14.
144. Avissar N, Ornt DB, Yagil Y, Horowitz S, Watkins RH, Kerl EA, Takahashi K, Palmer IS, Cohen HJ. Human kidney proximal tubules are the main source of plasma glutathione peroxidase. *Am J Physiol.* 1994; 266(2 Pt 1):C367-75.
145. Pawlowicz Z, Zachara BA, Trafikowska U, Maciag A, Marchaluk E, Nowicki A. Blood selenium concentrations and glutathione peroxidase activities in patients with breast cancer and with advanced gastrointestinal cancer. *J Trace Elem Electrolytes Health Dis.* 1991; 5(4):275-7.
146. Lee OJ, Schneider-Stock R, McChesney PA, Kuester D, Roessner A, Vieth M, Moskaluk CA, El-Rifai W. Hypermethylation and loss of expression of glutathione peroxidase-3 in Barrett's tumorigenesis. *Neoplasia.* 2005; 7(9):854-61.

147. Yu YP, Yu G, Tseng G, Cieply K, Nelson J, Defrances M, Zarnegar R, Michalopoulos G, Luo JH. Glutathione peroxidase 3, deleted or methylated in prostate cancer, suppresses prostate cancer growth and metastasis. *Cancer Res.* 2007; 67(17):8043-50.
148. Peng DF, Razvi M, Chen H, Washington K, Roessner A, Schneider-Stock R, El-Rifai W. DNA hypermethylation regulates the expression of members of the Mu-class glutathione S-transferases and glutathione peroxidases in Barrett's adenocarcinoma. *Gut.* 2009; 58(1):5-15.
149. Dreher I, Schmutzler C, Jakob F, Kohrle J. Expression of selenoproteins in various rat and human tissues and cell lines. *J Trace Elem Med Biol.* 1997; 11(2):83-91.
150. Chu F-F, Esworthy R, Chu P, Lonmate J, Huycke M, Wilczynski S, Doroshov J. Bacteria-induced intestinal cancer in mice with disrupted Gpx1 and Gpx2 genes. *Cancer Research.* 2004; 64(962-968).
151. Esworthy RS, Aranda R, Martin MG, Doroshov JH, Binder SW, Chu FF. Mice with combined disruption of Gpx1 and Gpx2 genes have colitis. *Am J Physiol Gastrointest Liver Physiol.* 2001; 281:G848-G55.
152. Esworthy RS, Yang L, Frankel PH, Chu FF. Epithelium-specific glutathione peroxidase, Gpx2, is involved in the prevention of intestinal inflammation in selenium-deficient mice. *J Nutr.* 2005; 135(4):740-5.
153. Mork H, al-Taie OH, Bahr K, Zierer A, Beck C, Scheurlen M, Jakob F, Kohrle J. Inverse mRNA expression of the selenocysteine-containing proteins GI-GPx and SeP in colorectal adenomas compared with adjacent normal mucosa. *Nutr Cancer.* 2000; 37(1):108-16.
154. Mork H, Scheurlen M, Al-Taie O, Zierer A, Kraus M, Schottker K, Jakob F, Kohrle J. Glutathione peroxidase isoforms as part of the local antioxidative defense system in normal and Barrett's esophagus. *Int J Cancer.* 2003; 105(3):300-4.
155. Al-Taie OH, Uceyler N, Eubner U, Jakob F, Mork H, Scheurlen M, Brigelius-Flohe R, Schottker K, Abel J, Thalheimer A, Katzenberger T, Illert B, Melcher R, Kohrle J. Expression profiling and genetic alterations of the selenoproteins GI-GPx and SePP in colorectal carcinogenesis. *Nutr Cancer.* 2004; 48(1):6-14.
156. Cho HY, Jedlicka AE, Reddy SP, Kensler TW, Yamamoto M, Zhang LY, Kleeberger SR. Role of NRF2 in protection against hyperoxic lung injury in mice. *Am J Respir Cell Mol Biol.* 2002; 26(2):175-82.
157. Singh A, Rangasamy T, Thimmulappa RK, Lee H, Osburn WO, Brigelius-Flohe R, Kensler TW, Yamamoto M, Biswal S. Glutathione peroxidase 2, the major cigarette smoke-

- inducible isoform of GPX in lungs, is regulated by Nrf2. *Am J Respir Cell Mol Biol*. 2006; 35(6):639-50.
158. Florian S, Wingler K, Schmehl K, Jacobasch G, Kreuzer OJ, Meyerhof W, Brigelius-Flohe R. Cellular and subcellular localization of gastrointestinal glutathione peroxidase in normal and malignant human intestinal tissue. *Free Radic Res*. 2001; 35(6):655-63.
 159. Ursini F, Maiorino M, Valente M, Ferri L, Gregolin C. Purification from pig liver of a protein which protects liposomes and biomembranes from peroxidative degradation and exhibits glutathione peroxidase activity on phosphatidylcholine hydroperoxides. *Biochim Biophys Acta*. 1982; 710(2):197-211.
 160. Maiorino M, Thomas JP, Girotti AW, Ursini F. Reactivity of phospholipid hydroperoxide glutathione peroxidase with membrane and lipoprotein lipid hydroperoxides. *Free Radic Res Commun*. 1991; 12-13 Pt 1:131-5.
 161. Maiorino M, Scapin M, Ursini F, Biasolo M, Bosello V, Flohe L. Distinct promoters determine alternative transcription of gpx-4 into phospholipid-hydroperoxide glutathione peroxidase variants. *J Biol Chem*. 2003; 278(36):34286-90.
 162. Imai H, Hirao F, Sakamoto T, Sekine K, Mizukura Y, Saito M, Kitamoto T, Hayasaka M, Hanaoka K, Nakagawa Y. Early embryonic lethality caused by targeted disruption of the mouse PHGPx gene. *Biochem Biophys Res Commun*. 2003; 305(2):278-86.
 163. Yant LJ, Ran Q, Rao L, Van Remmen H, Shibatani T, Belter JG, Motta L, Richardson A, Prolla TA. The selenoprotein GPX4 is essential for mouse development and protects from radiation and oxidative damage insults. *Free Radic Biol Med*. 2003; 34(4):496-502.
 164. Ursini F, Heim S, Kiess M, Maiorino M, Roveri A, Wissing J, Flohe L. Dual function of the selenoprotein PHGPx during sperm maturation. *Science*. 1999; 285(5432):1393-6.
 165. Imai H, Suzuki K, Ishizaka K, Ichinose S, Oshima H, Okayasu I, Emoto K, Umeda M, Nakagawa Y. Failure of the expression of phospholipid hydroperoxide glutathione peroxidase in the spermatozoa of human infertile males. *Biol Reprod*. 2001; 64(2):674-83.
 166. Scheerer P, Borchert A, Krauss N, Wessner H, Gerth C, Hohne W, Kuhn H. Structural basis for catalytic activity and enzyme polymerization of phospholipid hydroperoxide glutathione peroxidase-4 (GPx4). *Biochemistry*. 2007; 46(31):9041-9.
 167. Schneider M, Forster H, Boersma A, Seiler A, Wehnes H, Sinowatz F, Neumuller C, Deutsch MJ, Walch A, Hrabe de Angelis M, Wurst W, Ursini F, Roveri A, Maleszewski

- M, Maiorino M, Conrad M. Mitochondrial glutathione peroxidase 4 disruption causes male infertility. *FASEB J.* 2009; 23(9):3233-42.
168. Imai H, Nakagawa Y. Biological significance of phospholipid hydroperoxide glutathione peroxidase (PHGPx, GPx4) in mammalian cells. *Free Radic Biol Med.* 2003; 34(2):145-69.
169. Nomura K, Imai H, Koumura T, Arai M, Nakagawa Y. Mitochondrial phospholipid hydroperoxide glutathione peroxidase suppresses apoptosis mediated by a mitochondrial death pathway. *J Biol Chem.* 1999; 274(41):29294-302.
170. Imai H, Narashima K, Arai M, Sakamoto H, Chiba N, Nakagawa Y. Suppression of leukotriene formation in RBL-2H3 cells that overexpressed phospholipid hydroperoxide glutathione peroxidase. *J Biol Chem.* 1998; 273(4):1990-7.
171. Chen CJ, Huang HS, Chang WC. Depletion of phospholipid hydroperoxide glutathione peroxidase up-regulates arachidonate metabolism by 12S-lipoxygenase and cyclooxygenase 1 in human epidermoid carcinoma A431 cells. *FASEB J.* 2003; 17(12):1694-6.
172. Schneider M, Wortmann M, Mandal PK, Arpornchayanon W, Jannasch K, Alves F, Strieth S, Conrad M, Beck H. Absence of glutathione peroxidase 4 affects tumor angiogenesis through increased 12/15-lipoxygenase activity. *Neoplasia.* 2010; 12(3):254-63.
173. Cejas P, Garcia-Cabezas MA, Casado E, Belda-Iniesta C, De Castro J, Fresno JA, Sereno M, Barriuso J, Espinosa E, Zamora P, Feliu J, Redondo A, Hardisson DA, Renart J, Gonzalez-Baron M. Phospholipid hydroperoxide glutathione peroxidase (PHGPx) expression is downregulated in poorly differentiated breast invasive ductal carcinoma. *Free Radic Res.* 2007; 41(6):681-7.
174. Flohe L, Gunzler WA, Schock HH. Glutathione peroxidase: a selenoenzyme. *FEBS Letter.* 1973; 32(1):132-34.
175. Esworthy RS, Ho YS, Chu FF. The Gpx1 gene encodes mitochondrial glutathione peroxidase in the mouse liver. *Arch Biochem Biophys.* 1997; 340(1):59-63.
176. Thu VT, Kim HK, Ha SH, Yoo JY, Park WS, Kim N, Oh GT, Han J. Glutathione peroxidase 1 protects mitochondria against hypoxia/reoxygenation damage in mouse hearts. *Pflugers Arch.* 2010; 460(1):55-68.
177. Handy DE, Lubos E, Yang Y, Galbraith JD, Kelly N, Zhang YY, Leopold JA, Loscalzo J. Glutathione peroxidase-1 regulates mitochondrial function to modulate redox-dependent cellular responses. *J Biol Chem.* 2009; 284:11913-21.

178. Legault J, Carrier C, Petrov P, Renard P, Remacle J, Mirault ME. Mitochondrial GPx1 decreases induced but not basal oxidative damage to mtDNA in T47D cells. *Biochem Biophys Res Commun.* 2000; 272(2):416-22.
179. Ho YS, Magnenat JL, Bronson RT, Cao J, Gargano M, Sugawara M, Funk CD. Mice deficient in cellular glutathione peroxidase develop normally and show no increased sensitivity to hyperoxia. *J Biol Chem.* 1997; 272(26):16644-51.
180. de Haan JB, Bladier C, Griffiths P, Kelner M, O'Shea RD, Cheung NS, Bronson RT, Silvestro MJ, Wild S, Zheng SS, Beart PM, Hertzog PJ, Kola I. Mice with a homozygous null mutation for the most abundant glutathione peroxidase, Gpx1, show increased susceptibility to the oxidative stress-inducing agents paraquat and hydrogen peroxide. *J Biol Chem.* 1998; 273(35):22528-36.
181. Duong C, Seow HJ, Bozinovski S, Crack PJ, Anderson GP, Vlahos R. Glutathione peroxidase-1 protects against cigarette smoke-induced lung inflammation in mice. *Am J Physiol Lung Cell Mol Physiol.* 2010; 299(3):L425-33.
182. Hockenbery DM, Oltvai ZN, Yin XM, Millman CL, Korsmeyer SJ. Bcl-2 functions in an antioxidant pathway to prevent apoptosis. *Cell.* 1993; 75(2):241-51.
183. Gouaze V, Mirault ME, Carpentier S, Salvayre R, Levade T, Andrieu-Abadie N. Glutathione peroxidase-1 overexpression prevents ceramide production and partially inhibits apoptosis in doxorubicin-treated human breast carcinoma cells. *Mol Pharmacol.* 2001; 60(3):488-96.
184. Gouaze V, Andrieu-Abadie N, Cuvillier O, Malagarie-Cazenave S, Frisach MF, Mirault ME, Levade T. Glutathione peroxidase-1 protects from CD95-induced apoptosis. *J Biol Chem.* 2002; 277(45):42867-74.
185. Faucher K, Rabinovitch-Chable H, Cook-Moreau J, Barriere G, Sturtz F, Rigaud M. Overexpression of human GPX1 modifies Bax to Bcl-2 apoptotic ratio in human endothelial cells. *Mol Cell Biochem.* 2005; 277(1-2):81-7.
186. Fu Y, Sies H, Lei XG. Opposite roles of selenium-dependent glutathione peroxidase-1 in superoxide generator diquat- and peroxynitrite-induced apoptosis and signaling. *J Biol Chem.* 2001; 276(46):43004-9.
187. Hu YJ, Diamond AM. Role of glutathione peroxidase 1 in breast cancer: loss of heterozygosity and allelic differences in the response to selenium. *Cancer Res.* 2003; 63(12):3347-51.

188. Baliga MS, Wang H, Zhuo P, Schwartz JL, Diamond AM. Selenium and GPx-1 overexpression protect mammalian cells against UV-induced DNA damage. *Biol Trace Elem Res.* 2007; 115(3):227-42.
189. Zhang Y, Ikeno Y, Qi W, Chaudhuri A, Li Y, Bokov A, Thorpe SR, Baynes JW, Epstein C, Richardson A, Van Remmen H. Mice deficient in both Mn superoxide dismutase and glutathione peroxidase-1 have increased oxidative damage and a greater incidence of pathology but no reduction in longevity. *J Gerontol A Biol Sci Med Sci.* 2009; 64(12):1212-20.
190. Won HY, Sohn JH, Min HJ, Lee K, Woo HA, Ho YS, Park JW, Rhee SG, Hwang ES. Glutathione peroxidase 1 deficiency attenuates allergen-induced airway inflammation by suppressing Th2 and Th17 cell development. *Antioxid Redox Signal.* 2010; 13(5):575-87.
191. Ardanaz N, Yang XP, Cifuentes ME, Haurani MJ, Jackson KW, Liao TD, Carretero OA, Pagano PJ. Lack of Glutathione Peroxidase 1 Accelerates Cardiac-Specific Hypertrophy and Dysfunction in Angiotensin II Hypertension. *Hypertension.* 2009.
192. Hu Y, Benya RV, Carroll RE, Diamond AM. Allelic loss of the gene for the GPX1 selenium-containing protein is a common event in cancer. *J Nutr.* 2005; 135(12 Suppl):3021S-24S.
193. Hu YJ, Dolan E, Bae R, Yee H, Roy M, Glickman R, Kiremidjian-Schumacher L, Diamond AM. Allelic loss of GPx-1 locus in cancer of the head and neck. *Biological Trace Element Research.* 2004; 101(2):97-106.
194. Hardie LJ, Briggs JA, Davidson LA, Allan JM, King RF, Williams GI, Wild CP. The effect of hOGG1 and glutathione peroxidase I genotypes and 3p chromosomal loss on 8-hydroxydeoxyguanosine levels in lung cancer. *Carcinogenesis.* 2000; 21(2):167-72.
195. Moscow JA, Schmidt L, Ingram DT, Gnarr J, Johnson B, Cowan KH. Loss of heterozygosity of the human cytosolic glutathione peroxidase I gene in lung cancer. *Carcinogenesis.* 1994; 15(12):2769-73.
196. Foster CB, Aswath K, Chanock SJ, McKay HF, Peters U. Polymorphism analysis of six selenoprotein genes: support for a selective sweep at the glutathione peroxidase 1 locus (3p21) in Asian populations. *BMC Genet.* 2006; 7:56.
197. Vincent HK, Powers SK, Stewart DJ, Shanely RA, Demirel H, Naito H. Obesity is associated with increased myocardial oxidative stress. *Int J Obes Relat Metab Disord.* 1999; 23(1):67-74.

198. Hotta K, Funahashi T, Bodkin NL, Ortmeyer HK, Arita Y, Hansen BC, Matsuzawa Y. Circulating concentrations of the adipocyte protein adiponectin are decreased in parallel with reduced insulin sensitivity during the progression to type 2 diabetes in rhesus monkeys. *Diabetes*. 2001; 50(5):1126-33.
199. Zhuo P, Goldberg M, Herman L, Lee BS, Wang H, Brown RL, Foster CB, Peters U, Diamond AM. Molecular consequences of genetic variations in the glutathione peroxidase 1 selenoenzyme. *Cancer Res*. 2009; 69(20):8183-90.
200. Bastaki M, Huen K, Manzanillo P, Chande N, Chen C, Balmes JR, Tager IB, Holland N. Genotype-activity relationship for Mn-superoxide dismutase, glutathione peroxidase 1 and catalase in humans. *Pharmacogenet Genomics*. 2006; 16(4):279-86.
201. Malling TH, Sigsgaard T, Andersen HR, Frischknecht L, Deguchi Y, Skadhauge L, Sherson D, Thomsen G, Baelum J, Pedersen JK, Omland O. Sex determines the influence of smoking and gene polymorphism on glutathione peroxidase activity in erythrocytes. *Scand J Clin Lab Invest*. 2009; 69(2):295-302.
202. Jablonska E, Gromadzinska J, Reszka E, Wasowicz W, Sobala W, Szeszenia-Dabrowska N, Boffetta P. Association between GPx1 Pro198Leu polymorphism, GPx1 activity and plasma selenium concentration in humans. *Eur J Nutr*. 2009; 48(6):383-6.
203. Miller JC, Thomson CD, Williams SM, van Havre N, Wilkins GT, Morison IM, Ludgate JL, Skeaff CM. Influence of the glutathione peroxidase 1 Pro200Leu polymorphism on the response of glutathione peroxidase activity to selenium supplementation: a randomized controlled trial. *Am J Clin Nutr*. 2012.
204. Kucukgergin C, Sanli O, Amasyali AS, Tefik T, Seckin S. Genetic variants of MnSOD and GPX1 and susceptibility to bladder cancer in a Turkish population. *Med Oncol*. 2012; 29(3):1928-34.
205. Cox DG, Tamimi RM, Hunter DJ. Gene x Gene interaction between MnSOD and GPX-1 and breast cancer risk: a nested case-control study. *BMC Cancer*. 2006; 6:217.
206. Ratnasinghe D, Tangrea JA, Andersen MR, Barrett MJ, Virtamo J, Taylor PR, Albanes D. Glutathione peroxidase codon 198 polymorphism variant increases lung cancer risk. *Cancer Res*. 2000; 60(22):6381-3.
207. Yang P, Bamlet WR, Ebbert JO, Taylor WR, de Andrade M. Glutathione pathway genes and lung cancer risk in young and old populations. *Carcinogenesis*. 2004; 25(10):1935-44.

208. Ichimura Y, Habuchi T, Tsuchiya N, Wang L, Oyama C, Sato K, Nishiyama H, Ogawa O, Kato T. Increased risk of bladder cancer associated with a glutathione peroxidase 1 codon 198 variant. *J Urol.* 2004; 172(2):728-32.
209. Sutton A, Nahon P, Pessayre D, Rufat P, Poire A, Zioli M, Vidaud D, Barget N, Ganne-Carrie N, Charnaux N, Trinchet JC, Gattegno L, Beaugrand M. Genetic polymorphisms in antioxidant enzymes modulate hepatic iron accumulation and hepatocellular carcinoma development in patients with alcohol-induced cirrhosis. *Cancer Res.* 2006; 66(5):2844-52.
210. Lightfoot TJ, Skibola CF, Smith AG, Forrest MS, Adamson PJ, Morgan GJ, Bracci PM, Roman E, Smith MT, Holly EA. Polymorphisms in the oxidative stress genes, superoxide dismutase, glutathione peroxidase and catalase and risk of non-Hodgkin's lymphoma. *Haematologica.* 2006; 91(9):1222-7.
211. Arsova-Sarafinovska Z, Matevska N, Eken A, Petrovski D, Banev S, Dzikova S, Georgiev V, Sikole A, Erdem O, Sayal A, Aydin A, Dimovski AJ. Glutathione peroxidase 1 (GPX1) genetic polymorphism, erythrocyte GPX activity, and prostate cancer risk. *Int Urol Nephrol.* 2009; 41(1):63-70.
212. Hong Z, Tian C, Zhang X. GPX1 gene Pro200Leu polymorphism, erythrocyte GPX activity, and cancer risk. *Mol Biol Rep.* 2013; 40(2):1801-12.
213. Liwei L, Wei Z, Ruifa H, Chunyu L. Association between genetic variants in glutathione peroxidase 1 gene and risk of prostate cancer: a meta-analysis. *Mol Biol Rep.* 2012; 39(9):8615-9.
214. Hansen RD, Krath BN, Frederiksen K, Tjonneland A, Overvad K, Roswall N, Loft S, Dragsted LO, Vogel U, Raaschou-Nielsen O. GPX1 Pro(198)Leu polymorphism, erythrocyte GPX activity, interaction with alcohol consumption and smoking, and risk of colorectal cancer. *Mutat Res.* 2009; 664(1-2):13-9.
215. Choi JY, Neuhaus ML, Barnett M, Hudson M, Kristal AR, Thornquist M, King IB, Goodman GE, Ambrosone CB. Polymorphisms in oxidative stress-related genes are not associated with prostate cancer risk in heavy smokers. *Cancer Epidemiol Biomarkers Prev.* 2007; 16(6):1115-20.
216. Carey DG, Jenkins AB, Campbell LV, Freund J, Chisholm DJ. Abdominal fat and insulin resistance in normal and overweight women: Direct measurements reveal a strong relationship in subjects at both low and high risk of NIDDM. *Diabetes.* 1996; 45(5):633-8.
217. Savill P. Identifying patients at risk of type 2 diabetes. *Practitioner.* 2012; 256(1753):25-7, 3.

218. Yang S, Zhu H, Li Y, Lin H, Gabrielson K, Trush MA, Diehl AM. Mitochondrial adaptations to obesity-related oxidant stress. *Arch Biochem Biophys*. 2000; 378(2):259-68.
219. Faienza MF, Francavilla R, Goffredo R, Ventura A, Marzano F, Panzarino G, Marinelli G, Cavallo L, Di Bitonto G. Oxidative stress in obesity and metabolic syndrome in children and adolescents. *Horm Res Paediatr*. 2012; 78(3):158-64.
220. McClung JP, Roneker CA, Mu W, Lisk DJ, Langlais P, Liu F, Lei XG. Development of insulin resistance and obesity in mice overexpressing cellular glutathione peroxidase. *Proc Natl Acad Sci U S A*. 2004; 101(24):8852-7.
221. Chen X, Scholl TO, Leskiw MJ, Donaldson MR, Stein TP. Association of glutathione peroxidase activity with insulin resistance and dietary fat intake during normal pregnancy. *J Clin Endocrinol Metab*. 2003; 88(12):5963-8.
222. Zeng MS, Li X, Liu Y, Zhao H, Zhou JC, Li K, Huang JQ, Sun LH, Tang JY, Xia XJ, Wang KN, Lei XG. A high-selenium diet induces insulin resistance in gestating rats and their offspring. *Free Radic Biol Med*. 2012; 52(8):1335-42.
223. Wang X, Vatamaniuk MZ, Roneker CA, Pepper MP, Hu LG, Simmons RA, Lei XG. Knockouts of SOD1 and GPX1 exert different impacts on murine islet function and pancreatic integrity. *Antioxid Redox Signal*. 2011; 14(3):391-401.
224. Loh K, Deng H, Fukushima A, Cai X, Boivin B, Galic S, Bruce C, Shields BJ, Skiba B, Ooms LM, Stepto N, Wu B, Mitchell CA, Tonks NK, Watt MJ, Febbraio MA, Crack PJ, Andrikopoulos S, Tiganis T. Reactive oxygen species enhance insulin sensitivity. *Cell Metab*. 2009; 10(4):260-72.
225. Harmon JS, Bogdani M, Parazzoli SD, Mak SS, Oseid EA, Berghmans M, Leboeuf RC, Robertson RP. beta-Cell-specific overexpression of glutathione peroxidase preserves intranuclear MafA and reverses diabetes in db/db mice. *Endocrinology*. 2009; 150(11):4855-62.
226. Yang FY, Lin ZH, Li SG, Guo BQ, Yin YS. Keshan disease--an endemic mitochondrial cardiomyopathy in China. *J Trace Elem Electrolytes Health Dis*. 1988; 2(3):157-63.
227. Alfthan G, Xu GL, Tan WH, Aro A, Wu J, Yang YX, Liang WS, Xue WL, Kong LH. Selenium supplementation of children in a selenium-deficient area in China: blood selenium levels and glutathione peroxidase activities. *Biol Trace Elem Res*. 2000; 73(2):113-25.

228. Li Y, Peng T, Yang Y, Niu C, Archard LC, Zhang H. High prevalence of enteroviral genomic sequences in myocardium from cases of endemic cardiomyopathy (Keshan disease) in China. *Heart*. 2000; 83(6):696-701.
229. Levander OA, Beck MA. Interacting nutritional and infectious etiologies of Keshan disease. Insights from coxsackie virus B-induced myocarditis in mice deficient in selenium or vitamin E. *Biol Trace Elem Res*. 1997; 56(1):5-21.
230. Beck MA, Esworthy RS, Ho YS, Chu FF. Glutathione peroxidase protects mice from viral-induced myocarditis. *FASEB J*. 1998; 12(12):1143-9.
231. Xiong Y, Liu X, Lee CP, Chua BH, Ho YS. Attenuation of doxorubicin-induced contractile and mitochondrial dysfunction in mouse heart by cellular glutathione peroxidase. *Free Radic Biol Med*. 2006; 41(1):46-55.
232. Cao C, Leng Y, Huang W, Liu X, Kufe D. Glutathione peroxidase 1 is regulated by the c-Abl and Arg tyrosine kinases. *J Biol Chem*. 2003; 278(41):39609-14.
233. Kim SC, Sprung R, Chen Y, Xu Y, Ball H, Pei J, Cheng T, Kho Y, Xiao H, Xiao L, Grishin NV, White M, Yang XJ, Zhao Y. Substrate and functional diversity of lysine acetylation revealed by a proteomics survey. *Mol Cell*. 2006; 23(4):607-18.
234. Cowan DB, Weisel RD, Williams WG, Mickle DA. Identification of oxygen responsive elements in the 5'-flanking region of the human glutathione peroxidase gene. *J Biol Chem*. 1993; 268(36):26904-10.
235. Tan M, Li S, Swaroop M, Guan K, Oberley LW, Sun Y. Transcriptional activation of the human glutathione peroxidase promoter by p53. *J Biol Chem*. 1999; 274(17):12061-6.
236. Zhou LZ, Johnson AP, Rando TA. NF kappa B and AP-1 mediate transcriptional responses to oxidative stress in skeletal muscle cells. *Free Radic Biol Med*. 2001; 31(11):1405-16.
237. Hussain SP, Amstad P, He P, Robles A, Lupold S, Kaneko I, Ichimiya M, Sengupta S, Mechanic L, Okamura S, Hofseth LJ, Moake M, Nagashima M, Forrester KS, Harris CC. p53-induced up-regulation of MnSOD and GPx but not catalase increases oxidative stress and apoptosis. *Cancer Res*. 2004; 64(7):2350-6.
238. Sun Y, Oberley LW. Redox regulation of transcriptional activators. *Free Radic Biol Med*. 1996; 21(3):335-48.
239. Das KC, Lewis-Molock Y, White CW. Activation of NF-kappa B and elevation of MnSOD gene expression by thiol reducing agents in lung adenocarcinoma (A549) cells. *Am J Physiol*. 1995; 269(5 Pt 1):L588-602.

240. Chambers I, Frampton J, Goldfarb P, Affara N, McBain W, Harrison PR. The structure of the mouse glutathione peroxidase gene: the selenocysteine in the active site is encoded by the 'termination' codon, TGA. *Embo J.* 1986; 5(6):1221-7.
241. Le Hir H, Gatfield D, Izaurralde E, Moore MJ. The exon-exon junction complex provides a binding platform for factors involved in mRNA export and nonsense-mediated mRNA decay. *Embo J.* 2001; 20(17):4987-97.
242. Hubert N, Walczak R, Carbon P, Krol A. A protein binds the selenocysteine insertion element in the 3'-UTR of mammalian selenoprotein mRNAs. *Nucleic Acids Res.* 1996; 24(3):464-9.
243. Copeland PR, Driscoll DM. Purification, redox sensitivity, and RNA binding properties of SECIS-binding protein 2, a protein involved in selenoprotein biosynthesis. *J Biol Chem.* 1999; 274(36):25447-54.
244. Fagegaltier D, Hubert N, Yamada K, Mizutani T, Carbon P, Krol A. Characterization of mSelB, a novel mammalian elongation factor for selenoprotein translation. *Embo J.* 2000; 19(17):4796-805.
245. Papp LV, Lu J, Holmgren A, Khanna KK. From selenium to selenoproteins: synthesis, identity, and their role in human health. *Antioxid Redox Signal.* 2007; 9(7):775-806.
246. Schoenmakers E, Agostini M, Mitchell C, Schoenmakers N, Papp L, Rajanayagam O, Padidela R, Ceron-Gutierrez L, Doffinger R, Prevosto C, Luan J, Montano S, Lu J, Castanet M, Clemons N, Groeneveld M, Castets P, Karbaschi M, Aitken S, Dixon A, Williams J, Campi I, Blount M, Burton H, Muntoni F, O'Donovan D, Dean A, Warren A, Brierley C, Baguley D, Guicheney P, Fitzgerald R, Coles A, Gaston H, Todd P, Holmgren A, Khanna KK, Cooke M, Semple R, Halsall D, Wareham N, Schwabe J, Grasso L, Beck-Peccoz P, Ogunko A, Dattani M, Gurnell M, Chatterjee K. Mutations in the selenocysteine insertion sequence-binding protein 2 gene lead to a multisystem selenoprotein deficiency disorder in humans. *J Clin Invest.* 2010; 120(12):4220-35.
247. Diamond AM, Choi IS, Crain PF, Hashizume T, Pomerantz SC, Cruz R, Steer CJ, Hill KE, Burk RF, McCloskey JA, Hatfield DL. Dietary Selenium Affects Methylation of the Wobble Nucleoside in the Anticodon of Selenocysteine tRNA^{(Ser)Sec}. *Journal of Biological Chemistry.* 1993; 268(19):14215-23.
248. Moustafa ME, Carlson BA, El-Saadani MA, Kryukov GV, Sun QA, Harney JW, Hill KE, Combs GF, Feigenbaum L, Mansur DB, Burk RF, Berry MJ, Diamond AM, Lee BJ, Gladyshev VN, Hatfield DL. Selective inhibition of selenocysteine tRNA maturation and selenoprotein synthesis in transgenic mice expressing isopentenyladenosine-deficient selenocysteine tRNA. *Mol Cell Biol.* 2001; 21(11):3840-52.

249. Xu XM, Mix H, Carlson BA, Grabowski PJ, Gladyshev VN, Berry MJ, Hatfield DL. Evidence for direct roles of two additional factors, SECp43 and soluble liver antigen, in the selenoprotein synthesis machinery. *J Biol Chem.* 2005; 280(50):41568-75.
250. Blum J, Fridovich I. Inactivation of glutathione peroxidase by superoxide radical. *Arch Biochem Biophys.* 1985; 240(2):500-8.
251. Cho CS, Lee S, Lee GT, Woo HA, Choi EJ, Rhee SG. Irreversible inactivation of glutathione peroxidase 1 and reversible inactivation of peroxiredoxin II by H₂O₂ in red blood cells. *Antioxid Redox Signal.* 2010; 12(11):1235-46.
252. Fritz KS, Galligan JJ, Hirschey MD, Verdin E, Petersen DR. Mitochondrial acetylome analysis in a mouse model of alcohol-induced liver injury utilizing SIRT3 knockout mice. *J Proteome Res.* 2012; 11(3):1633-43.
253. Shepard BD, Tuma DJ, Tuma PL. Chronic ethanol consumption induces global hepatic protein hyperacetylation. *Alcohol Clin Exp Res.* 2010; 34(2):280-91.
254. Yu HS, Oyama T, Isse T, Kitagawa K, Pham TT, Tanaka M, Kawamoto T. Formation of acetaldehyde-derived DNA adducts due to alcohol exposure. *Chem Biol Interact.* 2010; 188(3):367-75.
255. Lee SH, Altenberg GA. Expression of functional multidrug-resistance protein 1 in *Saccharomyces cerevisiae*: effects of N- and C-terminal affinity tags. *Biochem Biophys Res Commun.* 2003; 306(3):644-9.
256. Galli F, Floridi AG, Floridi A, Buoncristiani U. Accumulation of vitamin E metabolites in the blood of renal failure patients. *Clin Nutr.* 2004; 23(2):205-12.
257. Buchdunger E, Zimmermann J, Mett H, Meyer T, Muller M, Druker BJ, Lydon NB. Inhibition of the Abl protein-tyrosine kinase in vitro and in vivo by a 2-phenylaminopyrimidine derivative. *Cancer Res.* 1996; 56(1):100-4.
258. Heinrich MC, Griffith DJ, Druker BJ, Wait CL, Ott KA, Zigler AJ. Inhibition of c-kit receptor tyrosine kinase activity by STI 571, a selective tyrosine kinase inhibitor. *Blood.* 2000; 96(3):925-32.
259. Naldini L, Stacchini A, Cirillo DM, Aglietta M, Gavosto F, Comoglio PM. Phosphotyrosine antibodies identify the p210c-abl tyrosine kinase and proteins phosphorylated on tyrosine in human chronic myelogenous leukemia cells. *Mol Cell Biol.* 1986; 6(5):1803-11.
260. Deininger M, Buchdunger E, Druker BJ. The development of imatinib as a therapeutic agent for chronic myeloid leukemia. *Blood.* 2005; 105(7):2640-53.

261. Kim JH, Chu SC, Gramlich JL, Pride YB, Babendreier E, Chauhan D, Salgia R, Podar K, Griffin JD, Sattler M. Activation of the PI3K/mTOR pathway by BCR-ABL contributes to increased production of reactive oxygen species. *Blood*. 2005; 105(4):1717-23.
262. Collins SJ, Kubonishi I, Miyoshi I, Groudine MT. Altered transcription of the c-abl oncogene in K-562 and other chronic myelogenous leukemia cells. *Science*. 1984; 225(4657):72-4.
263. Shtivelman E, Lifshitz B, Gale RP, Canaani E. Fused transcript of abl and bcr genes in chronic myelogenous leukaemia. *Nature*. 1985; 315(6020):550-4.
264. Samuels BA, Murray JL, Cohen MB, Safa AR, Sinha BK, Townsend AJ, Beckett MA, Weichselbaum RR. Increased glutathione peroxidase activity in human sarcoma cell line with inherent doxorubicin resistance. *Cancer Research*. 1991; 51:521-27.
265. Terry EN, Gann PH, Molokie R, Deininger M, Diamond AM. Changes in the activity of the GPx-1 anti-oxidant selenoenzyme in mononuclear cells following imatinib treatment. *Leuk Res*. 2011; 35(6):831-3.
266. Bradford MM. A rapid and sensitive method for the quantitation of microgram quantities of protein utilizing the principle of protein-dye binding. *Analytical Biochemistry*. 1976; 72:248-54.
267. Livak KJ, Schmittgen TD. Analysis of relative gene expression data using real-time quantitative PCR and the 2(-Delta Delta C(T)) Method. *Methods*. 2001; 25(4):402-8.
268. Miller AD, Rosman GJ. Improved retroviral vectors for gene transfer and expression. *Biotechniques*. 1989; 7:980-90.
269. Jameson RR, Diamond AM. A regulatory role for Sec tRNA[Ser]Sec in selenoprotein synthesis. *RNA*. 2004; 10(7):1142-52.
270. Kishi K. A new leukemia cell line with Philadelphia chromosome characterized as basophil precursors. *Leuk Res*. 1985; 9(3):381-90.
271. Ogura M, Morishima Y, Ohno R, Kato Y, Hirabayashi N, Nagura H, Saito H. Establishment of a novel human megakaryoblastic leukemia cell line, MEG-01, with positive Philadelphia chromosome. *Blood*. 1985; 66(6):1384-92.
272. Horoszewicz JS, Leong SS, Chu TM, Wajsman ZL, Friedman M, Papsidero L, Kim U, Chai LS, Kakati S, Arya SK, Sandberg AA. The LNCaP cell line--a new model for studies on human prostatic carcinoma. *Prog Clin Biol Res*. 1980; 37:115-32.

273. Ly C, Arechiga AF, Melo JV, Walsh CM, Ong ST. Bcr-Abl kinase modulates the translation regulators ribosomal protein S6 and 4E-BP1 in chronic myelogenous leukemia cells via the mammalian target of rapamycin. *Cancer Res.* 2003; 63(18):5716-22.
274. Brown EJ, Albers MW, Shin TB, Ichikawa K, Keith CT, Lane WS, Schreiber SL. A mammalian protein targeted by G1-arresting rapamycin-receptor complex. *Nature.* 1994; 369(6483):756-8.
275. Fingar DC, Salama S, Tsou C, Harlow E, Blenis J. Mammalian cell size is controlled by mTOR and its downstream targets S6K1 and 4EBP1/eIF4E. *Genes Dev.* 2002; 16(12):1472-87.
276. Cao C, Leng Y, Kufe D. Catalase activity is regulated by c-Abl and Arg in the oxidative stress response. *J Biol Chem.* 2003; 278(32):29667-75.
277. Zang C, Liu H, Waechter M, Eucker J, Bertz J, Possinger K, Koeffler HP, Elstner E. Dual PPARalpha/gamma ligand TZD18 either alone or in combination with imatinib inhibits proliferation and induces apoptosis of human CML cell lines. *Cell Cycle.* 2006; 5(19):2237-43.
278. Aichberger KJ, Mayerhofer M, Vales A, Krauth MT, Gleixner KV, Bilban M, Esterbauer H, Sonneck K, Florian S, Derdak S, Pickl WF, Agis H, Falus A, Sillaber C, Valent P. The CML-related oncoprotein BCR/ABL induces expression of histidine decarboxylase (HDC) and the synthesis of histamine in leukemic cells. *Blood.* 2006; 108(10):3538-47.
279. Kawano T, Ito M, Raina D, Wu Z, Rosenblatt J, Avigan D, Stone R, Kufe D. MUC1 oncoprotein regulates Bcr-Abl stability and pathogenesis in chronic myelogenous leukemia cells. *Cancer Res.* 2007; 67(24):11576-84.
280. Lin LC, Yeh CT, Kuo CC, Lee CM, Yen GC, Wang LS, Wu CH, Yang WC, Wu AT. Sulforaphane potentiates the efficacy of imatinib against chronic leukemia cancer stem cells through enhanced abrogation of Wnt/beta-catenin function. *J Agric Food Chem.* 2012; 60(28):7031-9.
281. Baran Y, Ural AU, Gunduz U. Mechanisms of cellular resistance to imatinib in human chronic myeloid leukemia cells. *Hematology.* 2007; 12(6):497-503.
282. Liu JH, Liu CC, Yen CC, Gau JP, Wang WS, Tzeng CH. Pml and TAp73 interacting at nuclear body mediate imatinib-induced p53-independent apoptosis of chronic myeloid leukemia cells. *Int J Cancer.* 2009; 125(1):71-7.
283. Salih J, Hilpert J, Placke T, Grunebach F, Steinle A, Salih HR, Krusch M. The BCR/ABL-inhibitors imatinib, nilotinib and dasatinib differentially affect NK cell reactivity. *Int J Cancer.* 2010; 127(9):2119-28.

284. Wong GH, Goeddel DV. Induction of manganous superoxide dismutase by tumor necrosis factor: possible protective mechanism. *Science*. 1988; 242(4880):941-4.
285. Borrello S, Demple B. NF kappa B-independent transcriptional induction of the human manganous superoxide dismutase gene. *Arch Biochem Biophys*. 1997; 348(2):289-94.
286. Sakurai A, Nishimoto M, Himeno S, Imura N, Tsujimoto M, Kunimoto M, Hara S. Transcriptional regulation of thioredoxin reductase 1 expression by cadmium in vascular endothelial cells: role of NF-E2-related factor-2. *J Cell Physiol*. 2005; 203(3):529-37.
287. Rundlof AK, Arner ES. Regulation of the mammalian selenoprotein thioredoxin reductase 1 in relation to cellular phenotype, growth, and signaling events. *Antioxid Redox Signal*. 2004; 6(1):41-52.
288. Forsberg L, Lyrenas L, de Faire U, Morgenstern R. A common functional C-T substitution polymorphism in the promoter region of the human catalase gene influences transcription factor binding, reporter gene transcription and is correlated to blood catalase levels. *Free Radic Biol Med*. 2001; 30(5):500-5.
289. Knopp EA, Arndt TL, Eng KL, Caldwell M, LeBoeuf RC, Deeb SS, O'Brien KD. Murine phospholipid hydroperoxide glutathione peroxidase: cDNA sequence, tissue expression, and mapping. *Mamm Genome*. 1999; 10(6):601-5.
290. Ufer C, Borchert A, Kuhn H. Functional characterization of cis- and trans-regulatory elements involved in expression of phospholipid hydroperoxide glutathione peroxidase. *Nucleic Acids Res*. 2003; 31(15):4293-303.
291. Squires JE, Stoytchev I, Forry EP, Berry MJ. SBP2 binding affinity is a major determinant in differential selenoprotein mRNA translation and sensitivity to nonsense-mediated decay. *Mol Cell Biol*. 2007; 27(22):7848-55.
292. Usuki F, Yamashita A, Fujimura M. Post-transcriptional defects of antioxidant selenoenzymes cause oxidative stress under methylmercury exposure. *J Biol Chem*. 2011; 286(8):6641-9.
293. Davis CA, Monnier JM, Nick HS. A coding region determinant of instability regulates levels of manganese superoxide dismutase mRNA. *J Biol Chem*. 2001; 276(40):37317-26.
294. Sutton A, Imbert A, Igoudjil A, Descatoire V, Cazanave S, Pessayre D, Degoul F. The manganese superoxide dismutase Ala16Val dimorphism modulates both mitochondrial import and mRNA stability. *Pharmacogenet Genomics*. 2005; 15(5):311-9.
295. Chung DJ, Clerch LB. RNA in polysomes is an inhibitor of manganese superoxide dismutase RNA-binding protein activity. *Am J Physiol*. 1997; 272(4 Pt 1):L714-9.

296. Fazzzone H, Wangner A, Clerch LB. Rat lung contains a developmentally regulated manganese superoxide dismutase mRNA-binding protein. *J Clin Invest.* 1993; 92(3):1278-81.
297. Knirsch L, Clerch LB. Tyrosine phosphorylation regulates manganese superoxide dismutase (MnSOD) RNA-binding protein activity and MnSOD protein expression. *Biochemistry.* 2001; 40(26):7890-5.
298. Altschul SF, Gish W, Miller W, Myers EW, Lipman DJ. Basic local alignment search tool. *J Mol Biol.* 1990; 215(3):403-10.
299. Zhang Z, Schwartz S, Wagner L, Miller W. A greedy algorithm for aligning DNA sequences. *J Comput Biol.* 2000; 7(1-2):203-14.
300. Li JJ, Oberley LW. Overexpression of manganese-containing superoxide dismutase confers resistance to the cytotoxicity of tumor necrosis factor alpha and/or hyperthermia. *Cancer Res.* 1997; 57(10):1991-8.
301. St Clair DK, Wan XS, Oberley TD, Muse KE, St Clair WH. Suppression of radiation-induced neoplastic transformation by overexpression of mitochondrial superoxide dismutase. *Mol Carcinog.* 1992; 6(4):238-42.
302. Cheng WH, Ho YS, Ross DA, Valentine BA, Combs GF, Lei XG. Cellular glutathione peroxidase knockout mice express normal levels of selenium-dependent plasma and phospholipid hydroperoxide glutathione peroxidases in various tissues. *J Nutr.* 1997; 127(8):1445-50.
303. Li S, Yan T, Yang JQ, Oberley TD, Oberley LW. The role of cellular glutathione peroxidase redox regulation in the suppression of tumor cell growth by manganese superoxide dismutase. *Cancer Res.* 2000; 60(14):3927-39.
304. Liu J, Hinkhouse MM, Sun W, Weydert CJ, Ritchie JM, Oberley LW, Cullen JJ. Redox regulation of pancreatic cancer cell growth: role of glutathione peroxidase in the suppression of the malignant phenotype. *Hum Gene Ther.* 2004; 15(3):239-50.
305. Nalvarte I, Damdimopoulos AE, Nystom C, Nordman T, Miranda-Vizuete A, Olsson JM, Eriksson L, Bjornstedt M, Arner ES, Spyrou G. Overexpression of enzymatically active human cytosolic and mitochondrial thioredoxin reductase in HEK-293 cells. Effect on cell growth and differentiation. *J Biol Chem.* 2004; 279(52):54510-7.
306. Sordillo LM, O'Boyle N, Gandy JC, Corl CM, Hamilton E. Shifts in thioredoxin reductase activity and oxidant status in mononuclear cells obtained from transition dairy cattle. *J Dairy Sci.* 2007; 90(3):1186-92.

307. Hofmann ER, Boyanapalli M, Lindner DJ, Weihua X, Hassel BA, Jagus R, Gutierrez PL, Kalvakolanu DV. Thioredoxin reductase mediates cell death effects of the combination of beta interferon and retinoic acid. *Mol Cell Biol.* 1998; 18(11):6493-504.
308. Lu G, Shimizu I, Cui X, Itonaga M, Tamaki K, Fukuno H, Inoue H, Honda H, Ito S. Interferon-alpha enhances biological defense activities against oxidative stress in cultured rat hepatocytes and hepatic stellate cells. *J Med Invest.* 2002; 49(3-4):172-81.
309. Obrig TG, Culp WJ, McKeehan WL, Hardesty B. The mechanism by which cycloheximide and related glutarimide antibiotics inhibit peptide synthesis on reticulocyte ribosomes. *J Biol Chem.* 1971; 246(1):174-81.
310. Schneider-Poetsch T, Ju J, Eyler DE, Dang Y, Bhat S, Merrick WC, Green R, Shen B, Liu JO. Inhibition of eukaryotic translation elongation by cycloheximide and lactimidomycin. *Nat Chem Biol.* 2010; 6(3):209-17.
311. Hopper RK, Carroll S, Aponte AM, Johnson DT, French S, Shen RF, Witzmann FA, Harris RA, Balaban RS. Mitochondrial matrix phosphoproteome: effect of extra mitochondrial calcium. *Biochemistry.* 2006; 45(8):2524-36.
312. Huguet F, Giocanti N, Hennequin C, Croisy M, Touboul E, Favaudon V. Growth inhibition by STI571 in combination with radiation in human chronic myelogenous leukemia K562 cells. *Mol Cancer Ther.* 2008; 7(2):398-406.
313. Obenauer JC, Cantley LC, Yaffe MB. Scansite 2.0: Proteome-wide prediction of cell signaling interactions using short sequence motifs. *Nucleic Acids Res.* 2003; 31(13):3635-41.
314. Lombard DB, Alt FW, Cheng HL, Bunkenborg J, Streeper RS, Mostoslavsky R, Kim J, Yancopoulos G, Valenzuela D, Murphy A, Yang Y, Chen Y, Hirschey MD, Bronson RT, Haigis M, Guarente LP, Farese RV, Jr., Weissman S, Verdin E, Schwer B. Mammalian Sir2 homolog SIRT3 regulates global mitochondrial lysine acetylation. *Mol Cell Biol.* 2007; 27(24):8807-14.
315. Lundby A, Lage K, Weinert BT, Bekker-Jensen DB, Secher A, Skovgaard T, Kelstrup CD, Dmytriiev A, Choudhary C, Lundby C, Olsen JV. Proteomic analysis of lysine acetylation sites in rat tissues reveals organ specificity and subcellular patterns. *Cell Rep.* 2012; 2(2):419-31.
316. Rix U, Hantschel O, Durnberger G, Remsing Rix LL, Planyavsky M, Fernbach NV, Kaupé I, Bennett KL, Valent P, Colinge J, Kocher T, Superti-Furga G. Chemical proteomic profiles of the BCR-ABL inhibitors imatinib, nilotinib, and dasatinib reveal novel kinase and nonkinase targets. *Blood.* 2007; 110(12):4055-63.

317. Winger JA, Hantschel O, Superti-Furga G, Kuriyan J. The structure of the leukemia drug imatinib bound to human quinone reductase 2 (NQO2). *BMC Struct Biol.* 2009; 9:7.
318. Melo JV, Chuah C. Resistance to imatinib mesylate in chronic myeloid leukaemia. *Cancer Lett.* 2007; 249(2):121-32.
319. Zhao Y, Sun Y. Targeting the mTOR-DEPTOR pathway by CRL E3 ubiquitin ligases: therapeutic application. *Neoplasia.* 2012; 14(5):360-7.
320. Patterson C, Mapera S, Li HH, Madamanchi N, Hilliard E, Lineberger R, Herrmann R, Charles P. Comparative effects of paclitaxel and rapamycin on smooth muscle migration and survival: role of AKT-dependent signaling. *Arterioscler Thromb Vasc Biol.* 2006; 26(7):1473-80.
321. Heuer M, Benko T, Cicinnati VR, Kaiser GM, Sotiropoulos GC, Baba HA, Treckmann JW, Broelsch CE, Paul A. Effect of low-dose rapamycin on tumor growth in two human hepatocellular cancer cell lines. *Transplant Proc.* 2009; 41(1):359-65.
322. Schieke SM, Phillips D, McCoy JP, Jr., Aponte AM, Shen RF, Balaban RS, Finkel T. The mammalian target of rapamycin (mTOR) pathway regulates mitochondrial oxygen consumption and oxidative capacity. *J Biol Chem.* 2006; 281(37):27643-52.
323. Chen C, Liu Y, Liu R, Ikenoue T, Guan KL, Liu Y, Zheng P. TSC-mTOR maintains quiescence and function of hematopoietic stem cells by repressing mitochondrial biogenesis and reactive oxygen species. *J Exp Med.* 2008; 205(10):2397-408.
324. Nussbaum RL, Orrison BM, Janne PA, Charnas L, Chinault AC. Physical mapping and genomic structure of the Lowe syndrome gene OCRL1. *Hum Genet.* 1997; 99(2):145-50.
325. Baxi SM, Walls M, Cheng H, Yin MJ. Targeting the mTOR pathway in tumor malignancy. *Curr Cancer Drug Targets.* 2013.
326. Thoreen CC, Kang SA, Chang JW, Liu Q, Zhang J, Gao Y, Reichling LJ, Sim T, Sabatini DM, Gray NS. An ATP-competitive mammalian target of rapamycin inhibitor reveals rapamycin-resistant functions of mTORC1. *J Biol Chem.* 2009; 284(12):8023-32.
327. Yu K, Toral-Barza L, Shi C, Zhang WG, Lucas J, Shor B, Kim J, Verheijen J, Curran K, Malwitz DJ, Cole DC, Ellingboe J, Ayril-Kaloustian S, Mansour TS, Gibbons JJ, Abraham RT, Nowak P, Zask A. Biochemical, cellular, and in vivo activity of novel ATP-competitive and selective inhibitors of the mammalian target of rapamycin. *Cancer Res.* 2009; 69(15):6232-40.

328. Sarbassov DD, Ali SM, Sengupta S, Sheen JH, Hsu PP, Bagley AF, Markhard AL, Sabatini DM. Prolonged rapamycin treatment inhibits mTORC2 assembly and Akt/PKB. *Mol Cell*. 2006; 22(2):159-68.
329. Kloo B, Nagel D, Pfeifer M, Grau M, Duwel M, Vincendeau M, Dorken B, Lenz P, Lenz G, Krappmann D. Critical role of PI3K signaling for NF-kappaB-dependent survival in a subset of activated B-cell-like diffuse large B-cell lymphoma cells. *Proc Natl Acad Sci U S A*. 2011; 108(1):272-7.
330. Li J, Li F, Wang H, Wang X, Jiang Y, Li D. Wortmannin reduces metastasis and angiogenesis of human breast cancer cells via nuclear factor-kappaB-dependent matrix metalloproteinase-9 and interleukin-8 pathways. *J Int Med Res*. 2012; 40(3):867-76.
331. Ballif BA, Roux PP, Gerber SA, MacKeigan JP, Blenis J, Gygi SP. Quantitative phosphorylation profiling of the ERK/p90 ribosomal S6 kinase-signaling cassette and its targets, the tuberous sclerosis tumor suppressors. *Proc Natl Acad Sci U S A*. 2005; 102(3):667-72.
332. Ma L, Chen Z, Erdjument-Bromage H, Tempst P, Pandolfi PP. Phosphorylation and functional inactivation of TSC2 by Erk implications for tuberous sclerosis and cancer pathogenesis. *Cell*. 2005; 121(2):179-93.
333. Ma L, Teruya-Feldstein J, Bonner P, Bernardi R, Franz DN, Witte D, Cordon-Cardo C, Pandolfi PP. Identification of S664 TSC2 phosphorylation as a marker for extracellular signal-regulated kinase mediated mTOR activation in tuberous sclerosis and human cancer. *Cancer Res*. 2007; 67(15):7106-12.
334. Tee AR, Anjum R, Blenis J. Inactivation of the tuberous sclerosis complex-1 and -2 gene products occurs by phosphoinositide 3-kinase/Akt-dependent and -independent phosphorylation of tuberlin. *J Biol Chem*. 2003; 278(39):37288-96.
335. Ohdate T, Izawa S, Kita K, Inoue Y. Regulatory mechanism for expression of GPX1 in response to glucose starvation and Ca in *Saccharomyces cerevisiae*: involvement of Snf1 and Ras/cAMP pathway in Ca signaling. *Genes Cells*. 2010; 15(1):59-75.
336. Squires JE, Berry MJ. Eukaryotic selenoprotein synthesis: mechanistic insight incorporating new factors and new functions for old factors. *IUBMB Life*. 2008; 60(4):232-5.
337. Ufer C, Wang CC, Fahling M, Schiebel H, Thiele BJ, Billett EE, Kuhn H, Borchert A. Translational regulation of glutathione peroxidase 4 expression through guanine-rich sequence-binding factor 1 is essential for embryonic brain development. *Genes Dev*. 2008; 22(13):1838-50.

338. Blackinton J, Kumaran R, van der Brug MP, Ahmad R, Olson L, Galter D, Lees A, Bandopadhyay R, Cookson MR. Post-transcriptional regulation of mRNA associated with DJ-1 in sporadic Parkinson disease. *Neurosci Lett*. 2009; 452(1):8-11.
339. Taira T, Saito Y, Niki T, Iguchi-Ariga SM, Takahashi K, Ariga H. DJ-1 has a role in antioxidative stress to prevent cell death. *EMBO Rep*. 2004; 5(2):213-8.
340. van der Brug MP, Blackinton J, Chandran J, Hao LY, Lal A, Mazan-Mamczarz K, Martindale J, Xie C, Ahmad R, Thomas KJ, Beilina A, Gibbs JR, Ding J, Myers AJ, Zhan M, Cai H, Bonini NM, Gorospe M, Cookson MR. RNA binding activity of the recessive parkinsonism protein DJ-1 supports involvement in multiple cellular pathways. *Proc Natl Acad Sci U S A*. 2008; 105(29):10244-9.
341. Vasseur S, Afzal S, Tardivel-Lacombe J, Park DS, Iovanna JL, Mak TW. DJ-1/PARK7 is an important mediator of hypoxia-induced cellular responses. *Proc Natl Acad Sci U S A*. 2009; 106(4):1111-6.
342. Martin GW, 3rd, Berry MJ. Selenocysteine codons decrease polysome association on endogenous selenoprotein mRNAs. *Genes Cells*. 2001; 6(2):121-9.
343. Fletcher JE, Copeland PR, Driscoll DM. Polysome distribution of phospholipid hydroperoxide glutathione peroxidase mRNA: evidence for a block in elongation at the UGA/selenocysteine codon. *RNA*. 2000; 6(11):1573-84.
344. Meyuhas O, Thompson EA, Jr., Perry RP. Glucocorticoids selectively inhibit translation of ribosomal protein mRNAs in P1798 lymphosarcoma cells. *Mol Cell Biol*. 1987; 7(8):2691-9.
345. Berry MJ, Harney JW, Ohama T, Hatfield DL. Selenocysteine insertion or termination: factors affecting UGA codon fate and complementary anticodon:codon mutations. *Nucleic Acids Res*. 1994; 22(18):3753-9.
346. Grundner-Culemann E, Martin GW, 3rd, Tujebajeva R, Harney JW, Berry MJ. Interplay between termination and translation machinery in eukaryotic selenoprotein synthesis. *J Mol Biol*. 2001; 310(4):699-707.
347. Gupta M, Copeland PR. Functional analysis of the interplay between translation termination, selenocysteine codon context, and selenocysteine insertion sequence-binding protein 2. *J Biol Chem*. 2007; 282(51):36797-807.
348. Brigelius-Flohe R, Kipp A. Glutathione peroxidases in different stages of carcinogenesis. *Biochim Biophys Acta*. 2009; 1790(11):1555-68.

349. Singh RK, Tripathi AK, Tripathi P, Singh S, Singh R, Ahmad R. Studies on biomarkers for oxidative stress in patients with chronic myeloid leukemia. *Hematol Oncol Stem Cell Ther.* 2009; 2(1):285-8.

VITA

Emily N. (Terry) Reinke, MS

EDUCATION

Formal education

Bachelor of Sciences, 2:1 classification	Animal Biology
University of St Andrews	June 2006 St. Andrews, Scotland
Master of Sciences	Animal Sciences
Washington State University	May 2008 Pullman, WA
Doctor of Philosophy	Pathology
University of Illinois at Chicago	In progress Chicago, IL

Major subjects

Undergraduate: Animal Biology
 Graduate: Animal Sciences, Pathology,

Thesis subjects

BSc Honors- Influence of Embryonic Incubation Temperature on White Muscle Fibre Recruitment in Atlantic Salmon (*Salmo salar L.*)
 M.S.- Regulation of Selected Selenoproteins in Porcine and Bovine Skeletal Muscle
 PhD- Post-transcriptional regulation of antioxidant enzymes

Scholarships and Fellowships

Vacation Scholarship (Animal Genetics and Genomics)	April 2006	Genesis Faraday
Veenhuizen Scholarship	April 2007	WSU- Animal Sciences
Fred W. Frasier Memorial Scholarship	April 2007	WSU- Animal Sciences
Graduate School Travel Grant	February 2008	WSU-Graduate School
GPSA Registration Grant	February 2008	WSU- GPSA
ASEE SMART Scholarship	August 2011	American Society for Engineering Education

EMPLOYMENT

Dates	Title	Address
July 2003-Aug 2004	Veterinary Assistant	Evergreen Veterinary Hospital, Kirkland, WA
Aug. 2006-May 2008	Graduate Teaching Assistant	Washington State University
Aug. 2008- Present	Graduate Assistant	University of Illinois at Chicago

COURSES TAUGHT

Institution	Name	Years
Washington State University	Introduction to Animal Sciences	Fall 2006
	Dr. Jerry Reeves	
	Reproduction of Farm Animals	Spring 2007
	Dr. Derek McLean	
	Introduction to Animal Sciences	Fall 2007
	Dr. Charles Gaskins	
	Reproduction of Farm Animals	Spring 2008
	Dr. Derek McLean	

MEMBERSHIPSProfessional

American Association for Cancer Research	2011-Present
Society of Toxicology	2011-Present
American Society of Clinical Oncology	2012-Present
American Society for Nutrition	2007-2008
Graduate Women in Science- Psi Chapter	Washington State University
Animal Sciences Graduate Student Association	Washington State University
Secretary/Treasurer 2007-2008	
Biological Society	University of St Andrews

COMMITTEE SERVICEUniversity

Graduate Student Council	University of Illinois at Chicago
Graduate and Professional Students Association	Washington State University
Biology Staff and Student Council	University of St Andrews

MANUSCRIPTS

- Terry, E.N.**, Michal, J.J., Hostetler, C.E., Kincaid, R.L. Levels of mRNA for three selenoproteins in skeletal muscle of fetal and newborn pigs. *Livest Sci* 2009;129 (1-3): 21-25.
- Brennan, K.M., **Terry, E. N.**, Michal, J. J., Kincaid, R. L., Johnson, K. A.. Body weight loss in beef cows: II. Increased antioxidant messenger ribonucleic acid levels in skeletal muscle but not erythrocyte antioxidant activity. *J Anim Sci.* 2009; 89(9):2867-2873
- Terry, EN**, Gann, P.H., Molokie, R., Deininger, M. and Diamond, A.M.. Changes in the activity of the GPx1 anti-oxidant selenoenzyme in mononuclear cells following imatinib treatment. *Leukemia Res.* 2011;35(6):831-833

BOOK CHAPTERS

- Terry, E.N.** and Diamond, A.M., Selenium. in *Present Knowledge in Nutrition*. Eds. Erdman, J., MacDonald, I., Zeisel, S. 10 ed. Washington, D.C. ILSI Press. 2012. Chapter 37.

EXTERNAL PRESENTATIONS

- Kincaid, R. L. and **E. N. Terry**. 2007. The role of selenoproteins in fetal development. Presented at: Symposium on the Nutrition and Management of the Transition Cow. Ottawa, Canada.
- E.N. Terry** 2012. Altered antioxidant levels in the treatment of chronic myelogenous leukemia. Presented at: Toxicology Directorate, U.S. Army Public Health Command. Aberdeen Proving Grounds, Edgewood, MD.

ABSTRACTS

- Emily N. Terry**, Jennifer J. Michal, Chris E. Hostetler, Ronald L. Kincaid. Effect of maternal selenium intake on mRNA levels of selenoprotein W, N, and glutathione peroxidase I in fetal and neonatal porcine skeletal muscle. Experimental Biology, 2008. San Diego, CA. April 5-9, 2008
- E Terry**, K Brennan, J Michal, K Johnson, R Kincaid. Selenoprotein expression is induced during oxidative stress in beef cows. ADSA-ASAS 2008. Indianapolis, IN. July 7-11, 2008.
- Emily N. Terry** and Alan M. Diamond. Post-transcriptional activation of anti-oxidant enzymes by imatinib. AACR 2012. Chicago, IL. March 31- April 4, 2012.